~~X70-79735~~

GRAVITY GRADIENT BOOM STABILIZATION SYSTEM
for the
APPLICATIONS TECHNOLOGY SATELLITE (ATS-E)

Final Report Vol I
Contract No. NAS 5-10285

Technical Officer: R. J. Wirth

Prepared for
GODDARD SPACE FLIGHT CENTER
Greenbelt, Maryland

by

WESTINGHOUSE DEFENSE AND SPACE CENTER
Aerospace and Electronic Systems
Baltimore, Maryland

GRAVITY GRADIENT BOOM STABILIZATION SYSTEM
for the
APPLICATIONS TECHNOLOGY SATELLITE (ATS-E)

Final Report Vol I
Contract No. NAS 5-10285

Technical Officer: R. J. Wirth

January 1970

Prepared for

GODDARD SPACE FLIGHT CENTER
Greenbelt, Maryland

By

B.S. Shephard, Mechanical Design
D.W. Zehner, Electrical Design
O.R. Shively, Technical Director

Approved: S. May, Program Manager

WESTINGHOUSE DEFENSE AND SPACE CENTER
Aerospace and Electronic Systems Division
Baltimore, Maryland

TABLE OF CONTENTS

LIST OF ILLUSTRATIONS

LIST OF TABLES

1.0 Introduction

This report is intended to describe the Westinghouse ATS-E boom system and how it functions; to discuss the capability of the system to withstand vibrational and operational loads; to describe the qualification and acceptance testing and the results thereof; and to evaluate the boom system in light of the above testing and analysis. Section 2.0 is devoted to the system description. Section 3.0 presents an analysis of certain critical system elements, as to how they withstand vibrational and operational loadings.

For this analysis, the final flight configuration was used so that, wherever applicable, the resulting system evaluation would complement the results of the qualification and acceptance tests; e.g., the test results verify that the system passed thrust axis vibration while the analytical results give some indication of the factors of safety involved in passing the test. Volume II describes the qualification and acceptance test procedures, the results of these tests, and the system design changes required in order to successfully complete the test programs.

2.0 Discussion of System

A discussion of the ATS-E Boom System composition and operation is as follows:

2.1 Description of the system - (see appendix-P for a full set of assembly drawings)

The Westinghouse ATS-E Boom System consists of the following basic components.

(1) deployer

(2) scissor mechanism

(3) tip mass release mechanism

(4) control circuit assembly

(5) squib firing circuit assembly

There are two separate identical packages (thereafter referred to as half systems) required for the ATS-E satellite, each of which consists of (2) deployers, (2) tip mass release mechanisms, (1) scissor mechanism, (1) control circuit assembly, (1) squib firing circuit assembly and the structure, wiring and hardware required to create a functional assembly. Each deployer within a given half system is capable of extending and retracting a gravity gradient boom upon command. The boom is a half inch diameter, interlocked seam, thermally stable hollow tube with a wall thickness of .002 inch. Each deployer provides means for continuously monitoring the length of boom deployed (via a linear potentiometer) and for automatically terminating deployment at a length of 123 feet (via the limit switch assembly). The control circuit assembly uses the output of the deployer potentiometers to produce coordination between the two booms being deployed from a given half system. The scissor mechanism rotates both deployers at the same rate but in opposite directions within the housing structure so that the included angle between the two half system booms

can be varied by 30°. The scissor mechanism contains a linear potentiometer to monitor the angles of the two booms. The scissoring action is automatically terminated at the limits of the scissor angle range by limit switches attached to the housing structure. The tip mass release mechanisms secure each tip mass (8 lb mass attached to the end of the boom) while subjected to the pre-launch and launch environments and release the masses upon command, once in space. A limit switch is actuated on each assembly which confirms successful release of the tip mass. The tip mass is released by cutting any one of two functionally redundant cables via squib actuated guillotine cable cutters. The explosive charge within each guillotine cable cutter squib is activated by an electronic signal generated by the squib firing circuit assembly.

The physical arrangement and configuration of the above half system elements can be seen in appendix-P. Provisions have been made to electrically isolate the boom from the deployer housings and the deployer housings from the half system housing structure. This will enable the booms to be used as antennas as well as for gravity gradient stabilization.

In every case in which two or more surfaces must move relative to one another to achieve successful operation in space, one or all of the sliding surfaces are coated with a suitable barrior coat to prevent cold welding. In most cases, the barrior is a bonded Molybdenum Disulfide compound developed by the Naval Air Material Laboratory, Philadelphia, Penn.

2.2 Description of major system component operation

2.2.1 Booms and Deployers

2.2.1.1 Booms (see fig 2-1)

The boom which was produced by Westinghouse for NASA under contract No. NAS5-10285 as part of the ATS-E gravity gradient stabilization system is made of .002 inch thick Beryllium copper that is formed into the 1/2" dia

interlocked tubular configuration. It is flattened and rolled onto a cylinder for storage, and when it is deployed it interlocks and assumes the tubular configuration. The boom has two improved features over other booms of this type. These improvements are increased torsional strength and rigidity, and minimized thermal bending.

The basic improvement in strength and rigidity results from the method of seam joining (interlocking), as can be seen from Figure 2-1. The interlocking is achieved by the interweaving of two opposing tabs, one of which is bent slightly toward the center of the X section. The roots of the opposing V-notches are locked together by the steep sides of the notches, and they are held together by elastic pressure which results from the nominal tube diameter being made smaller than the assembled diameter. The shape of the notch is made such that it is narrow and steep sided with a radius at the root. The location of engagement is defined within the radius of the notch root and the steep sides prevent the notches from sliding apart due to the shearing action produced by torsion on the boom. Thus, the torsional strength and rigidity are greatly increased over an open seam. The torsional backlash created by the radius at the root of each notch can be varied by increasing or decreasing the magnitude of this radius. In the limit, a perfectly sharp notch results in zero backlash.* The ATS-E Westinghouse boom design produces a backlash of 1 full twist of the boom in 30 feet. The torque required to twist the boom in the backlash region is 2.0 oz. in. The full torsional strength of the current Westinghouse boom is greater than 3.0 lb. in. The bending strength of the Westinghouse boom is 6 lb. in. minimum and the boom bending stiffness

*There are other methods developed by Westinghouse for eliminating the backlash which do not have the manufacturing and structural disadvantages of a sharp notch.

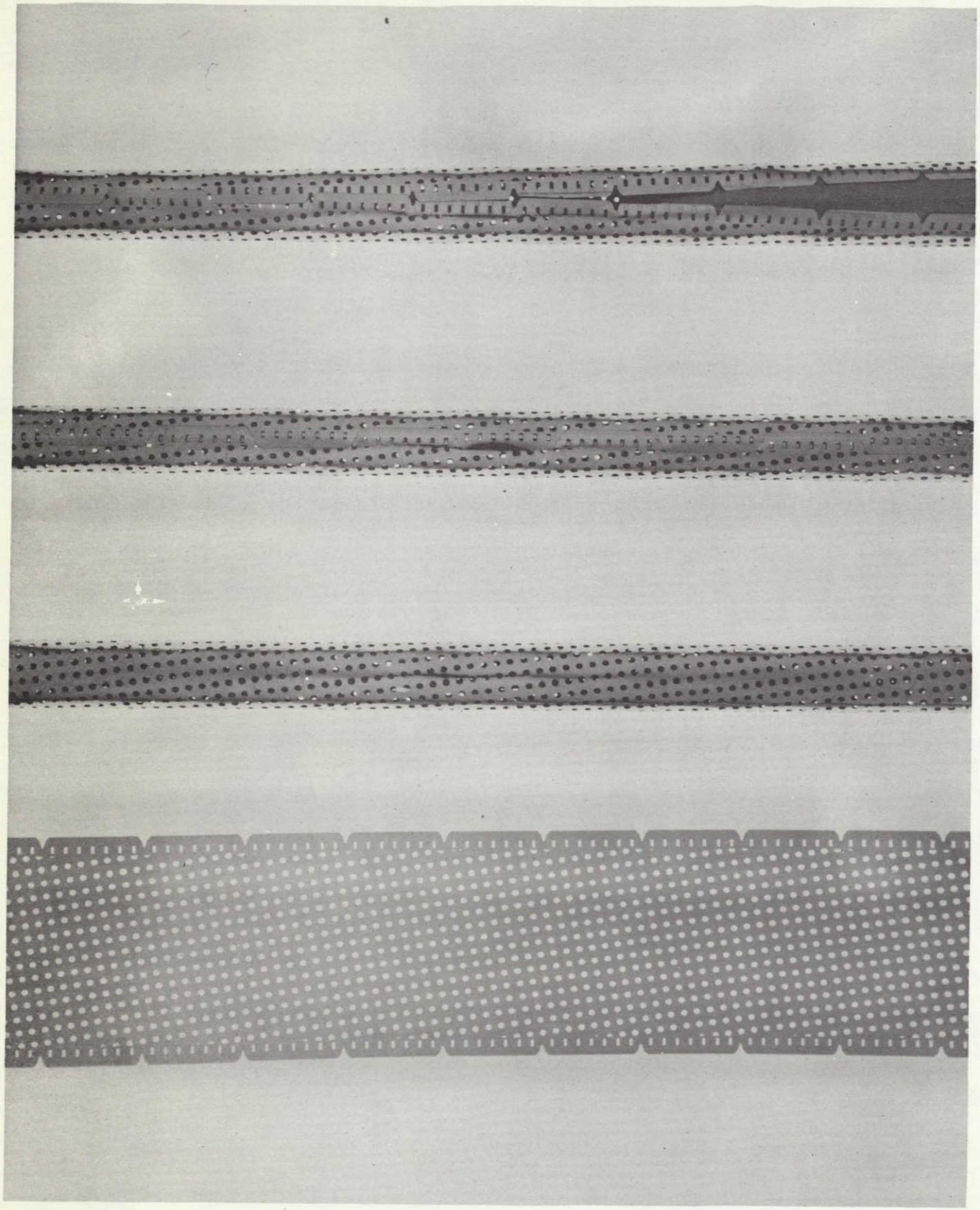

BOOM SEGMENTS

FIGURE 2-1

and torsional stiffness are both greater than 1000 lb-in^2.

The thermal bending of the boom is minimized through the use of window, or hole, patterns and surface coatings to equalize heat absorption across diameters. The windows permit a controlled amount of sunlight to strike the inside of the back wall, and the surface coatings are chosen to provide the same amount of heat absorption by the back and front walls. The window area is 17% of the boom surface area and the surface coatings are vapor deposited aluminum on the outside surface and "ebonal C" on the inside surface. The window pattern is layed out such that a constant proportionality between front and back exposure is maintained regardless of sun angle. This constant proportionality is upset slightly at the seam. However, since the seam tabs overlap both sides of the seam and bear hard against the opposite walls due to elastic forces in the boom, the resulting thermal conductive path tends to minimize adverse thermal effects at the seam. A photograph of a section of boom is shown in Figure 2-1. The effective projected area of the boom will be less than 6 in^2/ft. The straightness of the Westinghouse boom is controlled by the induced spiraling of the interlocked seam which distributes curvature in the boom in a helical pattern about an average center line.

2.2.1.2 Deployer - (see fig 2-2)

The Westinghouse boom deployer is capable of extending, retracting and storing the Westinghouse interlocked seam thermally stable boom per the requirements of component specification.

The deployer drive elements consist of a field wound D.C. motor, two slip clutches, an overrunning clutch and appropriate gears and bearings. The operational elements of the deployer are (in addition to the drive elements) a storage reel to store the flattened boom (tape); a set of drive rollers to deploy the boom; a contoured support to provide buckling strength

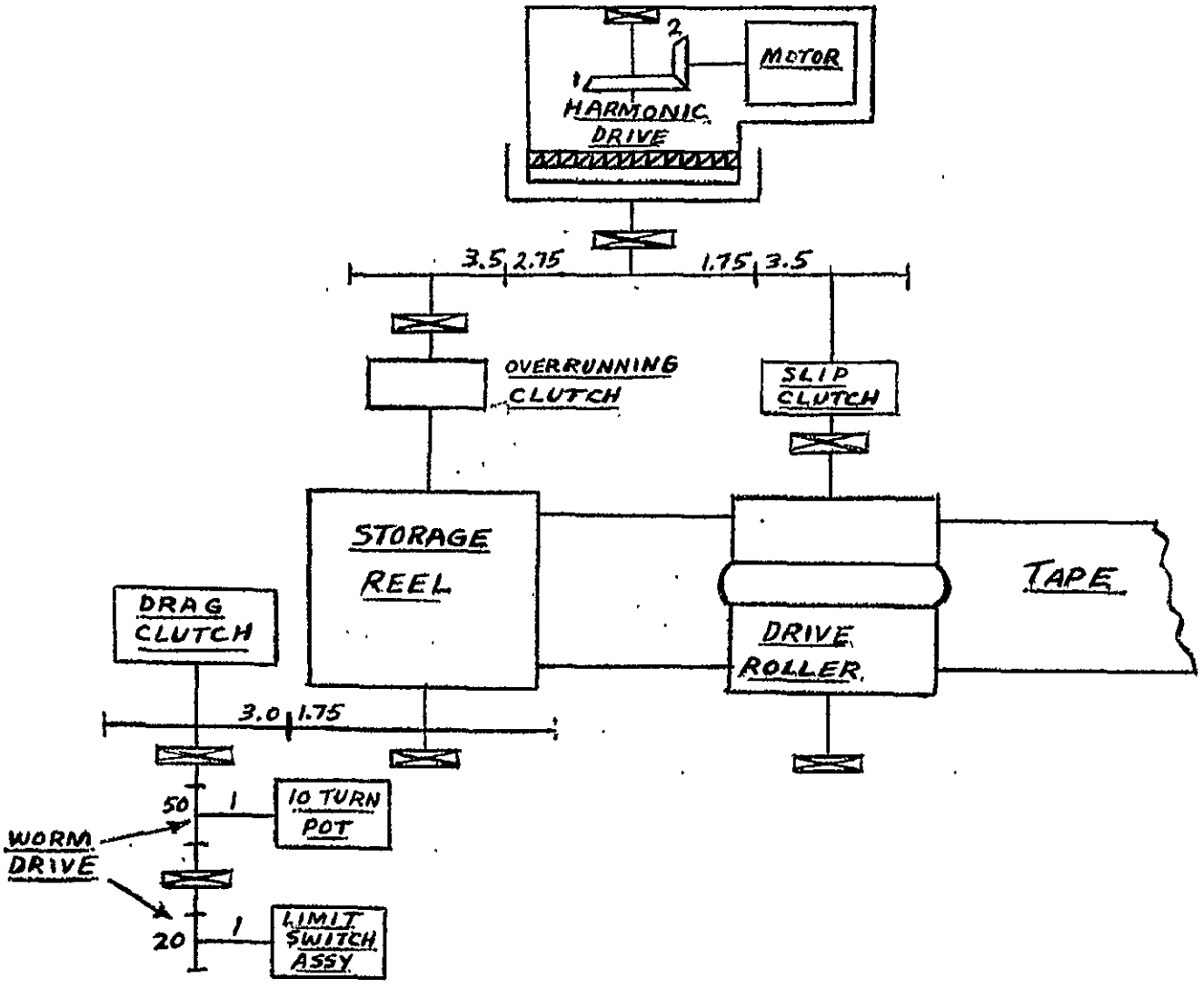

ATS DEPLOYER MECHANICAL SCHEMATIC

FIGURE 2-2

for the boom in the transition between the tubular and flat states (shoe); a zippering device to assure positive interlocking of the boom tabs; a guide support to support the fully tubular boom as it leaves the deployer exit; a linear 10 turn potentiometer to monitor the length of deployed boom; and a limit switch device to stop deployment at 123 feet. In addition, there is a housing to align and support these operational elements.

Figure 2-2 shows the conceptual schematic of the deployment mechanism. The motor simultaneously drives the input to the storage reel overrunning clutch and the input to the drive roller slip clutch. In the deploy mode the drive roller pulls the tape off the storage reel which has been uncoupled from the drive train via the overrunning clutch. Tension in the tape needed for positive boom tracking during deployment is provided by the drag slip clutch geared to the storage reel. The motion of the storage reel is geared to the length monitoring potentiometer and the full extension limit switch device. The extension length monitoring potentiometer will be capable of monitoring the tip mass position for any fractional increment of deployment or retraction within $\pm$ 6 inches. The position of the tip mass at any extension increment will remain fixed within 1/4 inch (excluding temperature effects). The full extension limit switch assembly will terminate deployment with the tip mass 123' $\pm$ 2 inches. In the retract mode the direction of motor rotation is reversed. The overrunning clutch now drives the storage reel which pulls the tape into the deployer. By virtue of the requirement that the storage reel uncpuple in the deploy mode, the storage reel, drive roller and the appropriate gearing have been sized such that during retraction the drive roller is forced to rotate faster than the input to the drive roller slip clutch. Consequently, the slip clutch slips. The tension from the slipping slip clutch is used to wrap the tape tightly onto the storage reel.

2.2.2 Scissor Mechanism - (see fig 2-3)

The scissor mechanism consists of a field wound D.C. motor, a 10 turn potentiometer, a turnbuckle, two screw arms, gearing and a housing designed to support these elements as well as to provide a hermetic seal. The mechanism operates as follows. The D.C. motor simultaneously drives the potentiometer and the "left-right threaded turnbuckle" thru appropriate gearing. The rotary motion of the "turnbuckle" is converted to axial motion of the "screw arms". This conversion occurs because the "screw arms" are prevented from rotating by the "rotary linkage". The axial motion of the "screw arms" (both arms move out or in together) is transmitted thru the rotating linkage to the "linkage pivot" which in turn causes each deployer to rotate about its "deployer pivot axis". The rotation of the potentiometer produces an analog signal used to determine the scissor angle. The D.C. motor and the brush type potentiometer each need to be operated in the presence of moisture. Thus, the mechanism is hermetically sealed with air, helium (used for leak detection) and water vapor. The bulk of the seal is provided by cementing sheet metal covers onto a base plate to which the mechanism elements are secured. The seal in the area of the "scissor arms" is provided by bellows which have one end soldered to the sensor arm and the other soldered to the sheet metal cover.

2.2.3 Tip Mass Release Mechanism - (see fig 2-4)

The major elements of the tip mass release mechanism consist of an 8 pound tip mass assembly, a clamping assembly* to secure (cage) and to release (uncage) the tip mass assembly, an end plate assembly* to support the tip mass assembly and the clamping assembly*, and appropriate hardware. The clamping

*The word assembly, in this case, refers to a functional assembly rather than a manufacturing assembly with its own assembly drawing and instructions

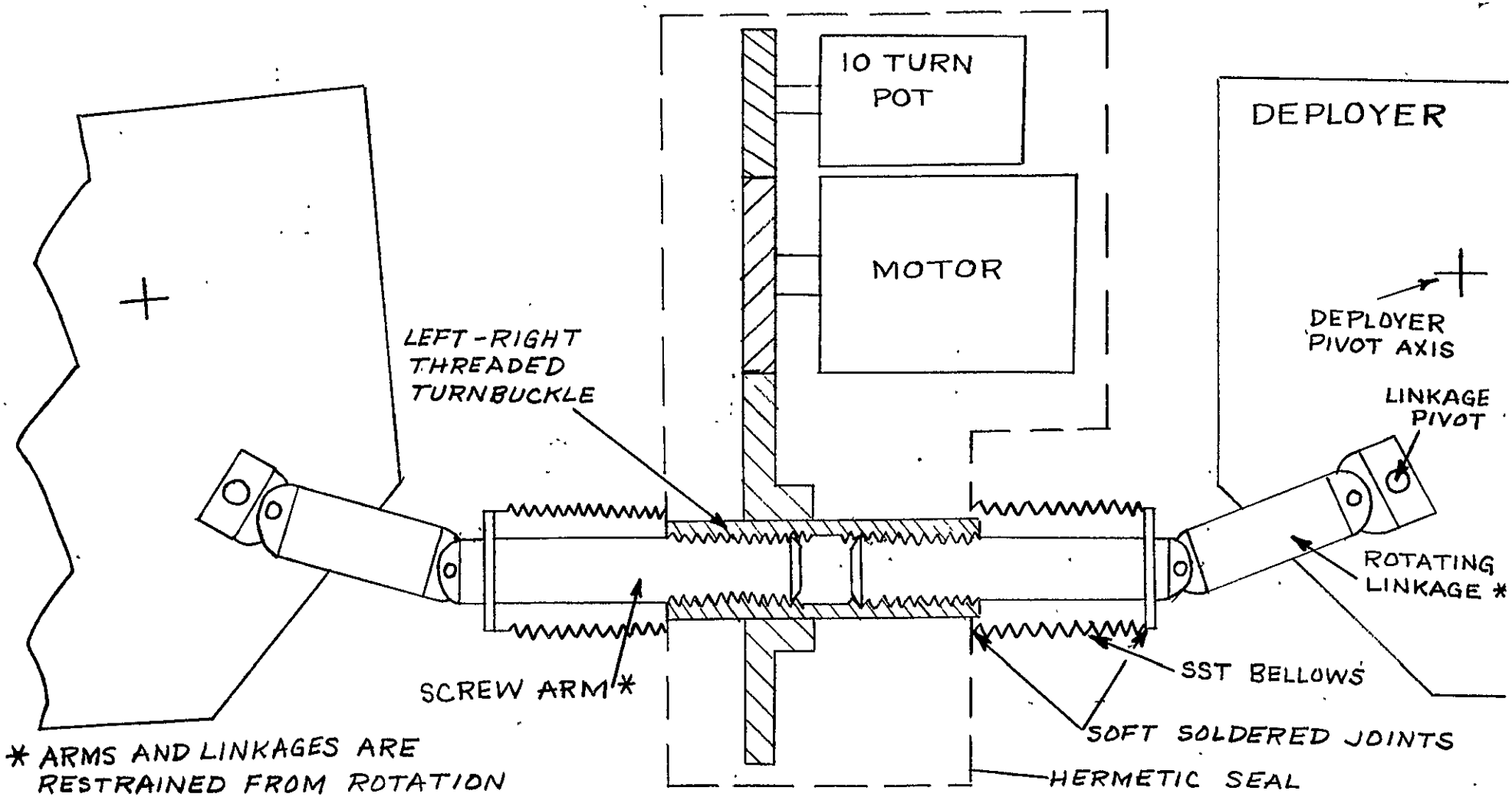

SCHEMATIC OF SCISSOR MECHANISM ATS DEPLOYER

FIGURE 2-3

assembly consists of a clamping lever which bears directly against the tip mass to secure it during launch; a support arm which supports (props-up) the clamping lever; a stranded stainless steel cable which holds the support arm in place; two squib actuated guillotine cable cutters any one of which will cut the cable and release the tip mass if activated; pins to allow the clamping lever and the support arm to rotate away from the tip mass after the cable is cut; torsion springs to cause this rotation; and metal beads, cemented to the cable, which restrain the cut sections of cable after release has been achieved. The end plate assembly consists of the end plate, which ties the entire assembly into the half system outer housing and provides direct support for the tip mass via the support posts, and means of securing the other elements of the end plate assembly*; the adjustment screw used to align the tip mass and act as a reaction point for preload and dynamic forces; a support post which provides a redundant support along with the adjustment screw; and structure to guide the cable and support its free ends. The tip mass assembly consists of the eight pound tip mass; the boom isolation assembly which connects the free end of the boom to the tip mass; a teflon bushing to electrically isolate the boom from the tip mass assembly; and a bowed retaining ring used to attach the boom isolation assembly to the tip mass.

The tip mass assembly is placed onto the support post. The clamping lever screw is brought into loose contact with the tip mass and the support arm wheel is held against the clamping lever stop by the cable. The cable tension adjustment and the clamping screw are alternately tightened, until sufficient strain energy has been stored in the clamping lever (the method of storing the strain energy is discussed in appendix I) and the

*The word assembly, in this case, refers to a functional assembly rather than a manufacturing assembly with its own assembly drawing and instructions

TIP MASS RELEASE MECHANISM

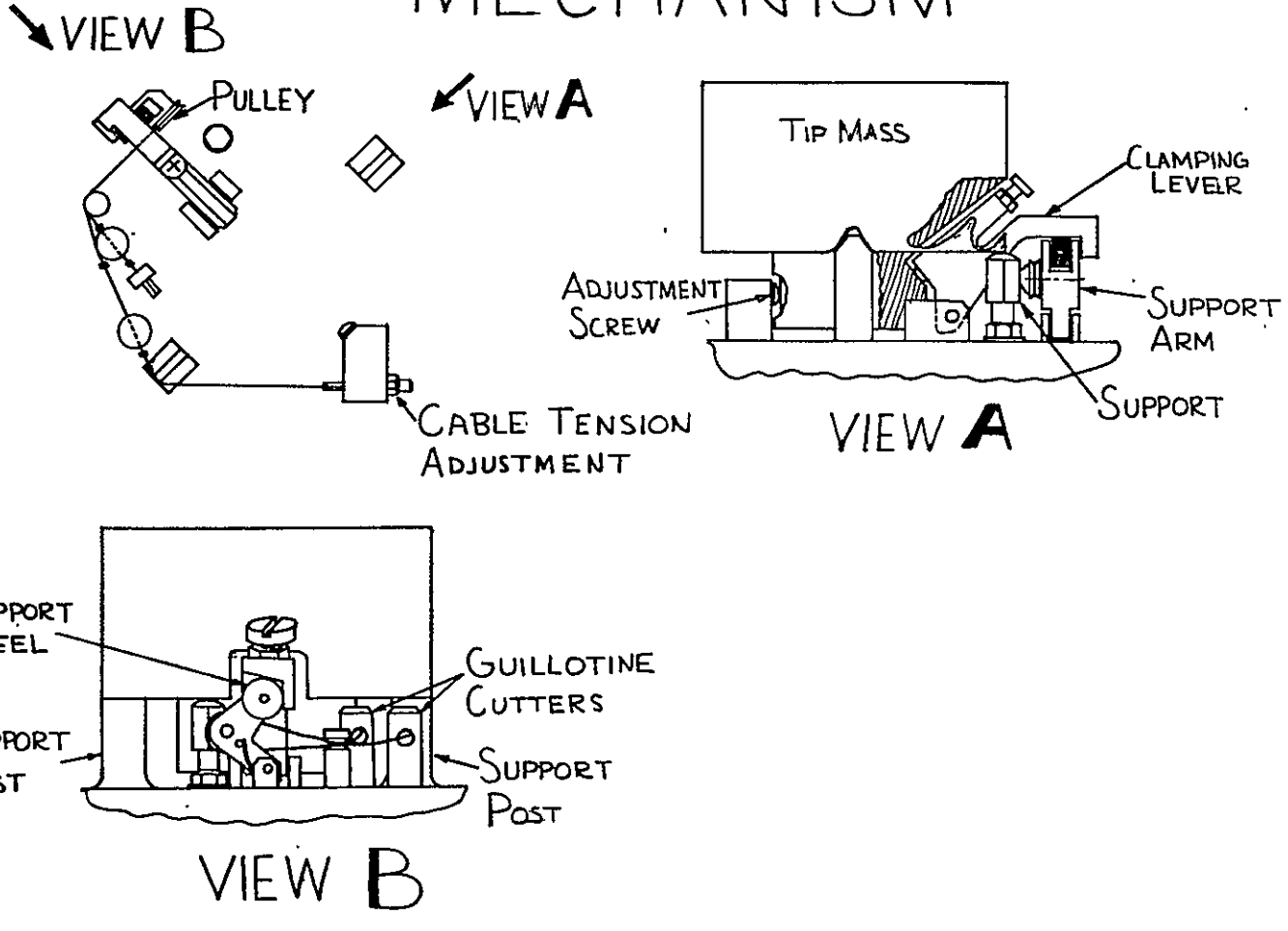

FIGURE 2-4

support wheel is just free of the stop on the clamping lever. The redundant support post is then adjusted to just touch the tip mass and is locked in place. Finally, all other clamping elements are locked. In this configuration the tip mass assembly is secure against the vibration environment (see appendix-I for the structural analysis of the tip mass release mechanism subjected to the most severe qualification level vibration inputs) encountered during launch. When the cable is cut by one or both of the other guillotine cable cutters, the strain energy stored in the clamping lever is now available to start the arm support rotating away from its clamped position. As the arm support rotates, the support wheel rolls up the inclined ramp of the clamping lever (see view B fig 2-3). A torsion spring acts on the arm support to assure that it rotates completely free of the clamping lever. A leaf spring on the clamping lever causes it to rotate free of the tip mass and hence the tip mass has been successfully released.

2.2.4 Control Circuit Assembly

The ATS-E Gravity Gradient experiment is conveniently divided into two identical half systems. Each consists of two mechanically independent gravity gradient booms to be electrically coordinated in length. The electrical control linking the two booms in each ATS-E half system replaces a mechanical linkage used on an earlier ATS-G/G system. To facilitate substitution of the W gravity gradient booms in the satellite, it is decreed that the existing electrical interface will be unchanged. Thus an interface intended to drive a single DC motor in the earlier ATS, must coordinate and control two separate motors for the ATS-E.

The interface consists of two leads intended to deliver a reversible voltage to the motor field establishing motor direction, and two leads intended to supply a nonreversible voltage to the motor armature. Both voltages originate with the unregulated bus. Control and coordination of the two booms in each ATS-E G/G half system is achieved by switching mode control of these power levels as they are routed to the motors. A regulated telemetry voltage and its return are also provided at the interface.

Initial deployment of the booms is essential to achieve even partial success of the G/G experiment, and the reliable performance of this function is stressed over the coordination requirement. Each pair of booms is also capable of being retracted to a length desired by the experimenter.

Boom length is monitored by a 10 turn potentiometer mechanically linked to each boom, the output of which provides telemetry information. Boom position information is also input to the coordinating and control circuit. The G/G boom coordinating system involves deployment of the MASTER boom subject to a telemetry command, and positioning of the SLAVE boom to match

the MASTER through a satellite boom control circuit. Note that the SLAVE is powered only for the duration of the T/M command; this is a consequence of the interface.

Coordination of MASTER and SLAVE G/G booms in the RETRACT direction involves the momentary interruption of power to the motor driving the boom most inboard to the satellite, i.e., least EXTENDED or most RETRACTED.

In the EXTEND direction, the coordinating influence available to the control circuit is to interrupt or reverse power to the SLAVE motor. Thus, during an EXTEND command in the unlikely situation where the SLAVE is farther EXTENDED than the MASTER, the SLAVE will RETRACT while the MASTER EXTENDS until matching is achieved. However normal operation should find both booms EXTENDING with the MASTER pacing the SLAVE throughout the deployment.

It can be seen that the SLAVE must possess a superior speed characteristic to that of the MASTER if matching during the EXTEND function is to be achieved. This is done by a process of selection, with the faster of two motors winding up as a SLAVE. Should the motor speed characteristics be altered as a result of launch vibration, at worst the MASTER will lead the SLAVE in a run to the LIMIT SWITCHES. Coordination in RETRACT is then unaffected by motor speed characteristics.

In the RETRACT direction the coordinating action is again to interrupt or reverse power to the SLAVE motor; in addition the MASTER motor is interrupted when the MASTER boom is inboard with respect to the SLAVE.

In a nutshell, the MASTER is subject to and obeys T/M command, and for the duration of the command the SLAVE will either DEPLOY or RETRACT to match the MASTER. The single exception to this general rule occurs in RETRACT operation. In RETRACT, should the MASTER be closest inboard to the

satellite, it is disabled to await the return of the SLAVE.

The few functional limitations of the G/G boom control are imposed chiefly to ensure reliability of deployment. Failure of a major portion of the control circuitry will not impair the ability to deploy both booms to their limit. This was achieved by cataloging failure modes, and designing for these to result in SLAVE deployment, with the MASTER remaining under the control of T/M command.

2.2 5 Squibb Firing Circuit Assembly

The tip masses attached to the Gravity Gradient Booms are secured to the satellite structure during launch with a spring loaded latch. The spring is restrained by a cable which is severed by a squibb fired guillotine to initiate release. Release is timed to follow orbital insertion and stabilization in inertial space, when external forces acting on the masses are essentially reduced to zero. Successful squibb firing and tip mass release is essential to mission achievement since Gravity Gradient is the only method provided for long term stabilization of the ATS-E.

The interface with which the ATS-E squibb firing circuit must mate is again defined by the earlier ATS versions, and consists of an "A" and "B" firing command on each G/G half system. Both "A" and "B" circuits are capable of producing a 26 $\pm$ 4 v, 7 amp time variable pulse, initiation and duration determined by T/M command. The ATS-E is designed to include a primary and redundant squibb on both MASTER and SLAVE mechanisms for a total of four squibbs per G/G half system. The recommended firing current for the squibbs is 5 amps which results in an average function time of 1.2 milliseconds. Minimum "all fire current", (the DC current at which all squibbs of this type function), is 3.5 amps. To achieve the recommended 5 amp function current with true redundancy, squibbs must be addressed alternately rather than in parallel.

The circuit that lends itself to this current steering application consists of a multivibrator (MV), furnishing time quadrature gating pulses to four silicon controlled rectifiers. Each SCR connects the 26 $\pm$ 4 volt bus to a squibb in series with a 5 ohm resistor. The 5 ohm resistors guarantee

* (A squibb is a pyrotechnic device requiring a current pulse (electric match), for detonation.)

survival of the "A" and "B" command circuits beyond the firing of the initial squibb since squibb bridgewire resistance is specified to be 1.1 ± 0.1 ohms. The SCR gating pulse must be long enough to ensure squibb firing at the low voltage end of the bus, (10 msec.), but short enough to allow several alternations between MASTER and SLAVE squibbs during the time period of the "A" and "B" fire command. The duration of the lettered commands is limited to prevent burn out of the 5 ohm series resistors should a squibb fail to fire. Assuring survival of a series resistor when a squibb fails to fire is questionable, but this at least permits readdressing the unfired squibb. The multivibrator was designed for a gate period of 40 msec. in conjunction with a lettered command of 200 msec. to permit addressing each squibb at least twice.

The operation can at this point be described in greater detail. The "A" command connects the 24 ± 4 v bus to an SCR cathode in each of the MASTER and SLAVE release mechanisms, and to the multivibrator. The MV initially gates SCR #1 in series with SLAVE squibb #1. The MV gate is designed to last for 40 msec., but current flows through SCR #1/squibb #1 until either the squibb bridgewire burns open or the "A" command terminates. After 40 msec the MV gates SCR #2 in series with MASTER squibb #2. Current now flows in SCR #2/ squibb #2, again until either the bridgewire burns open of the "A" command terminates. With the successful completion of this sequence, both tip masses are released, and boom deployment can proceed. Redundant operation results from the "B" command with SCR #3/squibb #3 of the MASTER release mechanism and SCR #4/squibb #4 of the SLAVE release mechanism receiving the attention. To prevent premature squibb firing resulting in parallel operation, the MV must produce an authentic 40 msec gate initially with the application of power. Start up circuitry is included in the MV to assure this.

The ATS-E squibb firing circuitry thus alternately steers the current from each lettered source to two squibbs, permitting the use of redundant squibbs from a single source. Failure of either lettered command or either MV gate will not impair the release of both MASTER and SLAVE tip masses. Failure of one squibb in each of the release mechanisms will also of itself not cause tip release failure.

3.0 System Analysis

3.1 Discussion

3.1.1 Description of the system

The system to be analyzed is described in section 2.1 of this report.

3.1.2 Scope of Analysis

This portion of the report is devoted to the stress analysis of certain critical mechanical elements of the ATS-E boom system. Section 3.2 of the analysis is concerned with the effects of vibration loading and Section 3.3 is concerned with the effects of operational loading on the pertinent critical mechanical elements. Section 3.2, with its associated appendices, determines the c.g. response of the major system subassemblies for the thrust axis qualification sinusoidal vibration input levels; defines the critical components and determines the critical load levels; and determines the maximum stress levels resulting from the dynamic loading. Section 3.3 with its associated appendices defines the critical operational modes; determines the corresponding load levels; and determines if these load levels will cause any problems from the standpoint of stress and/or acceptable system operation.

3.2 System Analysis - Vibration Loading

The vibration input loading has been chosen as the original thrust axis sinusoidal qualification test levels inspite of the fact that these levels were changed before qualification vibration testing was accomplished. The reason for this is because it is felt that the original specification levels are more severe than the final levels (original levels have 11.5 g's input at the system fundamental resonant frequency whereas the new levels have only 5 g's and consequently the following analysis should be conservative. The thrust axis has been chosen as the pertinent vibration axis for two reasons;

m_i = i^{th} system mass

δ_{ij} = deflection at i due to unit load at j (flexibility influence coefficient) = δ_{ji}

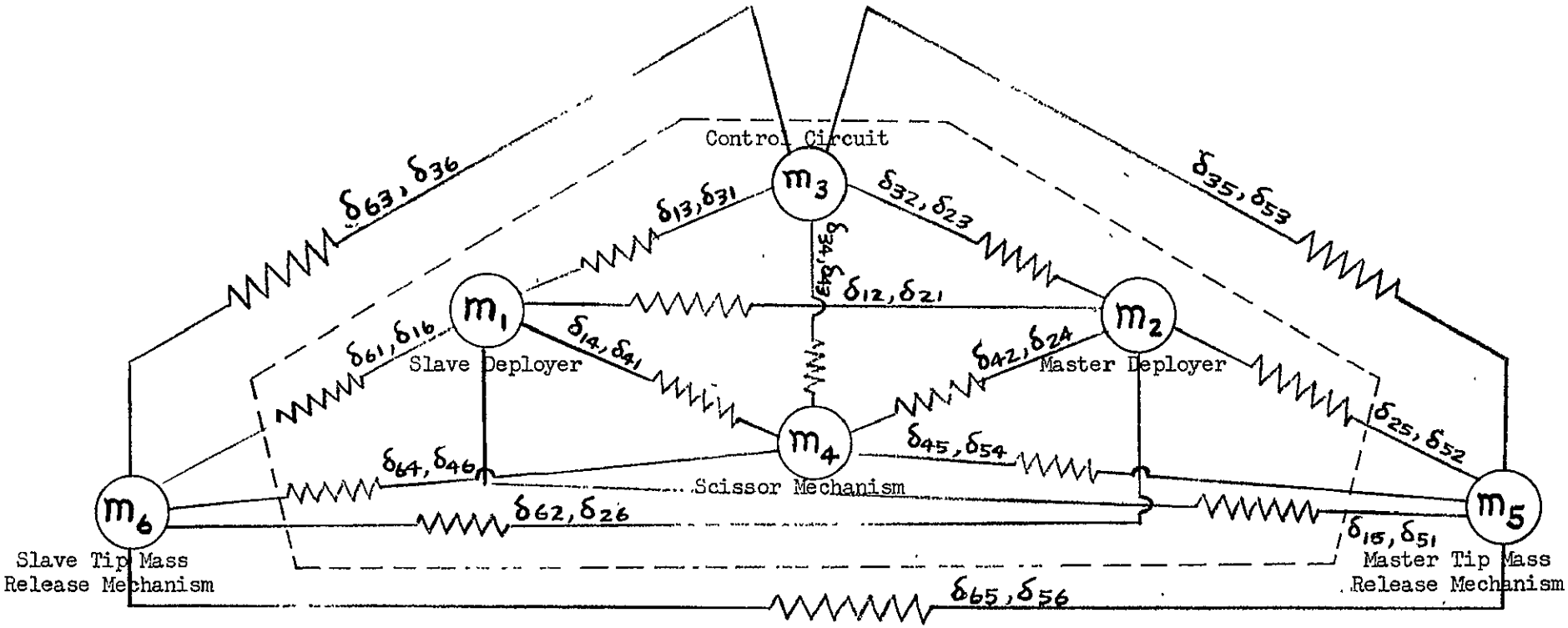

LUMPED MASS VIBRATION MODEL ATS-E BOOM SYSTEM

FIGURE 3-1

i.e., (1) the half system structure is the most flexible in this axis resulting in the lowest system fundamental natural frequency and consequently the largest vibration amplitude for a given input level, and (2) the input levels are the greatest in this axis at all frequencies.

3.2.1 Determination of system c.g. vibration response

Each half system can be thought of as a six degree of freedom lumped spring-mass system (see fig 3-1). The mass points correspond to the centers of gravity of the six major system components as shown in fig 3-1. The mass assigned to each mass point is assumed to act at that point, and consists of the component mass plus a portion of the mass of the half system housing structure. The masses are all dynamically uncoupled but are statically coupled thru the flexible structure. This coupling can be expressed in terms of flexibility influence coefficients, A_{ij}; where A_{ij} is defined as the deflection @ mass point "i" due to a unit load at mass point "j". The development of the equations for the response of each mass, resulting from a sinusoidal vibration input to the system, requires a knowledge of certain parameters developed in solving for the free vibration response of the system. The parameters of interest are the six natural frequencies (normal made frequencies) and the six sets of normalized displacement amplitudes (six amplitudes per set with all values normalized such that the largest amplitude is 1.0). The normalized displacement amplitudes are referred to as the normal mode shapes corresponding to a given normal mode frequency. The six equations of motion for the spring mass system in free vibration can be written as:

displacement vector

$$\begin{Bmatrix} X_1 \\ X_2 \\ X_3 \\ X_4 \\ X_5 \\ X_6 \end{Bmatrix} \begin{bmatrix} A_{11}M_1 & A_{12}M_2 & A_{13}M_3 & A_{14}M_4 & A_{15}M_5 & A_{16}M_6 \\ A_{21}M_1 & A_{22}M_2 & A_{23}M_3 & A_{24}M_4 & A_{25}M_5 & A_{26}M_6 \\ A_{31}M_1 & A_{32}M_2 & A_{33}M_3 & A_{34}M_4 & A_{35}M_5 & A_{36}M_6 \\ A_{41}M_1 & A_{42}M_2 & A_{43}M_3 & A_{44}M_4 & A_{45}M_5 & A_{46}M_6 \\ A_{51}M_1 & A_{52}M_2 & A_{53}M_3 & A_{54}M_4 & A_{55}M_5 & A_{56}M_6 \\ A_{61}M_1 & A_{62}M_2 & A_{63}M_3 & A_{64}M_4 & A_{65}M_5 & A_{66}M_6 \end{bmatrix} \times W^2 = \text{frequency} \begin{Bmatrix} X_1 \\ X_2 \\ X_3 \\ X_4 \\ X_5 \\ X_6 \end{Bmatrix}$$

The solution to these coupled equations gives six normal mode shapes and the corresponding six normal mode frequencies. The mathematical expression of any given mode shape is $\bar{X}_{ia}$ (mode shape for the $i^{\underline{th}}$ mass in the $a^{\underline{th}}$ mode) and for any mode frequency is W_a ($a^{\underline{th}}$ system natural frequency). The method of solving the above six equations of motion, expressed in matrix form, for the $\bar{X}_{ia}$'s and W_a's is the same as solving a standard eigen value - eigen vector problem. The details of the solution are not included in this report*; however, a computer program is presented in appendix-B, a portion of which is used to solve for the made shapes and mode frequencies.

The magnitude and phase of the response of any of the six masses due to a one "g" sinusoidal vibration input to the system can now be expressed as follows:

$$H_{i(W)} = \sqrt{\sum_{\substack{a=0 \\ K=0}}^{6} B_{ia} B_{ik} \operatorname{Cos} (\psi a - \psi k)}$$

*"Vibration Theory and Applications", William T. Thomson, Prentice Hall, page 222

$$\xi_{i(w)} = \tan^{-1}\left[\frac{\sum_{a=0}^{6} B_{ia} \sin \psi_a}{\sum_{a=0}^{6} B_{ia} \cos \psi_a}\right]$$

where:

$$B_{ia} = -\bar{X}_{ia} \left\{ \frac{\sum_{K=1}^{6} \left(M_K \bar{X}_{Ka}\right)\left(\frac{W}{W_a}\right)^2}{\left[\left(1-\left(\frac{W}{W_a}\right)^2\right)^2 + \gamma^2\right]^{\frac{1}{2}} \sum_{K=1}^{6}\left[M_K \bar{X}_{Ka}^2\right]} \right\}$$

$$B_{IO} = 1$$

$$\psi_a = \tan^{-1}\left[\frac{\gamma}{1-(W/W_a)^2}\right]$$

$$\psi_o = 0$$

M_K = Kth mass

$\bar{X}ia$ = mode shape for $i^{\underline{th}}$ mass in $a^{\underline{th}}$ mode

$\bar{X}_{Ka}$ = mode shape for $K^{\underline{th}}$ mass in $a^{\underline{th}}$ mode

W = frequency of external excitation

W_a = $a^{\underline{th}}$ normal mode frequency

γ = structural damping factor

$H_{i(W)}$ = response of $i^{\underline{th}}$ mass for a one "g" input to the system at a frequency of W - g's

$\xi_i(W)$ = phase angle between response of $i^{\underline{th}}$ mass and the input to the system - radians

Because of its complexity, the derivation of these equations is not presented in this report. The development of these equations is described in several references* although not in the same form as presented above. The relative displacement between masses 1 and 5 and between masses 1 and 4 are also of interest (see 3.2.2). The equations which define these displacements are:

$$(X_{REL})\ 1-5 = \sqrt{(H_1)^2 + (H_5)^2 - 2(H_1)(H_5)\cos(E_1 - E_5)}$$

$$(X_{REL})\ 1-4 = \sqrt{(H_1)^2 + (H_4)^2 - 2(H_1)(H_4)\cos(E_1 - E_4)}$$

The solution to the above equations was achieved by use of the computer program listed in appendix B. The absolute responses of each of the six mass points versus excitation frequency are shown in fig's 3-2 thru 3-7. The maximum mass accelerations and the maximum values of (X_{REL}) 1 - 5 and (X_{REL}) 1 - 4 are tabulated in table 3-1. The determination of the physical properties required to solve the response equations was, for the most part, done experimentally and is presented in appendix A. The input levels for which the half system response has been determined are listed in table 3-2.

*(1) "Elements of Normal Mode Theory", G. J. O'Hara & P. F. Cunniff, NRL Report 6002

(2) "Vibration Aanlysis of the EME/ATS-E System," R. M. Root, W report TM-179-MDD-267

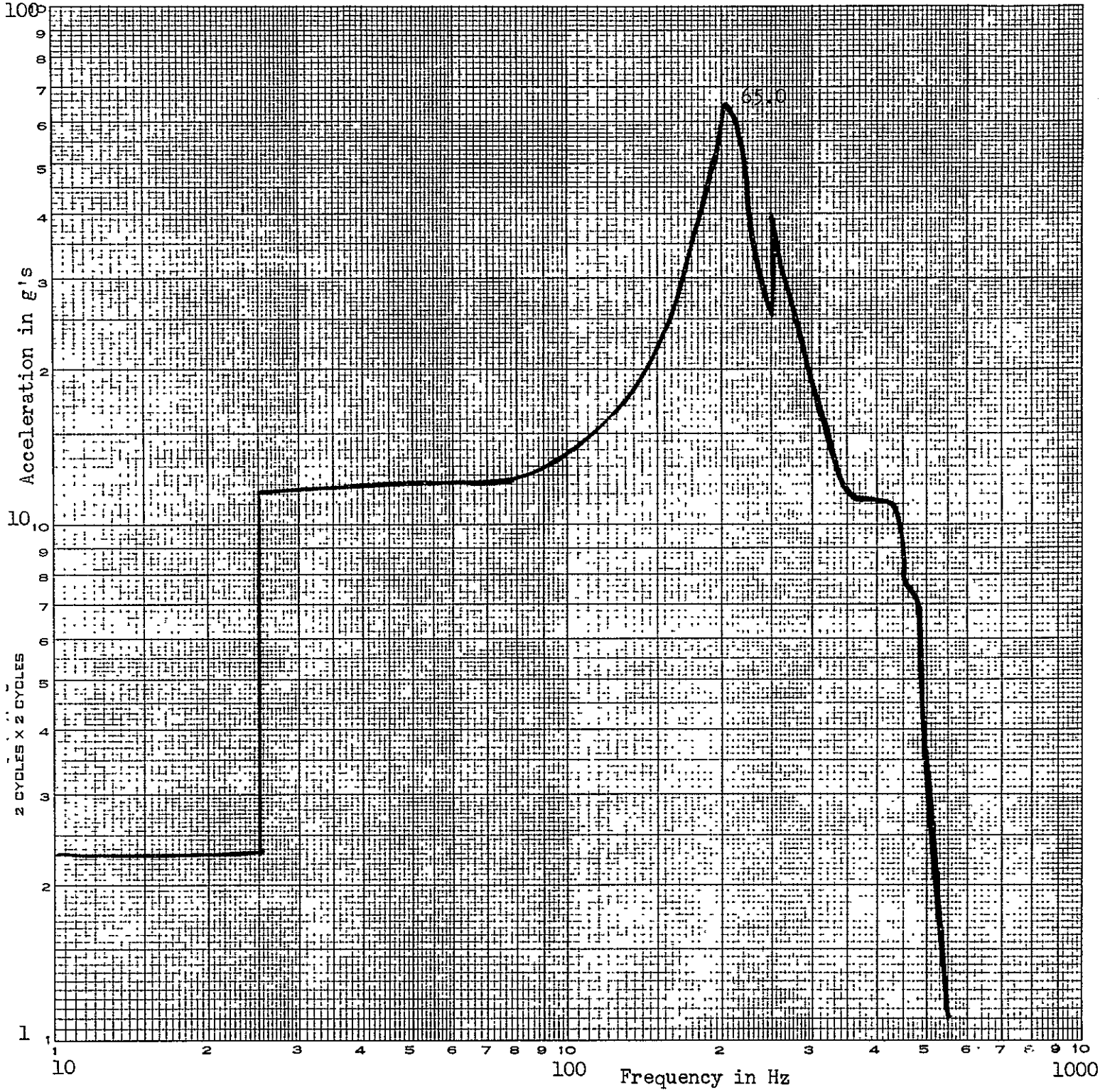

FREQUENCY RESPONSE MASS ONE

FIGURE 3-2

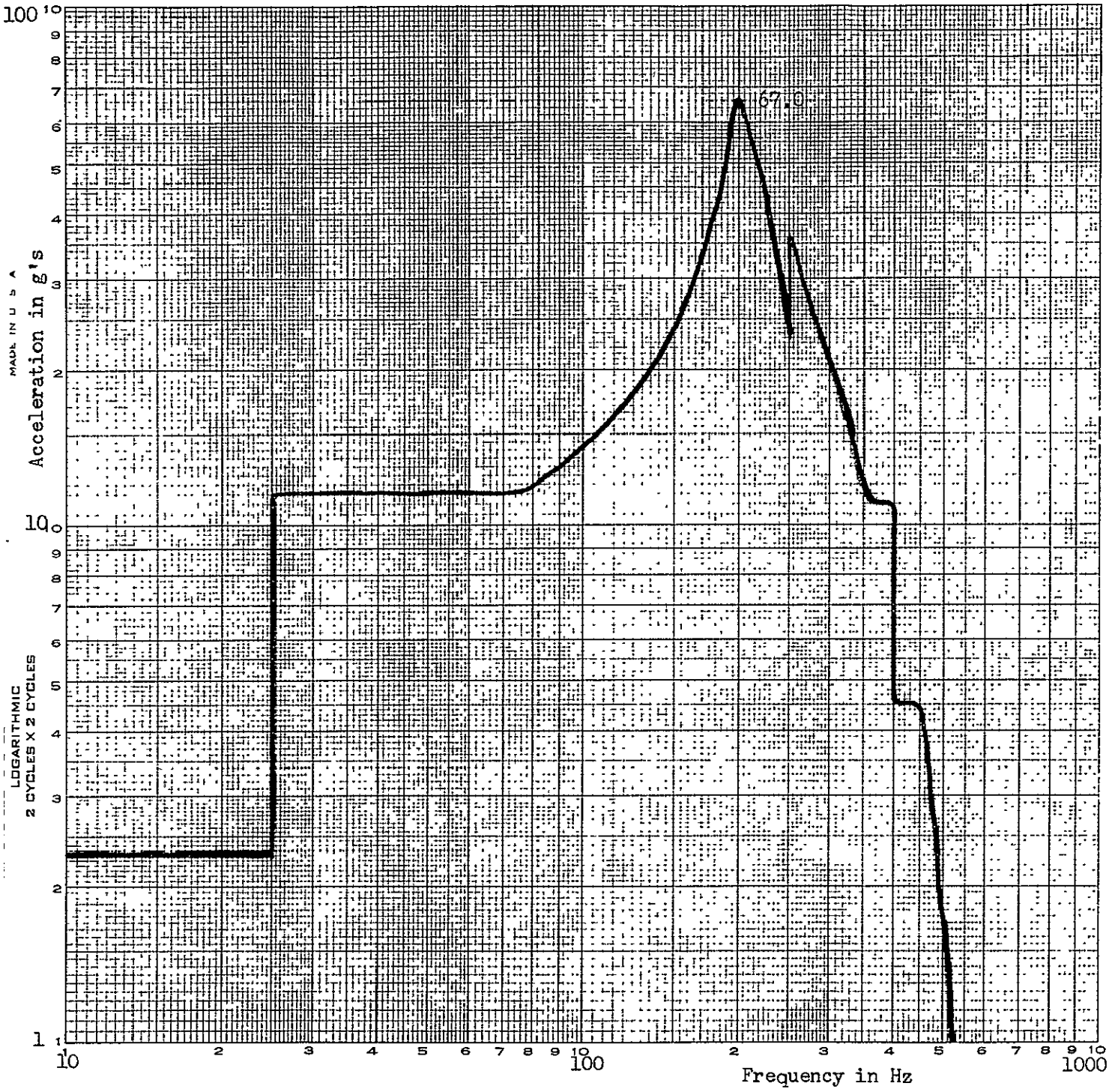

FREQUENCY RESPONSE MASS TWO

FIGURE 3-3

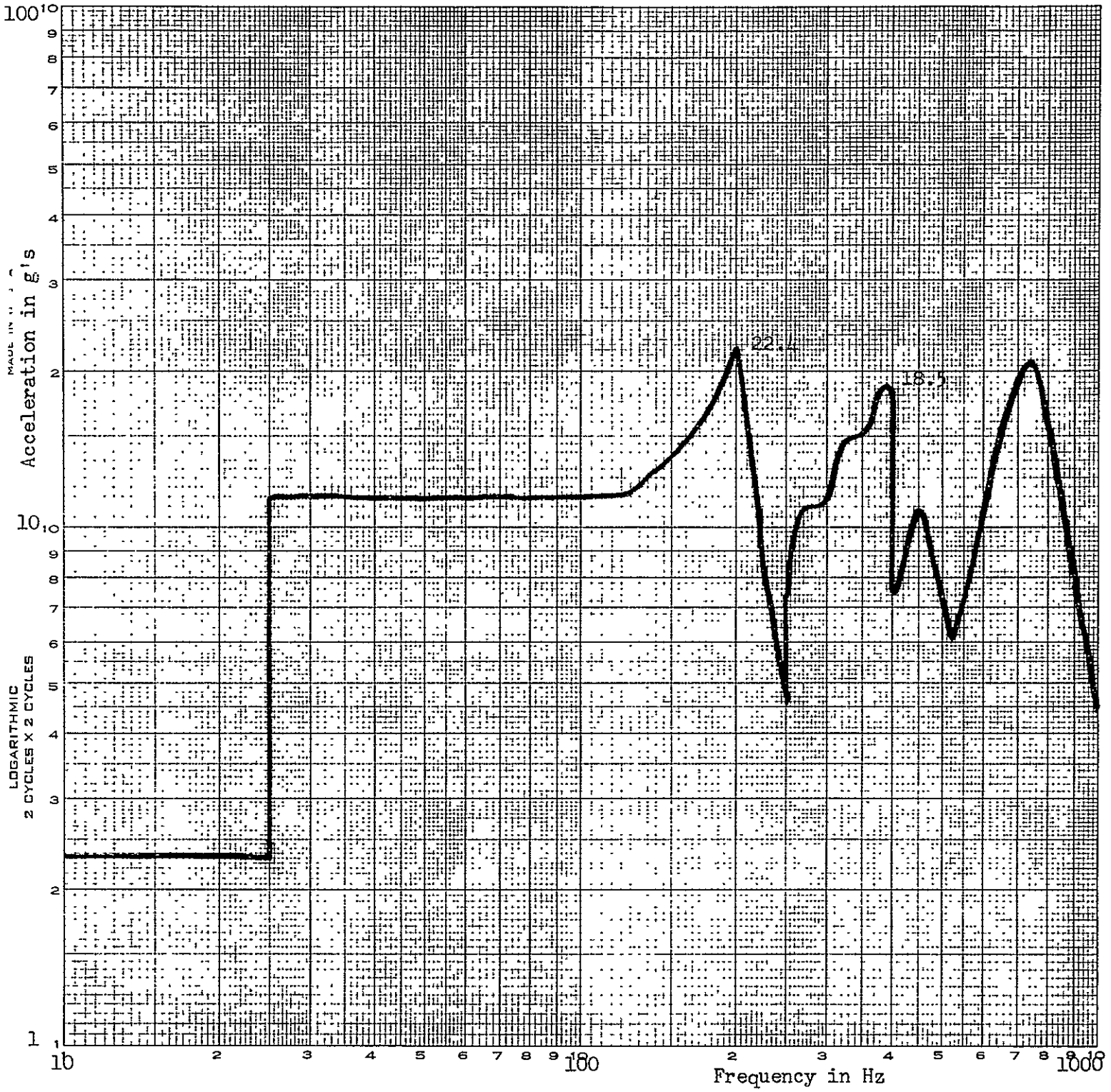

FREQUENCY RESPONSE MASS THREE

FIGURE 3-4

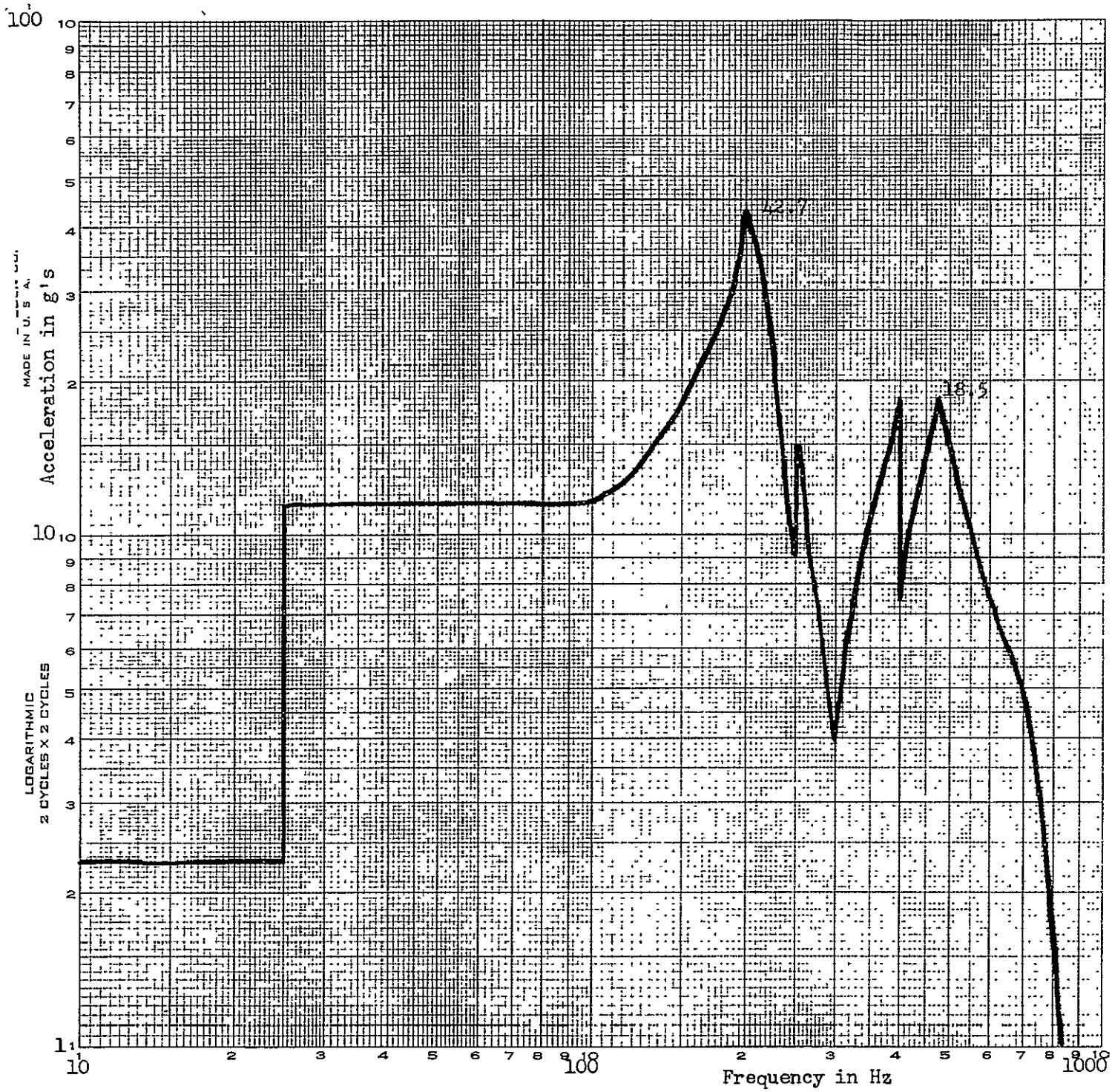

FREQUENCY RESPONSE MASS FOUR

FIGURE 3-5

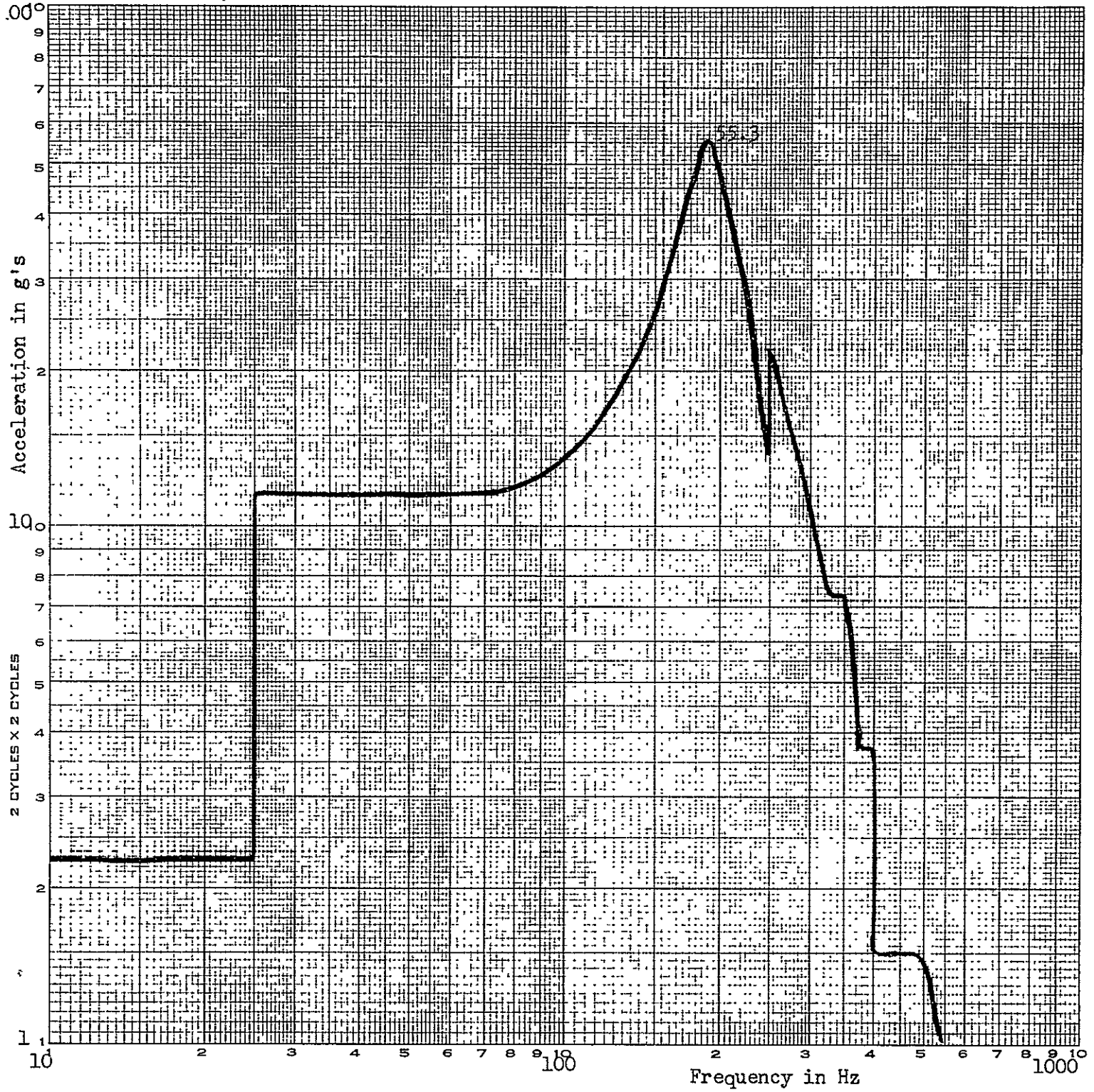

FREQUENCY RESPONSE MASS FIVE

FIGURE 3-6

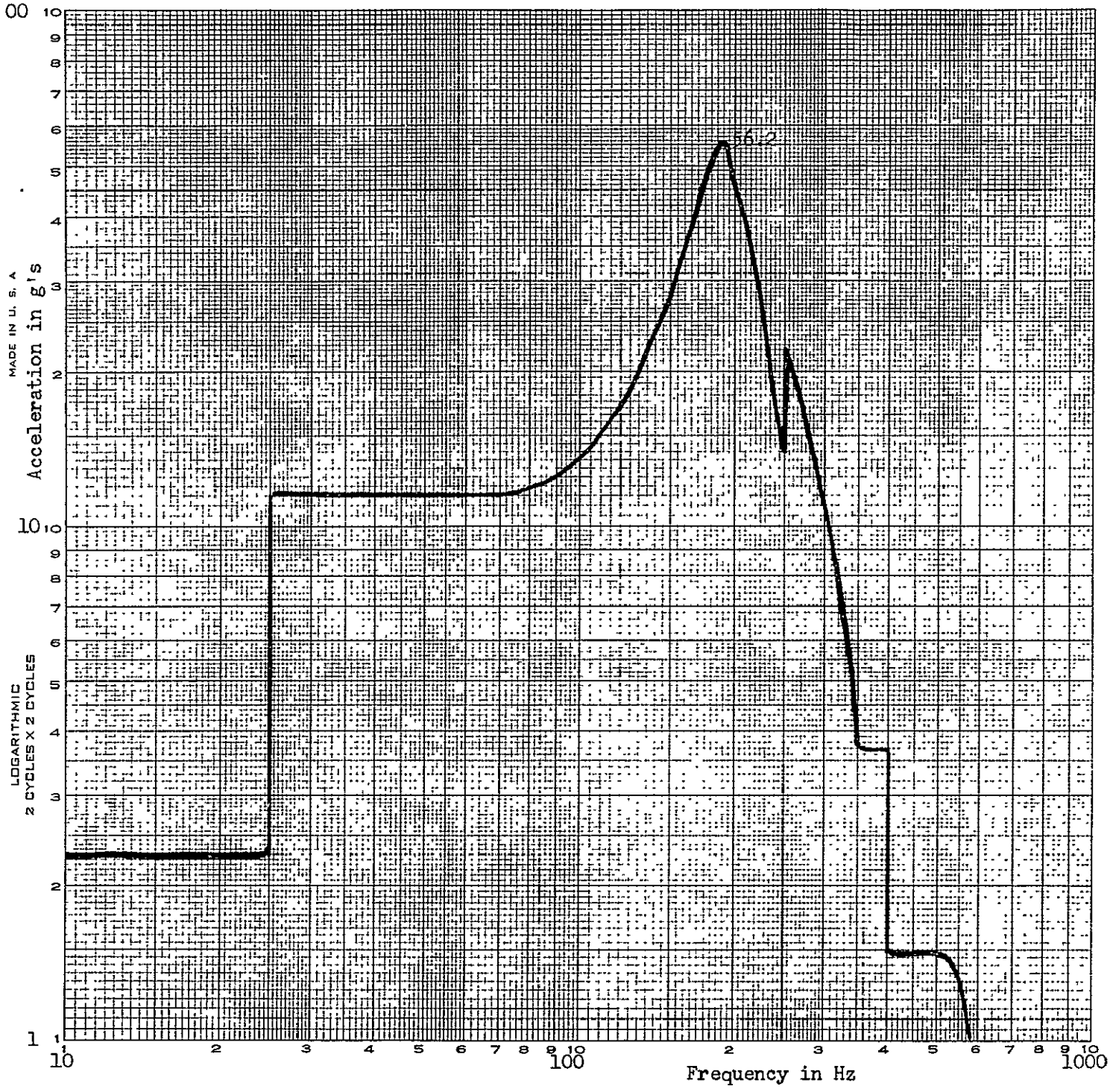

FREQUENCY RESPONSE MASS SIX

FIGURE 3-7

MASS POINT	MAXIMUM ACCELERATION g's	MAXIMUM RELATIVE DISPLACEMENT INCHES
1	65	--
2	67	--
3	22.4	--
4	42.7	--
5	55.3	--
6	56.2	--
1 to 5	--	.0277
1 to 4	--	.024
1 to Input	--	.015

MAXIMUM SYSTEM ACCELERATION AND RELATIVE DISPLACEMENTS

TABLE 3-1

FREQUENCY RANGE (Hz)	INPUT ACCELERATION LEVEL (g's)
10 - 25	2.3
25 - 250	11.5
250 - 400	18.5
400 - 2000	7.5

SYSTEM INPUT VIBRATION LEVELS - DYNAMIC ANALYSIS

TABLE 3-2

3.2.2 Determination of Critical Element Input Loads

This section is concerned with defining the critical elements and determining the corresponding critical input loads to these elements for the system subjected to thrust axis sinusoidal qualification level vibration inputs. The term "load" for this section can refer to an acceleration, or a displacement. The critical elements and the location and nature of each critical input load are identified as follows. A summary of the critical element element input load levels is given in table 3-3.

3.2.2.1 Drive Roller Spring Arms - (refer to fig C-1a and fig P-2)

The deployment friction torque required to deploy the boom is developed by a normal force between the drive roller and the following roller. This normal force, in turn, is provided by the strain of the spring arms which are machined out of the deployer housing side plates. In the static environment these arms are stressed to a maximum stress level of approximately 20,000 psi (see sect 3.3.3). A substantial variation of this stress level due to alternating strains induced by the vibration environment could cause fatigue problems with the 7075-T73 aluminum spring arms. Fracture of one or both of these arms would be catastrophic in that deployment could not be achieved. Consequently, the critical input load to the spring arms will be taken as the maximum acceleration of the base of the spring arms in the direction of the static deflection of the arms. The determination of this input level is discussed in appendix-C.

3.2.2.2 Scissor Mechanism Linkage - (refer to fig D-1 and fig P-3)

The scissor mechanism linkage consists of the elements needed to connect the scissor mechanism assembly to the deployers. There are two identical linkages, one to one deployer and one to the other deployer. Each linkage is defined to consist of the "linkage pivot", the "rotary linkage"

ASSEMBLY (-)	CRITICAL ELEMENT (-)	CRITICAL ACCELERATION (g's)	CRITICAL RELATIVE DEFLECTION (In)	FREQUENCY (Hz)
Deployer				
	drive roller	23.8		204
	tape reel	67.0		208
	deployer pivot bearings	67.0		208
Scissor Mechanism				
	scissor linkage	-	.024	208
Tip Mass Release Mechanism		56.2		189
Miscellaneous				
	outer housing side plate	-	.015	204
	boom isolation assembly	-	.0277	194

CRITICAL INPUT LOAD LEVELS*

TABLE 3-3

*The critical input load levels are the maximum input loads (accelerations or displacements) to the above subassemblies. The subassembly component loads are determined from these inputs.

and the "screw arm" and "turnbuckle" up to the "turnbuckle sleeve". In addition, there are two pivot pins and two polyimide bearings associated with the rotary linkage. Relative motion between the deployer ends ("linkage pivot") and the scissor mechanism ends ("turnbuckle sleeve") of these linkages produces stresses in the linkage elements which could cause fracture of one or both of the linkages resulting in a loss of scissoring capability. The critical input load will be chosen as the maximum relative displacement between the c.g. of the deployer (corresponds to motion of "linkage pivot") and the c.g. of the scissor mechanism (corresponds to motion of "turnbuckle sleeve"). This relative displacement is determined in sect 3.2.1.

3.2.2.3 Tape Reel Assembly - (refer to fig E-1 and fig P-2)

The tape reel assembly stores the flattened boom (tape) and contains the gearing and clutching necessary for normal deployment and retraction. The spool which houses the overrunning clutch and contains the tape is attached to the shaft by a retaining ring and a pinned collar. The shaft, in turn, is attached to the deployer housing side plates by a retaining ring on one side and a set screwed gear on the other side. The axis of vibration is along the axis of the reel shaft. A failure of either of the two retaining rings to carry the axial load, as well as a failure of the reel drive gear set screw to carry the axial load, will undoubtedly result in catastrophic failure in the primary deployment mode. In addition, excessive bearing loads (thrust) could degrade normal deployment operation to the point of preventing complete deployment. Consequently, the critical input load to the tape reel will be the maximum acceleration of the deployer housing in the vacinity of the tape reel bearings. It has been determined that this load level corresponds to the maximum acceleration of the deployer c.g. This acceleration is determined in sect 3.2.1.

3.2.2.4 Deployer Pivot Bearings - (refer to fig F-1a and fig P-1)

The deployer pivot bearings provide the main support for the deployers within the half system housing. Each deployer pivots on two of these bearings during scissoring. An ultimate fracture of the stainless steel washer and/or the polyimide bushing could result in the following: (1) loss of scissoring capability (the failure of the pivot bearing elements would expose the scissor linkage to large relative deflections and possible failure); (2) loss of scissor angle calibration even if scissor capability is retained; (3) loss of pointing accuracy of boom (maintaining the original boom centerline depends on the pivot bearings remaining in tact) and; (4) loss of stable reaction point for boom forces (if a deployer is not fixed to the spacecraft via the half system outer housing, the boom cannot react directly against the spacecraft). The input load which would cause these problems will be the maximum acceleration of the deployer c.g. (deployers are balanced so that the deployer c.g. lies along the deployer scissor pivot axis). This load is determined in section 3.2.1.

3.2.2.5 Outer Housing Side Plates - (refer to fig G-1 and fig P-1)

The half system outer housing side plates must be capable of withstanding the strains resulting from the thrust axis qualification vibration levels without fracturing or yielding in critical areas. A fracture anywhere in the plate is considered critical although yielding is only critical in the area of the deployer pivot bearings (yielding could cause the boom centerline to change from the pre-launch aligned position). It turns out that the highest plate stresses occur at the pivot bearing bores. Therefore, the critical input load will be taken as the maximum deflection of the side plate relative to the remaining housing structure. It will be assumed that the absolute deflection of the remaining housing structure is the same as the input

deflection. Thus, the critical input load is the maximum relative displacement of the deployer c.g. This is determined in section 3.2.1.

3.2.2.6 Boom Isolation Assembly - (refer to fig H-1 and fig P-4)

The "boom isolation assembly" connects the 8 lb tip mass to the free end of the boom. In the launch environment, one end of the assembly moves with the tip mass and the other end (soldered to the boom) moves with the "deployer guide support" ("boom plug" fits snuggly into "deployer guide support"). If the relative deflection between the two ends of the isolation assembly becomes too great, the isolation assembly could break resulting in primary mission failure (the boom without the attached tip mass is of little value). The critical load therefore is the relative deflection between the tip mass c.g. and the deployer c.g. (the deployer guide support and the c.g. are assumed to move together - conservative in that guide support motion will be somewhere between the deployer c.g. motion and tip mass motion). This critical load level is determined in section 3.2.1.

3.2.2.7 Tip Mass Release Mechanism - (refer to fig I-4 and fig P-5)

The tip mass release mechanism secures the tip mass during luanch and then releases the tip mass on command once the system is in space. Details of the construction and operation of the tip mass release mechanism are given in sections 2.1, 2.2.3 and in appendix-I. The elements of the mechanism must be capable of overcoming the acceleration forces acting through the tip mass c.g. The critical input load level will therefore be taken as the maximum acceleration of the tip mass c.g. as determined in section 3.2.1. The resulting dynamic loads on the critical elements of the assembly are determined in appendix I.

3.2.3 Effect of Critical Input Loads

This section is concerned with determining the effect of the critical

element input load levels on the critical components of the above listed critical elements. Each critical component is identified and the nature and location of the component critical mode parameters are discussed. The critical mode parameters are defined as either the maximum component load levels (for load sensitive components such as retaining rings) or the maximum stress levels within a given component (for stress sensitive components). The maximum stress levels are evaluated on the basis of the ultimate strength and/or fatigue life of the material in question. The maximum component loads are evaluated on the basis of the maximum rated load for the item. A summary of the component critical mode parameters, the resulting factors of safety, and references to the appropriate section of this report are given in table 3-4.

3.2.3.1 Drive Roller Spring Arms

The critical components are the spring arms themselves. The critical mode parameters are the maximum and minimum tensil bending stresses at the base of each spring arm. The determination of these stresses and the corresponding effect on the static and fatigue life of the arms is presented in appendix-C.

3.2.3.2 Scissor Mechanism Linkage

The critical components are the turnbuckle and the rotary linkage. The critical mode parameter is the maximum bending stress at the outermost surface of each component. The determination of the stress levels is given in appendix-D.

3.2.3.3 Tape Reel Assembly

The critical components are the two retaining rings, the set screw in the reel drive gear, and the bearings. The critical mode parameters are the maximum rated loads for these parts. For the retaining rings, the failure mode is shearing of the shaft material at the wall of the retaining ring groove.

TABLE 3-4 COMPONENT MODE PARAMETER LEVELS

ASSEMBLY	CRITICAL ELEMENT	CRITICAL COMPONENT	CRITICAL MODE PARAMETERS		FACTOR OF SAFETY*	APPROPRIATE REPORT REFERE
			MAXIMUM LOAD (LB)	MAXIMUM STRESS (PSI)		
Deployer	Drive Roller	Spring Arms	--	29,100	2.75 (1000)	Appendix C
	Tape Reel	Retaining Rings	127	--	2.55	Appendix E
		Bearings	127	--	1.07**	Appendix E
		Set Screw	127	--	2.44	Appendix E
	Deployer Pivot Bearings	Stainless Steel Washer	--	96,700	1.5	Appendix F
		Polyimide Bushing	--	5,800	2.0	Appendix F
Scissor Mechanism	Scissor Linkage	Turnbuckle	--	39,300	1.58 (1000)	Appendix D
Tip Mass Release Mechanism	N/A	Clamping Lever	--	157,000	1.78	Appendix I
		Clamping Lever Pivot Pin	--	45,500	2.78	Appendix I
		Clamping Lever Pivot Boss	--	8,050	3.73	Appendix I
		Support Arm Pivot Pin	--	34,000	3.7	Appendix I
		Cable	51	--	1.38	Appendix I
	End Plate	End Plate Support Posts	--	12,600	4.93	Appendix I
Miscellaneous	N/A	Outer Housing Side Plates	--	21,500	1.95 (4)	Appendix G
		Boom Isolation Assembly		144,000	1.78 (5)	Appendix H

*The values shown in parentheses are the fatigue factors of safety. The other values are the factors of safety based on static failure

**This factor of safety does not refer to bearing failure but to the threshold of smooth bearing operation

For the set screw, the failure mode is defined as an axial movement of the set screw of .01 inch or more. In the case of the bearings the failure mode is loss of smooth operation due to too large an axial load. The calculation of the effects of these critical component loads are shown in appendix-E.

3.2.3.4 Deployer Pivot Bearings

The critical components are the stainless steel washer and the polyimide bushing. The critical mode parameter is the maximum tangential stress at the diameter of the screw clearance hole for the washer and the maximum principle stress created by shearing and compressive stresses for the bushing. The determination and evaluation of these stresses is given in appendix-F.

3.2.3.5 Outer Housing Side Plates

The critical component is the half system housing side plate in the vacinity of the pivot bearing bore. The critical mode parameter (due to maximum deflection of side plate at the deployer pivot bearing) is the tangential stress at the bearing bore I.D. The determination and evaluation of this stress are presented in appendix-G.

3.2.3.6 Boom Isolation Assembly

The critical components of this assembly are the spring wire and the coil spring. The critical mode parameter is the maximum bending stress at each end of the wire and coil. The determination and evaluation of these stresses are discussed in appendix-H.

3.2.3.7 Tip Mass Release Mechanism

The critical components and critical mode parameters of this assembly are: (1) the clamping lever - maximum bending stress in spring arm; (2) cable - maximum tensil load in cable; (3) clamping lever and support arm pins - maximum shearing stresses in pins and pin supports; and (4) end plate support posts -

maximum bending stress at base of support. The determination and evaluation of these critical load parameters is presented in appendix-I.

3.3 System Analysis - (Operational loading)

The critical system elements subject to operational loading (loading, originating in the functional operation of the system, the assembly of the system or thermal expansion* characteristics of the system) which are considered in this report are:

(1) deployer gearing

(2) scissor mechanism gearing

(3) drive roller spring arms

(4) overrunning clutch

(5) drag clutch belleville washers

A detailed breakdown of each of these critical elements into its critical components, critical loading (nature of load and location), and critical mode parameters along with a reference to the pertinent appendix in which all calculations are presented, follows. Table 3-4 gives a summary of all component critical mode parameter levels and the corresponding factors of safety.

3.3.1 Deployer Gearing - (see fig J-1)

The deployer gearing consists of (2) miter gears, (4) spur gears, and two worm pairs. The critical loading is the tangential load at each gear mesh required to produce an operational or stall motor torque (whenever possible a stall condition is assumed). This load is assumed to act at the pitch circle of the gear in question and the entire load is assigned to one gear tooth. The critical mode parameter is the maximum tooth bending stress

*Thermal affects are negligible for all critical elements except the scissor mechanism gearing.

at the root of the tooth. The calculation and evaluation of the maximum tooth bending stress for each deployer gear appears in appendix-J.

3.3.2 Scissor Mechanism Gearing - (see fig K-4)

The scissor mechanism gearing consists of 7 spur gears. The critical loading is the tangential load, carried by 1 tooth per gear, required to produce the maximum operational torque occuring at the gear in question. The critical mode parameter is the maximum bending stress at the root of the tooth. Appendix-K presents the calculation and evaluation of the maximum tooth bending stresses.

3.3.3 Drive Roller Spring Arms - (see fig L-1a)

The drive roller spring arms are loaded by the strain induced (during assembly) in each arm to produce the normal force between the drive roller and the following roller required to deploy the boom. The critical mode parameter is the static maximum bending stress occuring at the base of each spring arm. The determination and evaluation of the spring arm stresses appears in appendix-L.

3.3.4 Overrunning Clutch - (see fig E-1)

The critical component of the overrunning clutch is the clutch coil. The critical mode parameters are (1) tensil and bending stresses in the coil (retract mode with motor stalled); (2) maximum load carrying capability in retract mode; and (3) slipping torque in free wheeling mode. The determination and evaluation of these mode parameters are presented in appendix-M.

3.3.5 Drag Clutch Belleville Washers - (see fig N-1)

The torque produced by the drag clutch is generated by straining the six belleville washers against the delrin friction discs. The critical mode parameter is the maximum tangential stress created at the I.D. of the washer. The calculation and evaluation of the maximum washer stress is presented in appendix-N.

APPENDIX A

DETERMINATION OF VIBRATION PARAMETERS

A.1 SCOPE

This appendix describes how the system parameters required to solve the equations of response (see Section 3.2.1), for the half system subjected to a 1 "g" sinusoidal input from 10 to 2000 Hz, have been determined and what these values are. The parameters of concern are: δ_{ij} (flexibility influence coefficient); M_i (mass of i^{th} masspoint); and γ (structural damping factor).

A.2 FLEXIBILITY INFLUENCE COEFFICIENTS - δ_{ij}

The flexibility influence coefficients were measured on the prototype half system housing. Every structural element which ties together the various system masses was accounted for except for the following: (1) the deployers were not assembled at this time so the connections between the deployers and the scissor mechanism and between each deployer and its corresponding tip mass were not accounted for; and (2) the scissor mechanism was not available so that the total stiffness of the half system side plate to which the scissor mechanism is normally attached was not simulated. Although the deployers were not available, the connection they provide between the two half system side plates at the scissor pivot bearings was accounted for by tying each set of pivot bearings together with a rigid cylindrical bar. The test set up for these measurements is as shown in figures A-1a and A-1b. A known load was applied at a mass point, and the resulting deflections of all of the mass points (including the point of applied force)

were measured. In this way the influence coefficient matrix was formed; where an individual influence coefficient, δ_{ij}, is defined as the deflection at mass point "i" due to a unit load at mass point "j". A known force was not applied at every mass point since $\delta_{ij} = \delta_{ji}$. The force was applied by a hand actuated hydraulic jack, and the force was measured by a calibrated load cell wedged between the jack piston and the half system mass point in question. The half system was mounted to the vibration fixture which, in turn, was supported within the cylindrical frame shown in figure A-1b. The applied loads were reacted between the half system and the cylindrical frame (AWG-10 radar vibration fixture). Deflections were measured by a dial indicator resting on the vibration fixture.

The values of δ_{55} and δ_{66} for the two tip mass release mechanisms were corrected for the fact that they were measured at the tip mass release mechanism end plates rather than at the c.g.'s of the tip masses. The value of δ_{44} for the scissor mechanism was measured on the aluminum side plate, on the opposite side of the housing from where the stainless steel scissor mechanism base-plate would have been mounted, at a point coincident with the scissor mechanism c.g. in the thrust axis direction. This value was consequently corrected to account for the stiffer stainless steel plate. The values of the other influence coefficients containing subscripts 4, 5, & 6 were not greatly affected by the above deviations from the true system configuration and, therefore, they were not altered from their measured values.

The symmetrical influence coefficient matrix is given in table A-1.

A.3 SYSTEM MASSES - M_i

The masses of each of the six mass points were measured and a portion of the weight of the half system housing was assigned to each mass point. The portion of the housing mass assigned to each mass was taken to be 1/3 of the mass of the more flexible portions of the housing support for that mass. This is in line with the practice of allowing 1/3 the mass of a beam, carrying a concentrated mass, to be added to that concentrated mass for the purpose of determining the system fundamental natural frequency. Table A-2 lists the six masses used in the analysis along with the mass point numbers and descriptions.

A.4 STRUCTURAL DAMPING COEFFICIENT -

The structural damping coefficient γ is defined as the inverse of the amplification factor occurring at the natural frequency of a single degree of freedom system, the spring element of which is made of the material in question and constructed in the same manner as the structure in question. For a structure composed mainly of aluminum plates, screwed together as with the ATS-E half system structure, experience has shown that the structural damping factor is no less than $\gamma = .2$. Thus, this value will be used.

TABLE A-1 - INFLUENCE COEFFICIENT MATRIX

$$\begin{bmatrix} 24.0 & -.29 & 2.57 & 5.70 & -2.57 & 2.62 \\ & 24.00 & 2.57 & 6.78 & 2.62 & -2.57 \\ & & 7.42 & 3.32 & -.43 & -.18 \\ & & & 13.00 & -.71 & -1.78 \\ & & & & 35.30 & -8.00 \\ & & & & & 35.30 \end{bmatrix} \times 10^{-6} \text{ IN/LB}$$

TABLE A-2 - SYSTEM MASSES

Mass Point	Mass Point Number	Mass (lbs.) Force
Slave Deployer	1	9.0
Master Deployer	2	9.0
Control Circuit Electronics	3	3.0
Scissor Mechanism	4	5.0
Master Tip Mass Release Mechanism	5	10.0
Slave Tip Mass Release Mechanism	6	10.0

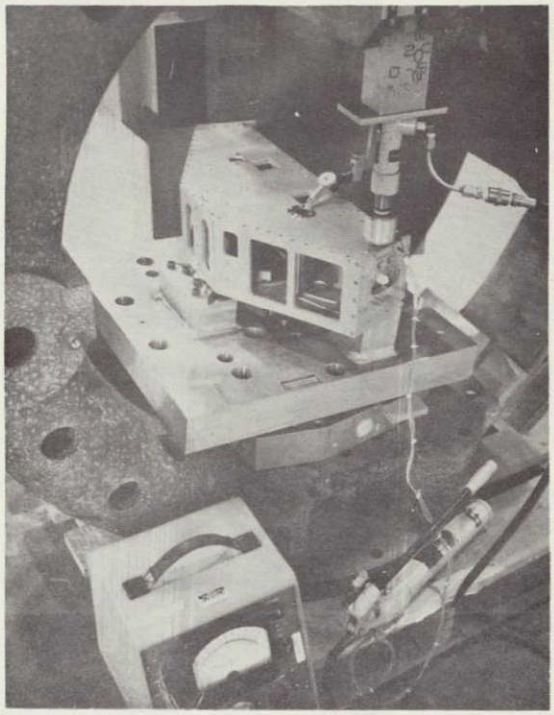

Figure A-1a

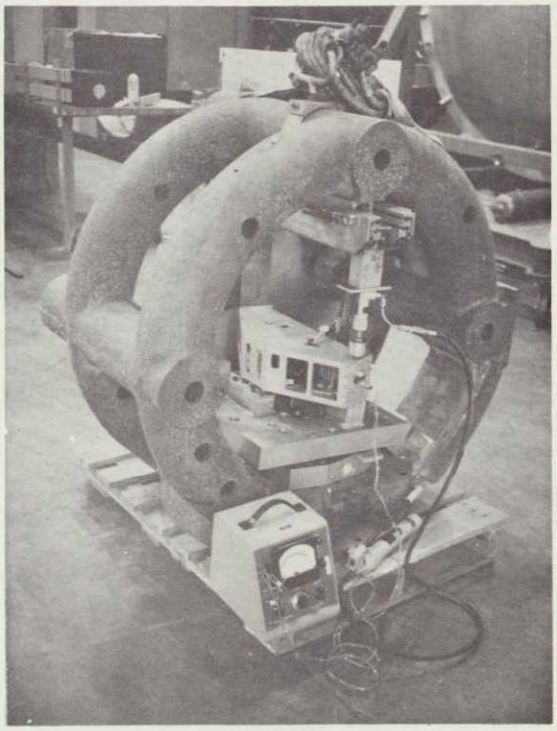

Figure A-1b

APPENDIX-B

Computer Programs - Vibration Analysis

The two computer programs required to solve for the dynamic response of the ATS-E boom system to thrust axis sinusoidal vibration are presented in this appendix. Program number I solves for the normal mode frequencies (Wa's) and the normal mode shapes (Xia's). Program number II uses these values as inputs and subsequently computes the peak acceleration response in g's of each system mass for various system driving frequencies (25 to 2000 Hz in 25 Hz increments) and for an input acceleration level of 1 g. The results of program II multiplied by the ATS-E input specification vibration levels gives the actual system responses (see figures 3-2 thru 3-7). Both programs were written in FORTRAN for use in analyzing the dynamic response of the EME package supplied by Westinghouse to NASA (GSFC) for ATS-E.

```
0$SAV
1$NDM
10  DIMENSIØN SM(20),C(20,20),E(20),V(20,20)
15 DIMENSIØN ANAME(20)
20  CALL ØPENF(1,"RMRØØT")
30  READ(1,)N
32  READ(1,130)AXIS
33 130 FØRMAT(A6)
35 DØ 15 I=1,N
36 15 READ(1,130)ANAME(I,
40 READ(1,)(SM(I),I=1,N)
50 DØ 20 I=1,N
60  20  SM(I)= (SM(I)/386.)**.5
70 DØ 30 I=1,N
80  30 READ(1,)(C(I,J),J=I,N)
90  DØ 32 I=1,N
100 DØ 32 J=I,N
105 C(I,J)=100.*C(I,J)
110  32 C(J,I)=C(I,J)
120  DØ 35 I=1,N
130  DØ 35 J=1,N
140  35  C(I,J)=C(I,J)*SM(I)*SM(J)
150 CALL JACØBI(N,C,1,NR,V)
160  DØ 37  I=1,N
170  DØ 37 J=1,N
180  37  V(I,J)=V(I,J)/SM(I)
190 WRITE(3;100)NR
200  100 FØRMAT(//12H ITERATIØNS= ,I5 //)
207 105 FØRMAT(A6,6H  AXIS )
210 DØ 40 J=1,N
220  S=V(1,J)
230 DØ 60 I=2,N
240  IF (ABS(V(I,J))-ABS(S)) 60,50,50
250 50 S=V(I,J)
260 60 CØNTINUE
270 DØ 70 I=1,N
280 70 V(I,J)=V(I,J)/S
285 IF( C(J,J) ) 38,40,40
286 38 C(J,J)=1.E-6
290 40 E(J)=10000./((C(J,J)**.5)*6.28319)
295 WRITE(3;105)AXIS
300 DØ 80 I=1,N
310 WRITE(3;110)I,E(I)
320  DØ 80 J=1,N
330 80 WRITE(3;120) V(J,I),ANAME(J)
340  110  FØRMAT(/ 18HNATURAL FREQUENCY  ,I2 ,1H=  , F8.2 , 4HCPS
350&   /11HMØDE SHAPE    )
360 120 FØRMAT(F10.5,2X,A6)
361  WRITE(2)N
362  DØ 90 I=1,N
363  SM(I)=SM(I)**2
```

```
364 WRITE(2) ANAME(I),SM(I),E(I)
366  90 WRITE(2) (V(I,J),J=1,N)
367  CALL CLØSEF(2,"DYDAT")
368 CALL CLØSEF(3,"DYNRES")
370 STØP
380 END
1080       SUBRØUTINE JACØBI(N,Q,JVEC,M,V)
1090       DIMENSIØN Q(20,20),V(20,20),X(20),IH(20)
1092 ABSF(X)=ABS(X)
1094 SQRTF(X)=SQRT(X)
1100       IF(JVEC) 1103,1110,1103
1110  1103 DØ 1109 I=1,N
1120       DØ 1109 J=1,N
1130       IF(I-J) 1108,1106,1108
1140  1106 V(I,J)=1.0
1150       GØ TØ 1109
1160  1108 V(I,J)=0.
1170  1109 CØNTINUE
1180  1110 M=0
1190  1111 MI=N-1
1200       DØ 1119 I=1,MI
1210       X(I)=0.
1220       MJ=I+1
1230       DØ 1119 J=MJ,N
1240  IF(X(I)-ABS(Q(I,J))) 1117,1117,1119
1250 1117 X(I)=ABS(Q(I,J))
1260       IH(I)=J
1270  1119 CØNTINUE
1280  1120 DØ 1126 I=1,MI
1290       IF(I-1) 1123,1123,1122
1300  1122 IF( XMAX-X(I) )1123,1126,1126
1310  1123 XMAX=X(I)
1320       IP=I
1330       JP=IH(I)
1340  1126 CØNTINUE
1350 EPSI=1.E-6
1360       IF( XMAX-EPSI) 1212,1212,1129
1370  1129 M=M+1
1380       IF( Q(IP,IP)-Q(JP,JP)) 1131,1135,1135
1390  1131 TANG=-2.*Q(IP,JP)/(ABSF(Q(IP,IP)-Q(JP,JP))
1400&  +SQRTF((Q(IP,IP)-Q(JP,JP))**2+4.*Q(IP,JP)**2))
1410       GØ TØ 1138
1420  1135 TANG= +2. * Q(IP,JP) / (ABSF( Q(IP,IP)-Q(JP,JP))
1430& +SQRTF((Q(IP,IP)-Q(JP,JP))**2+4.*Q(IP,JP)**2))
1440  1138 CØSN=(1.0+TANG**2)**(-.5)
1450       SINE=TANG*CØSN
1460       QII=Q(IP,IP)
1470  Q(IP,IP)=CØSN**2*(QII+TANG*(2.*Q(IP,JP)+TANG*Q(JP,JP)))
1480  Q(JP,JP)=CØSN**2*(Q(JP,JP)-TANG*(2.*Q(IP,JP)-TANG*QII))
1490       Q(IP,JP)=0.
1500       IF( Q(IP,IP)-Q(JP,JP) ) 1147,1156,1156
1510  1147 TEMP=Q(IP,IP)
1520       Q(IP,IP)=Q(JP,JP)
1530       Q(JP,JP)=TEMP
1540       IF(SINE) 1151,1153,1153
1550  1151  TEMP=CØSN
1560       GØ TØ 1154
1570  1153 TEMP=- CØSN
1580  1154 CØSN= ABSF(SINE)
1590       SINE=TEMP
1600  1156 DØ 1172 I=1,MI
```

```
      IF( I-IP) 1159,1172,1158
1158  IF(I-JP)  1159,1172,1159
1159  IF(IH(I)-IP) 1160,1161,1160
1160  IF(IH(I)-JP) 1172,1161,1172
1161  K=IH(I)
1162  TEMP= Q(I,K)
      Q(I,K)=0.
      MJ=I+1
      X(I)=0.
      DØ 1170 J=MJ,N
      IF( X(I)-ABSF( Q(I,J) ) )  1168,1168,1170
1168  X(I)=ABSF( Q(I,J) )
      IH(I)=J
1170  CØNTINUE
      Q(I,K)=TEMP
1172  CØNTINUE
      X(IP)=0.
      X(JP)=0.
      DØ 1205 I=1,N
      IF(I-IP) 1178,1205,1188
1178  TEMP=Q(I,IP)
      Q(I,IP)= CØSN*TEMP+SINE*Q(I,JP)
      IF( X(I)-ABSF( Q(I,IP))) 1181,1183,1183
1181  X(I)=ABSF(Q(I,IP))
      IH(I)=IP
1183  Q(I,JP)=-SINE*TEMP+CØSN*Q(I,JP)
      IF(X(I)-ABSF(Q(I,JP)))  1185,1205,1205
1185  X(I)=ABSF(Q(I,JP))
      IH(I)=JP
      GØ TØ 1205
1188  IF(I-JP) 1189,1205,1196
1189  TEMP=Q(IP,I)
      Q(IP,I)= CØSN*TEMP+SINE*Q(I,JP)
      IF(X(IP)-ABSF(Q(IP,I)))1192,1194,1194
1192  X(IP)=ABSF(Q(IP,I))
IH(IP)=I
1194  Q(I,JP)=-SINE*TEMP+CØSN*Q(I,JP)
      IF( X(I)-ABSF(Q(I,JP))) 1185,1205,1205
1196  TEMP=Q(IP,I)
      Q(IP,I)=CØSN*TEMP+SINE*Q(JP,I)
      IF( X(IP)-ABSF(Q(IP,I))) 1199,1201,1201
1199  X(IP)=ABSF( Q(IP,I) )
      IH(IP)=I
1201  Q(JP,I)=-SINE*TEMP+CØSN*Q(JP,I)
      IF( X(JP)-ABSF( Q(JP,I) ) ) 1203,1205,1205
1203  X(JP)=ABSF( Q(JP,I) )
      IH(JP)=I
1205  CØNTINUE
      IF( JVEC ) 1207,1120,1207
1207  DØ 1210 I=1,N
      TEMP=V(I,IP)
      V(I,IP)=CØSN*TEMP+SINE*V(I,JP)
1210  V(I,JP)=-SINE*TEMP+CØSN*V(I,JP)
      GØ TØ 1120
1212  RETURN
      END
```

```
100$SAV
110$NDM
120C RESPØN/RMR00T 8/29/69
130 DIMENSIØN Z(16,42)
140 DIMENSIØN ANAME(20)
150 DIMENSIØN SM(20),Y(20)
160 CØMMØN N,U(20),F(20,20),P(20),R(20),A1(20,21)
170 INTEGER FIRST
180 INTEGER TEMP1,TEMP2
190 CALL ØPENF(1,"DYDAT")
200 READ(1)N
210  DØ 10 I=1,N
220 READ(1) ANAME(I),SM(I),U(I)
230  10  READ(1)(F(I,J),J=1,N)
240  DØ 20 I=1,N
250  P(I)=0.
260  R(I)=0.
270  DØ 20 J=1,N
280  S=SM(J)*F(J,I)
290  P(I)=P(I)+S
300  20  R(I)=R(I)+S*F(J,I)
310 DØ 25 J=1,42
320  FREQ=50*J
330 CALL RSPN(FREQ,Y)
340 DØ 25 I=1,N
350  Z(I,J)=Y(I)
360 25 CØNTINUE
370 1000 FØRMAT(A6)
380 1010 FØRMAT( 70H      0....1....2....3....4....5....6....7....8....9
390&..10...11...12...          )
400 1020 FØRMAT(I5,V,1H*)
410  1030 FØRMAT(///)
420 WRITE(3,1030)
430 DØ 510 I=1,N
440 ND1=0
450 FIRST=0
460 NT1=11
470 NT2=11
480 TEMP1=0.
490 TEMP2=0.
500 WRITE(3,1000) ANAME(I)
510 WRITE(3,1010)
520 DØ 500 J=1,42
530 JM2=J-2
540  NFREQ=50*J
550 NY= 5.*Z(I,J)+6.5
560 IF(ND1) 100,110,100
570 110 FIRST=0
580 100 CØNTINUE
590 IF(NT1-NY) 150,150,160
600 160 IF(NT1-NT2) 150,150,140
610 140 ND1=1
620 GØ TØ 170
630 150 ND1=0
640 170 IF(ND1) 120,470,120
650 120 FIRST=1
660 WRITE(3,1020) TEMP2,NT2
670 FRQ=TEMP2
680 WRITE(4) FRQ,Z(I,JM2)
690 CALL MAX(TEMP2,FREQ,YMAX,I,MNY)
700 WRITE(3,1040) FREQ,YMAX,MNY
```

```
710 WRITE(4) FREQ,YMAX
720 470 IF(FIRST) 130,130,475
730 130 CØNTINUE
740 IF(J-1) 460,475,460
750 460 WRITE(3;1020)TEMP2,NT2
760 FRQ=TEMP2
770 WRITE(4) FREQ,Z(I,JM2)
780 475 CØNTINUE
790 NT2=NT1
800 NT1=NY
810 TEMP2=TEMP1
820 TEMP1=NFREQ
830 500 CØNTINUE
840 WRITE(3;1010)
850 510 WRITE(3;1030)
860 1040 FØRMAT(F6.0,F6.2,V,1H*)
870 CALL CLØSEF(3,"FREQRS")
880 CALL CLØSEF(4,"SPECIN")
890 STØP
900 END
910 SUBRØUTINE RSPN(FREQ,Y)
920 DIMENSIØN Q(20),V(21),Y(20)
930 CØMMØN N,U(20),F(20,20),P(20),R(20),A1(20,21)
940 G=.15
950  DØ 100 I=1,N
960 T=FREQ*FREQ/(U(I)*U(I))
970  TM1=1.-T
980  Q(I)=P(I)*T/(R(I)*((TM1*TM1+G*G)**.5))
990 A=G/TM1
1000 V(I)=ATAN(A)
1010 IF(A) 25,30,30
1020 25 V(I)=V(I)+3.14159
1030 30 DØ 35 I1=1,N
1040 35 A1(I1,I)=F(I1,I)*Q(I)
1050  NP1=N+1
1060  100  A1(I,NP1)=1.
1070 V(NP1)=0.
1080 DØ 200 I=1,N
1090 Y(I)=0.
1100 DØ 150 J1=1,NP1
1110 DØ 150 K=1,NP1
1120  150 Y(I)=Y(I)+A1(I,K)*A1(I,J1)*CØS(V(J1)-V(K))
1130 200 Y(I)= SQRT(Y(I))
1140 RETURN
1150 END
1160 SUBRØUTINE MAX(TEMP2,FREQ,YMAX,I,NY)
1170 DIMENSIØN Q(20),V(21),Y(20)
1180 CØMMØN N,U(20),F(20,20),P(20),R(20),A1(20,21)
1190 INTEGER TEMP2
1200 FREQ=TEMP2
1210 I9=I
1220 DF=10.
1230 LT=0
1240 TEMP=0.
1250 NP1=N+1
1260 G=.15
1270 1020 CØNTINUE
1280 DØ 100 I=1,N
1290 T=FREQ*FREQ/(U(I)*U(I))
1300  TM1=1.-T
1310  Q(I)=P(I)*T/(R(I)*((TM1*TM1+G*G)**.5))
1320 A=G/TM1
```

```
1330 V(I)=ATAN(A)
1340 IF(A) 25,30,30
1350 25 V(I)=V(I)+3.14159
1360 30 DØ 35 I1=1,N
1370 35 A1(I1,I)=F(I1,I)*Q(I)
1380 100 A1(I,NP1)=1.
1390 I=I9
1400 V(NP1)=0.
1410 Y(I)=0.
1420 DØ 150 J1=1,NP1
1430 DØ 150 K=1,NP1
1440  150 Y(I)=Y(I)+A1(I,K)*A1(I,J1)*CØS(V(J1)-V(K))
1450 200 Y(I)= SQRT(Y(I))
1460 IF(Y(I)-TEMP) 110,110,105
1470 105 TEMP=Y(I)
1480  FREQ=FREQ+DF
1490 GØ TØ 1020
1500 110 IF(LT-3)120,2290,120
1510 120 TP=TEMP
1520 TEMP=0.
1530 FREQ=FREQ-2.*DF
1540 LT=LT+1
1550 IF(LT-1) 140,130,140
1560 130 DF=5.
1570 GØ TØ 1020
1580 140 IF(LT-2) 2290,160,2290
1590 160 DF=1.
1600 GØ TØ 1020
1610 2290 YMAX=TP
1620  FREQ=FREQ+1.
1630 NY=5.*YMAX+6.5
1640 IF(NY-70) 170,170,180
1650 180 NY=70
1660 170 RETURN
1670 END
1630 NY=5.*YMAX+6.5
1260 G=.15
940 G=.1S
SAVE:RMRØØT
```

APPENDIX C

DETERMINATION OF THE STRUCTURAL INTEGRITY OF THE DEPLOYER DRIVE ROLLER SPRING ARMS - VIBRATION LOADING

C.1 SCOPE OF ANALYSIS - (See Figure C-1a)

This analysis will determine the structural integrity of the drive roller spring arms in the vibration environment. Although the vibration inputs are in the thrust (Z) axis, the pertinent motion of the spring arms is in the direction of the static deflection of the arms which is perpendicular to the thrust axis. Consequently, a coupling factor between the deployer motion in the thrust axis and the spring arm deflection motion will be employed. The analysis will initially concern itself with two conditions; i.e., (1) vibration at the natural frequency of the drive roller - spring arm system, and (2) at the fundamental natural frequency of the deployer c.g. In each case, the resulting dynamic deflection amplitude will be determined. The resulting dynamic stress levels will be determined for the greatest levels. A fatigue analysis will then follow to determine if the dynamic loading is a problem.

C.2 DEFLECTION ANALYSIS AT DRIVE ROLLER - SPRING ARM NATURAL FREQUENCY

C.2.1 DETERMINATION OF NATURAL FREQUENCY - (See Figure C-1b)

The natural frequency of the drive roller - spring arm system is given by:

$$f_n = \frac{1}{2\pi}\sqrt{\frac{K_1 + K_2}{M + \bar{M}/3}}$$ where $\bar{M}$ = mass of spring arms

The values of K_1 and K_2 will now be determined.

K_1: Both spring arms can be represented as shown in Fig. C-1c.

The deflection at point "A" due to load "F" is given by:

$$\delta = \frac{F}{EI}\left[\frac{\ell^3}{3} + \ell^2\ell' + \ell\ell'^2\right]$$

now $K_1 = K_a + K_b$, K_a = spring constant of arm on motor side plate

K_b = spring constant of arm on gear side plate

$$K_a = \frac{EI_a}{\frac{\ell a^3}{3} + \ell a^2 \ell' a + \ell a \ell' a^2}$$ where: $\ell a = .92$, $E = 10.6 \times 10^6$ psi

$\ell' a = .39$

and $I_a = \frac{(bh^3)a}{12}$ where: $b = .125$ for "a" & "b"

$h = .154$ for "a" & $.189$ for "b"

$I_a = .381 \times 10^{-4}$ IN^4

$\therefore K_a = 553$ lb/in

now $K_b = \frac{E\,Ib}{\frac{b^3}{3} + b^2\,b^1 + b\,b^2}$ where: $I_b = \frac{(bh^3)b}{12} = .7 \times 10^{-4}$ IN^4

$b = 1.075$

$b = .37$

$\therefore K_b = 725$ lb/in

$K_1 = K_a + K_b = 553 + 725$

$\boxed{K_1 = 1278 \text{ lb/in}}$

K_2 was measured and found to be:

$\boxed{K_2 = 2500 \text{ lb/in}}$

Thus, the fundamental natural frequency of the drive roller - spring arm system is given by:

$$f_n = \frac{1}{2\pi}\sqrt{\frac{K_1 + K_2}{M + \bar{M}/3}}$$

where:

$K_1 + K_2 = 3778$ lb/in

$M = 70$ gms

$\bar{M} = 9$ gms

$\therefore$ $\boxed{f_n = 480 \text{ Hz}}$

C.2.2 DETERMINATION OF DYNAMIC DEFLECTION

At this frequency, the input to the deployer c.g. is 3.8 g's (i.e., the input to the half system package is 7.5 g's and the amplification factor between the package mounting surface and the deployer c.g. is 1/2:1 - see fig. 3-2). It will be assumed that the coupling between the input axis and the axis of the spring arm deflection is 1 to 1 (very conservative). Thus, assuming that the amplification factor between the drive roller c.g. and the built-in end of the spring arms is 10:1 (very conservative considering that one of the springs is polyurethane), the maximum acceleration of the drive roller will be 38 g's. The deflection resulting from this acceleration will now be determined:

$$\delta = \frac{a \times 386}{\omega^2}$$

where: a = acceleration in g's = 38

$\omega = 2\pi f$, f = frequency of exertation = 480 Hz

δ = single amplitude deflection of c.g. of drive roller

$$\delta = \frac{38 \times 386}{(2\pi \times 480)^2} = .0016 \text{ IN}$$

C.3 DETERMINATION OF DYNAMIC DEFLECTION AT THE DEPLOYER c.g. FUNDAMENTAL NATURAL FREQUENCY

The anticipated deflection of the drive roller due to vibration at the fundamental natural frequency of the deployer c.g. will now be determined.

From the dynamic analysis, the deployer c.g. response @ its fundamental natural frequency (204 Hz) is 65 g's. Assuming that the coupling between the axis of the spring arm deflection and the thrust axis is 1/3 to 1 (conservative based on vibration of mock-up), we can expect a motion of the deployer c.g. in the axis of the spring deflection of 21.7 g's. The amplification factor at this frequency will be 1.1 assuming that the spring arm - drive roller system is a simple single degree of freedom spring mass system. Thus, the acceleration of the drive roller will be 23.8 g's @ 204 Hz. This results in a deflection given by:

$$\delta = \frac{a \times 386}{\omega^2} \qquad a = 23.8 \qquad \omega = 2\pi f = 2\pi(204)$$

$$\delta = .0057 \text{ in}$$

Since the stress in the spring arms is a function of deflection rather than load, the worst loading occurs at the deployer fundamental natural frequency (204 Hz). An analysis will now be made to see if any fatigue problems will result from this loading.

C.4 FATIGUE ANALYSIS

The stress incrment resulting from this deflection is given by: (see fig. 1c).

$$\Delta\sigma = \frac{MC}{I} = \frac{P(\ +\ ^{1})C}{I} = \frac{K\quad(\quad +\ ^{1})C}{I}$$

$\Delta\sigma_a$ = bending stress increment in motor side plate spring arm

$\Delta\sigma_b$ = bending stress increment in gear side plate spring arm

$$\Delta\sigma_a = \frac{K_a\,\delta\,(\ell_a + \ell'_a)C_a\,K'}{I_a}$$

where:

$C_a = h_a/2 = .077$ in

$I_a \approx .381 \times 10^{-4}$ in^4

$\ell_a = .92$ in

$\boxed{\Delta\sigma_a = 9800 \text{ psi}}$

$\ell'_a = .39$ in

$K'_a = 553$ lb/in

$\delta = .0057$

K^1 = stress concentration factor = 1.17

in like manner $\boxed{\Delta\sigma_b = 9750 \text{ psi}}$

Thus, a maximum alternating bending stress of 9800 psi must be superimposed upon the static bending stress due to the pre-loading of the spring arms of 19,300 psi (see Appendix L). Thus, the total maximum stress becomes:

$\boxed{\sigma_T = 29{,}100 \text{ psi}}$

Since the ultimate stress of 7075-T73 aluminum (material from which spring arms are made) is $\approx$ 75,000 psi, and the yield is 60,000 psi, there is no danger of low cycle fatigue failure; i.e., if a failure occurs it will require more than a few vibration cycles to produce it.

An investigation of the anticipated fatigue life follows:

The mean spring arm bending stress is 19,300 psi and the fluctuating stress is 9,800 psi. The fatigue strength diagram* for 7075-T6 (assumed to

* "Stress, Strain, and Strength," Robert C. Juvinall, McGraw Hill, pg. 273

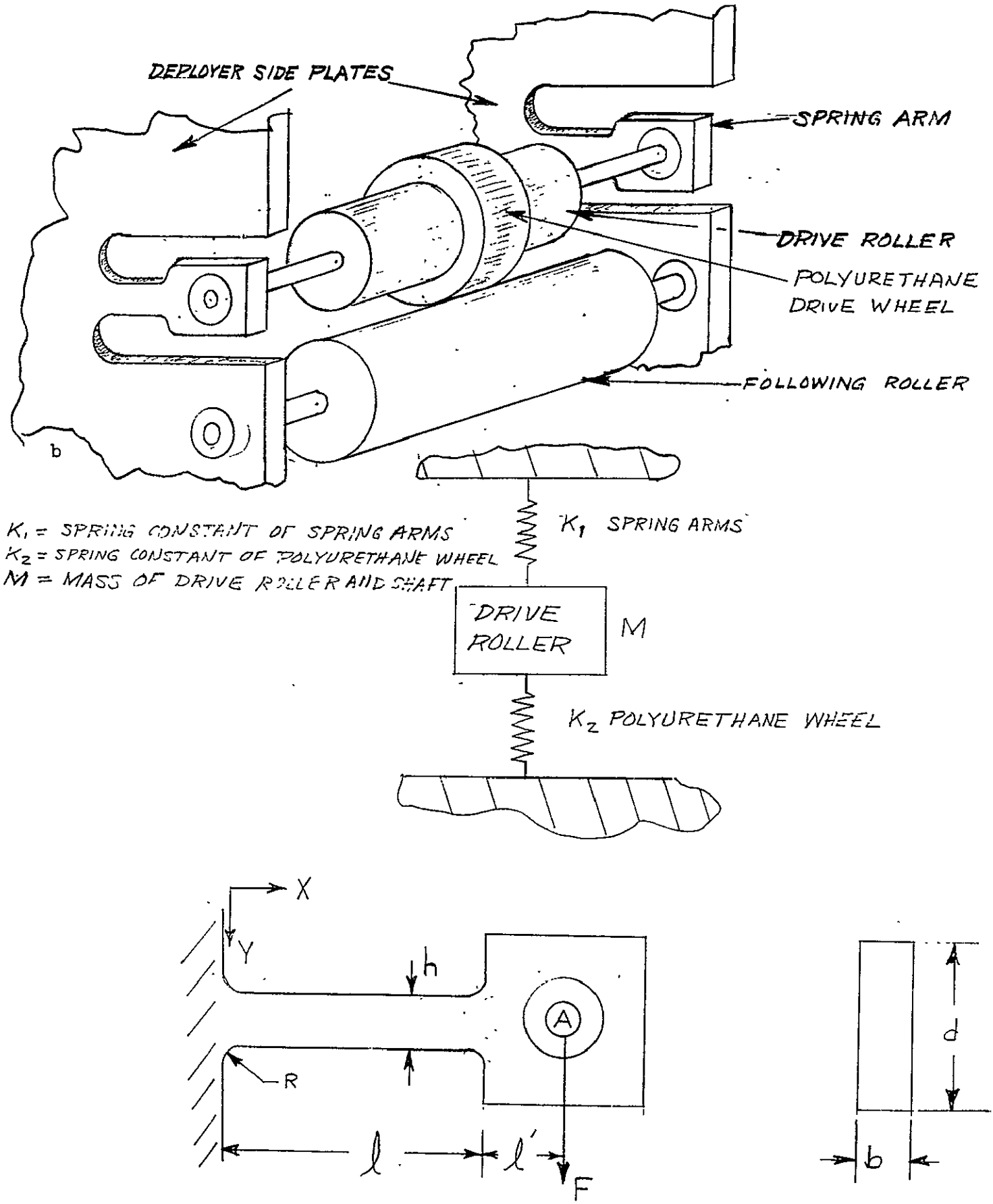

DRIVE ROLLER
SPRING ARMS

FIG C-1

apply to 7075-T73) aluminum indicates that for the above mean and fluctuating stresses, the fatigue life of the spring arms will be in excess of 10^9 cycles. The fact that the arm is in bending and not tension makes the 10^9 cycle life conservative.

During the entire qualification test, the total number of cycles is less than 10^6 cycles, most of which occur at lower stress levels than determined above. $\circ^{\circ}_{\circ}$ The combination of the static stress (19,300 psi) plus the fluctuation stress due to vibration (9,800 psi) will not cause a fatigue failure.

APPENDIX D

Stress Analysis of the Scissor Mechanism Linkage - Vibration Loading

D.1 Scope of Analysis

This analysis will concern itself with estimating the maximum stresses present in the linkage elements which connect the output of the scissor mechanism to two deployers. Since the two sets of linkage elements are nearly identical the analysis will be concerned with only one of the two linkage assemblies (see fig D-1). The full relative deflection between the c.g. of the deployer and the c.g. of the scissor mechanism (as determined in sect 3.2.1) is assumed to exist between the deployer pivot and the turnbuckle bearing. The resulting maximum bending stress in the turnbuckle is then determined. It has been determined that the maximum bending stress occurs at the turnbuckle and therefore no other points are considered in the analysis. The assumptions made in the course of the analysis are all conservative in nature.

D.2 Derivation of the Equation of Maximum Bending Stress

The motion of the scissor mechanism (see fig D-1) relative to the deployer during vibration causes stresses to be set up in the rotating link and the scissor arm-turnbuckle assembly (hereafter referred to as scissor mechanism linkage). This system can be mechanically represented as shown in fig D-2a. It will be assumed that the deployer moves relative to the scissor mechanism such that the members at each clamped end retain a zero slope. Thus the deflected case can be seen as shown in fig D-2b. Each section of the beam can be treated individually as shown in fig D-2c. Thus for beam segment 1 we have

$$M = M_1 - F_1 X$$

$$E_1 I_1 \frac{d^2 y}{dx^2} = M = M_1 - F_1 X$$

$$E_1 I_1 \frac{dy}{dx} = M_1 X - F_1 \frac{X^2}{2} + C_1$$

$$\frac{dy}{dx} = 0 \text{ at } X = 0 \quad C_1 = 0$$

$$E_1 I_1 Y = M_1 \frac{X^2}{2} - F_1 \frac{X^3}{6} + C_3$$

$$Y = 0 \text{ at } X = 0 \quad C_3 = 0$$

where:

E_1 = modulus of elasticity of beam segment 1

I_2 = moment of inertia of beam segment 1

Y_1 = deflection of beam segment 1 at $X = L_1$

and at $X = L_1$ we have

$$Y_1 = \frac{1}{E_1 I_1} M_1 \frac{L_1^2}{2} - \frac{1}{E_1 I_1} \frac{F_1 L_1^3}{6}, \text{ let } \frac{1}{E_1 I_1} = R_1$$

$$(1) \quad \boxed{Y_1 = \frac{R_1 L_1^2}{2} \left(M_1 - \frac{F_1 L_1}{3} \right)}$$

For beam segment 2 we have

$$M = M_2 - F_2 X$$

$$E_2 I_2 \frac{d^2 y}{dx^2} = M = M_2 - F_2 X$$

$$E_2 I_2 \frac{dy}{dx} = M_2 X - F_2 \frac{X^2}{2} + C_2$$

$$\frac{dy}{dx} = 0 \text{ at } X = 0; \; C_2 = 0$$

where:

E_2 = modulus of elasticity of beam segment 2

I_2 = moment of inertia of beam segment 2

Y_2 = deflection of beam segment 2 at $X = L_2$

$$E_2 I_2 Y = M_2 \frac{X^2}{2} - F_1 \frac{X^3}{6} + C_3$$

$$Y = 0 \quad \text{at } X = 0 \quad C_3 = 0$$

and at $X = L_2$ we have

$$Y_2 = \frac{M_2}{E_2 I_2} \frac{L_2^2}{2} - \frac{F_2 L_2^3}{6 E_2 I_2} \quad , \quad \text{let } R_2 = \frac{}{E_2 I_2}$$

$$(2) \quad \boxed{Y_2 = \frac{R_2 L_2^2}{2} \left(M_2 - \frac{F_2 L_2}{3} \right)}$$

also, we know that : (3) $\boxed{Y_1 + Y_2 = \delta}$ where δ is assumed to be known.
In addition to the above equations, we can write

$$\left(\frac{dy}{dx} \right)_{X = L_1} = Y_1' = \frac{1}{E_1 I_1} \left(M_1 L_1 - \frac{F_1 L_1^2}{2} \right)$$

$$\text{or} \quad (4) \quad \boxed{Y_1' = R_1 L_1 \left(M_1 - \frac{F_1 L_1}{2} \right)}$$

and, $\left(\frac{dy}{dx} \right)_{X = L_2}$ can likewise be written as:

$$(5) \quad \boxed{Y_2' = R_2 L_2 \left(M_2 - \frac{F_2 L_2}{2} \right)}$$

now at $X = L_1$ for segment 1 and $X = L_2$ for segment 2 we know that

$$\left(\frac{dy}{dx} \right)_{X = L_1} = \left(\frac{dy}{dx} \right)_{X = L_2}$$

$$\text{or} \quad (6) \quad \boxed{Y_1^1 = Y_2^1}$$

Finally, summing moments @ X = L_1 and summing forces in the "Y" direction we get:

(7) $\boxed{M_1 + M_2 = F_2 L}$

and (8) $\boxed{F_1 = F_2}$

Thus, there are 8 equations with 8 unknowns; i.e. M_1, M_2, F_1, F_2, Y_1, Y_2, Y_1', Y_2'. The solutions for M_1 and M_2 are given as follows:

$$M_2 = \frac{6L\left(2R_1LL_1 - R_1L_1^2 + R_2L_2^2\right)\delta}{R_1^2L_1^4L + 2R_1R_2L_1L_2L\,(3L_1L - 3L_1L_2 - 2L_1^2 - 2L_2^2 + 3L_2L) + R_2^2L_2^4L}$$

and $$M_1 = \left(\frac{2R_2LL_2 - R_2L_2^2 + R_1L_1^2}{2R_1LL_1 - R_1L_1^2 + R_2L_2^2}\right) M_2$$

where $R_1 = \frac{1}{E_1I_1}$, $R_2 = \frac{1}{E_2I_2}$

δ = relative deflection between constraints = .024 in (see table)

E_1 = modulus of elasticity of rotating link = 10.6×10^6 psi

E_2 = modulus of elasticity of turnbuckle

I_1 = moment of inertia of rotating link

I_2 = moment of inertia of turnbuckle scissor arm

D.3 Determination of the Maximum Bending Stress

It has been determined (not presented herein) that the maximum bending stress occurs in the turnbuckle at the turnbuckle bearing for M = M_2 (M_1 is greater than M_2 but the resulting stress at M_1 is less than at M_2). The analysis of the stress in the turnbuckle proceeds as follows:

$$I_1 = \frac{1}{12} (.375)(.44)^3 = 2.66 \times 10^{-3} \text{ in}^4$$

$$E_1 = 10^7 \text{ psi (aluminum)}$$

$$\overset{\circ}{\circ}\overset{\circ}{\circ} R_1 = 3.55 \times 10^{-5} \text{ in}^{-2} \text{ lb}^{-1}$$

The turnbuckle scissor arm assembly (see fig D-1) consists of two pieces each of a different material. For the purposes of this analysis it will be assumed that:

$$E_2 I_2 = E_a I_a + E_b I_b$$

but, $I_a = \frac{\pi}{4} (d_o^4 - d_i^4)$

$$= \frac{\pi}{4} \left[(.375)^4 - (.25)^4 \right]$$

$$I_a = .78 \times 10^{-3} \text{ in}^4$$

$$I_b = \frac{\pi}{4} (d_1^4) = \frac{\pi}{4} (.25)^4$$

$$I_b = .19 \times 10^{-3} \text{ in}^4$$

$$E_2 I_2 = 19 \times 10^6 \times .19 \times 10^{-3} + 10 \times 10^6 \times .78 \times 10^{-3}$$

$$E_2 I_2 = .144 \times 10^5$$

$$\overset{\circ}{\circ}\overset{\circ}{\circ} R_2 = 8.75 \times 10^{-5} \text{ in}^{-2} \text{ lb}^{-1}$$

where:

E_a = modulus of elasticity of turnbuckle = 10^7 psi (aluminum)

E_b = modulus of elasticity of scissor arm = 19×10^6 psi (BeCu)

I_a = moment of inertia of turnbuckle

I_b = moment of inertia of scissor arm

d_o = outer diameter of turnbuckle

d_i = inner diameter of turnbuckle

also $L_1 = 1.25$ in , $L = 3.55$ in

$L_2 = 2.3$ in

Hence, M_2 is found to be

$$M_2 = \frac{6x3.55(2x(3.35)^2x\,1.25-3.55x(1.25)^2+8.75(2.3)^2)x\delta x10^5}{(1.25)^4(3.55)^3+2x(3.55)^2x8.75x2.3(3x3.55x1.25-3x1.25x2.3-2(1.25)^2-2(2.3)^2 +3x2.3x3.55)x1.25+(8.75)^2x(2.3)^4x3.35}$$

but δ = .024 (see sect)

$$\boxed{M_2 = 203 \text{ lb in}}$$

The resulting maximum bending stress in the scissor arm turnbuckle is now given by

$$\sigma_2 = \frac{M_2 C_2}{I_2} \qquad C_2 = {}^{d_o}/_2 = .188 \text{ in}$$

$$I_2 = .97 \times 10^{-3} \text{ in}^4$$

$$\boxed{\sigma_2 = 39{,}300 \text{ psi}}$$

This stress occurs at the outer surface of the turnbuckle which is 2024-T4 aluminum with a yield of 40,000 psi and an ultimate of 62,000 psi. Thus the above stress would indicate a marginal condition with respect to yielding. Based on the ultimate strength however there is a factor of safety of 1.58. The above calculation is very conservative however from several standpoints. To begin with the aluminum turnbuckle does not nominally touch the BeCu scissor arm so that the two parts don't act like one shaft in the early stages of bending. Next, the scissor arm turnbuckle combination was assumed to be 3/8 in dia over its entire length of 2.3 inches where in reality the 3/8 in dia extends over only 1.0 inches with the remaining inch or so being only $\frac{1}{4}$ in dia. The above calculation neglected any allowable free play in the rotating linkage joints in the presence of which reduces the value of "δ" used in the stress equations and hence would reduce the calculated stress. In addition, the model itself is very conservative in assuming prefectly clamped ends and in its requirement that the slope of the deflection curve be the same for both segments at the point where they join. There is a great deal of radial play in the rotating linkage pivot pins as well as radial play in the bearing supporting the turnbuckle. Both sources of play

would reduce the calculated stress. For instance if the turnbuckle is considered fixed and the rotating linkage is assumed to be simply supported the maximum calculated stress at the turnbuckle would be reduced by a factor of 4:1. Finally, the value of "δ" used in the stress calculation was determined (vibration response analysis, sect) with the assumption that the scissor linkage did not exist. Consequently, the assumed configuration is not as rigid as the actual configuration (in this area of the system) and the assumed value of "δ" is likely to be larger than the actual value, contributing to an increase in the calculated stress.

In light of the above conservative assumptions, the actual stress level will be below the endurance limit of aluminum (20,000 psi) and therefore there will be no fatigue problems.

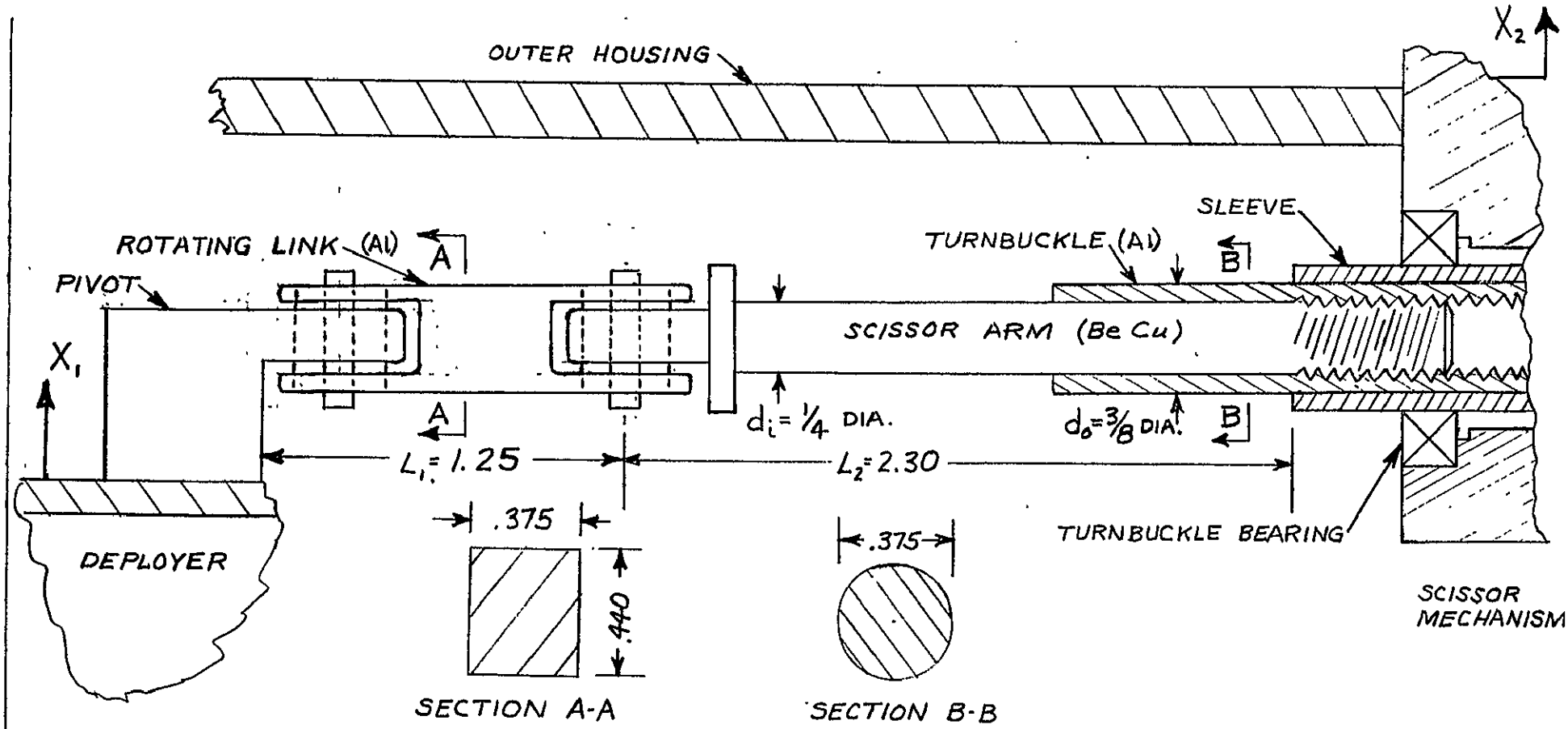

SCISSOR MECHANISM LINKAGE

FIG. D-1

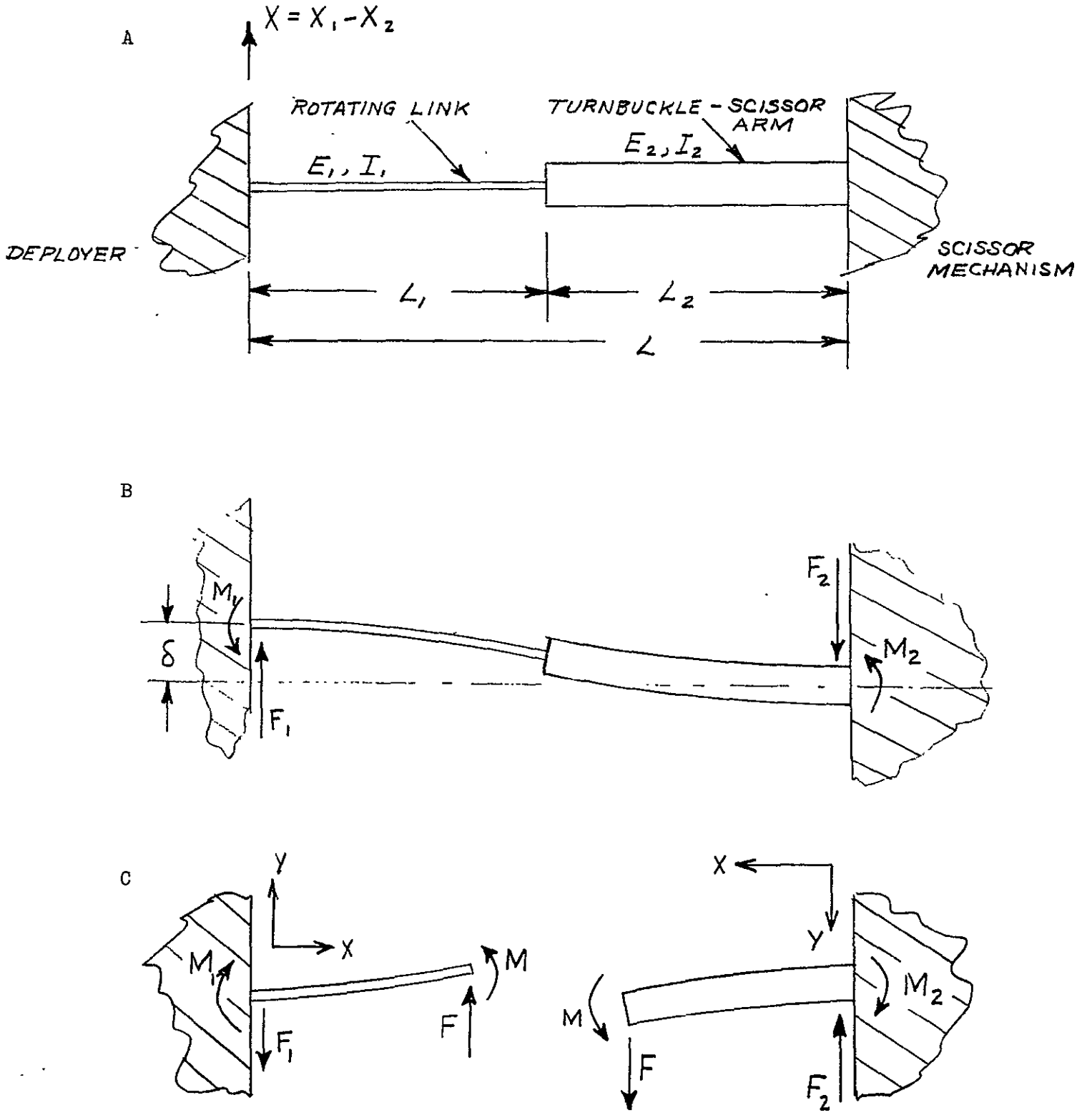

MODELS OF SCISSOR MECHANISM LINKAGE

FIG. D-2

APPENDIX - E

ANALYSIS OF STRUCTURAL INTEGRITY OF TAPE REEL ASSEMBLY - VIBRATION LOADING

E.1 Scope of Analysis

Referring to figure E-1, it is seen that the tape reel assembly consists of the tape storage reel (spool); an overrunning clutch (made up of a collar, a hub, and a coil spring); a shaft; two bearings; a retaining ring; a collar; and the tape (flattened stored boom). Furthermore, the tape reel assembly is secured to the deployer housing by a retaining ring on one side and the reel drive gear, which is set screwed to the shaft, on the other side. This analysis is concerned with the following critical elements; (1) the retaining rings, (2) the tape reel (and deployer) bearings, (3) the holding ability of the reel drive gear set screw. All other elements in the assembly are lightly loaded in relation to their ability to withstand dynamic loads, and are therefore not considered in the analysis.

E.2 Retaining Rings (See Detail A, Figure E-1)

Each retaining ring must alternately carry the full acceleration loading of the c.g. of the tape reel assembly. The maximum acceleration of the tape reel assembly c.g. is 67 g's, in the axial direction, at the deployer fundamental natural frequency (see section 3.2.1) of 204 Hz. Since the assembly weighs 1.9 lb. (fully loaded with tape), the load on the c.g. becomes 124 lb. Under this type of load, there are two possible failure modes; i.e., (1) the ring fracturing or springing from the groove, or (2) the groove material shearing. For the stainless steel shaft used

in this design, the second failure mode predominates. The equations* defining the maximum allowable vibratory acceleration loading are as follows:

(1) $a = \dfrac{1.037 P_g}{w}$

(2) $P_g = \dfrac{C_F S_d \pi \sigma_y}{F}$

where:

a = max. allowable acceleration, g's.

w = weight of vibrating mass, lb.

P_g = static thrust load limit (based on failure of groove), lb.

C_F = conversion factor

S = shaft dia. in.

d = groove depth

σ_y = tensile yield of groove material, psi.

F = factor of safety

For the retaining ring used in this design (Truarc-5100-external) "C_F" and "d" are found to be:

*$\begin{cases} C_F = 1.0 \\ d = .010 \end{cases}$

Since we are looking for the maximum allowable value of acceleration, "F" will be taken as 1.0. Also,

$S = .25$ in.

$\sigma y = 40{,}000$ psi (302 Stainless Steel)

Thus,

$P_g = 1.0 \times .25 \times .010 \times 3.14 \times 40{,}000$

$P_g = 314$ lb.

and $a = \dfrac{1.037 \times 314}{1.9}$

---

* - Technical Manual, Waldes Truarc Retaining Rings, 25th Edition, Pages 26 & 44.

$a = 171$ g's*

Since the maximum acceleration is only 67 g's, the retaining ring design is more than adequate.

E.3 Bearings

Each tape reel bearing and deployer housing bearing must alternately carry the 124 lb. peak vibration load. Assembly procedures have been established to remove all axial play from the bearings, and therefore it will be assumed that no suddenly applied loads will occur. The ability of the bearing to withstand vibration loading will be at least as good as the ability to withstand a constant thrust load equivalent to the peak harmonic load of 124 lbs. For the bearing in question (Barden flanged, 1/4 in. dia. bore, 5/8 dia. O.D. bearing - SFR4SS), the maximum static thrust load rating is 132 lb.** Thus, the bearings used appear to be adequate especially since the maximum static thrust load does not represent a failure of the bearing, but rather indicates the threshold of smooth bearing operation.

E.4 Drive Gear Set Screw - (See Figure E-1)

The tape reel assembly is restrained on one side of the deployer by the reel drive gear. The drive gear in turn is secured to the shaft by a #8-32 hardened steel, cone point, set screw which is tightened against a flat on the reel shaft and locked in place using "Locktite-E" screw thread

---

* - It should be noted that inherent in the equations used to determine the maximum allowable vibratory acceleration is the assumption that the side, which contains the sharp edge of the retaining ring I.D., carries the load. It is also assumed that the corners of the groove are sharp ($R < .003$ in). In addition, it is assumed that all of the free play between the retaining ring and the groove has been removed before application of the vibration loading. All of these assumptions have been satisfied by this design.

** - "Engineering Catalog G-3," Barden Precision Bearings, page 17.

retaining compound. In addition, there is a #8-32 pan head screw threaded into the end of the reel shaft which is snugged up against the gear hub (see fig. E-1) and locked via "Locktite-E". It will be assumed, for the sake of this analysis, that the #8-32 pan head screw does not exist and thus the set screw must carry the full dynamic load of 124 lbs. (This assumption is obviously very conservative). The axial holding power* of a #8-32 set screw torqued against a flat on a Stainless Steel shaft with a torque of 20 lb. in. has been measured to be 412 lbs.** The torque applied to the set screw in this design is 15 lb. in. This will reduce the above axial holding power by a factor of 15/20. Thus, the available axial holding power is 310 lb. and the set screw is more than adequate to support the expected maximum dynamic load.

---

* - Axial holding power is defined as the minimum axial load necessary to produce .01 in. of relative movement between the shaft and the collar being secured to the shaft.

** - "Key Factors in Set Screw," F. R. Kull, Machine Design, April 30, 1959, Pages 101-105.

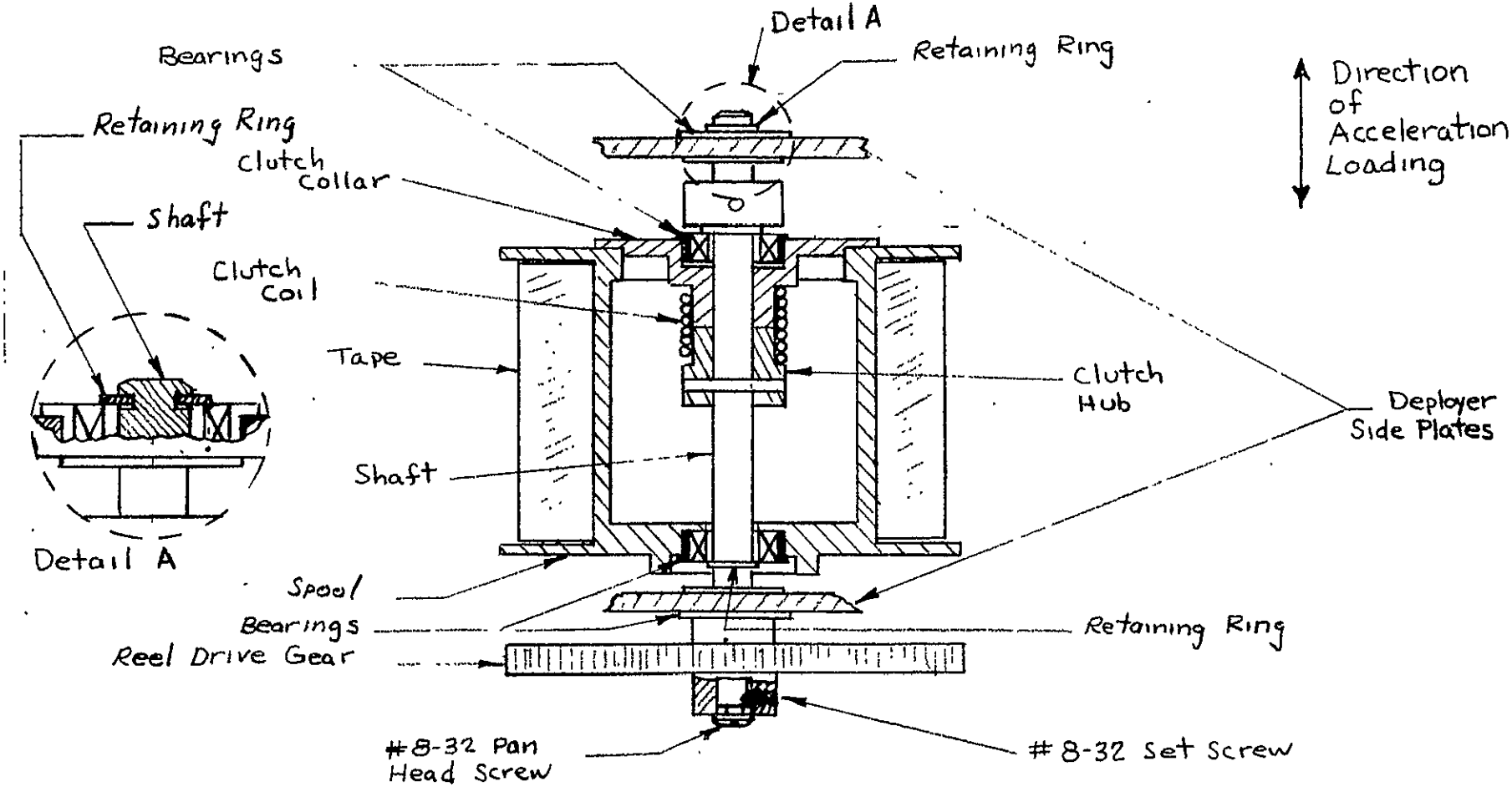

TAPE REEL ASSEMBLY

FIG. E-1

APPENDIX-F

Analysis of Deployer Pivot Bearing Elements -
Vibration Loading

F.1 Scope of Analysis

This analysis determines the critical stresses in the deployer pivot bearing elements due to a combination of pre-load and dynamic forces. The two elements found to be most sensitive to loading are the polyimide bushing and the stainless steel bearing load washer (see fig F-1).

F.2 Polyimide Bushing

F.2.1 Stress Equations - (see fig F-1)

F.2.1.1 Compressive stresses on bushing:

Assume bushing behaves as perfectly rigid member

Area "A" must bear total load of F lb.

$$\text{Area} = \pi(r_2^2 - r_1^2) = \frac{(3.14)(0.9^2 - 0.775^2)}{} = 0.165 \text{ in}^2$$

$$\text{Stress} = \text{Force} \div \text{Area} = \frac{F}{0.165}$$

F.2.1.2 Shear stress

Entire load of F lb. must be born in shear by the bushing area which interfaces the inner and outer portions of the bushing.

$$\text{Area} = \pi \times \text{diameter} \times \text{height}$$

$$= (3.14)(0.775)(0.06) = 0.146 \text{ in}^2$$

$$\text{Shear stress} = \text{Force} \div \text{area} = \frac{F}{0.146}$$

F.2.1.3 Tensile stress

The applied compressive and shear stresses produce tensile stresses in the polyimide perpendicular to the compressive stresses.

From Mohr's circle, $S_t = S_c + 2(S_s)$

F.2.2 Dynamic Load Plus Preload Stresses

Conservatively assume entire load must be born by the bushing.

Total load = 470 + 87.2* = 557.2 lb.

(1) Compressive stress $\frac{557.2}{0.146}$ = 3375 psi

(2) Shear stress $\frac{557.2}{0.146}$ = 3810 psi

(3) Tensile stress 2(3810)-3375 = 4245 psi

These stresses give a principle tensile stress of 5,800 psi

All the above stresses are well within acceptable limits.

($S_{ult\text{-}tensil}$ = 11,500 psi , $S_{ult\text{-}shear}$ 10,000 psi , $S_{ult\text{-}comp.}$ 12,000 psi for polyimide)

F.3 Washer Stresses

Washer bending stress is the only stress considered in this analysis because of its extremely large magnitude compared to other washer stresses. Assuming that the washers must bear the entire load produces values of bending stress which exceeded acceptable limits. Therefore an analysis to find the load distribution must be carried out before acceptable stress calculations can be made.

F.3.1 Load distribution between bushing and washers - (see fig F-2)

The load distribution can be determined by knowing the spring constants of the structural elements supporting the deployer. When the deployer is vibrating in the thrust axis the load at one of the two pivot bearings is carried by the stainless steel washer while the load @ the other bearing is carried by the polyimide bushing. Hence the deployer mass is attached to two spring elements (K_B & K_W). Each of these spring elements in

*The tensile pre-load comes from screwing the #10-32 screw into the deployer pivot block and tightening the head of the screw against the SST washer to a torque level of 10 lb in - see appendix-K

turn is attached to the outer housing frame structure via a frame spring of constant, K. The determination of these spring elements and the resulting load distribution follows:

F.3.1.1 Washer spring constant - K_W

$$* Y_{max} = \frac{-3W(m^2-1)}{2Em^2t^3}\left[\frac{(a^2-b^2)(3m+1)}{2(m+1)} - (b^2+r_o^2)\log\frac{a}{b} - \frac{r_o^2(a^2-b^2)(m-1)}{2a^2(m+1)}\right]$$

$$\frac{-6M(m^2-1)}{Emt^3}\left[\frac{b^2}{(m+1)} + \frac{2a^2b^2}{(a^2-b^2)(m-1)}\log\frac{a}{b}\right]$$

where $m = \frac{1}{\text{Poisons Ratio}} = 3.2$

E = Modulus of elasticity 5×10^5 psi

where $M = \frac{W}{8m}\left[(m-1) + 2(m+1)\log\frac{a}{r_o} - (m-1)\frac{r_o^2}{a^2}\right]$

$$W/Y = K_W = 1.11 \times 10^5 \text{ lb/in}$$

F.3.1.2 Bushing spring constant - K_B (see fig F-1)

Assume washers never contact top of deployer pivot shaft

$F = S \times A \quad e = S/E \quad K = F/e \times h$

$$K_B = \frac{S \times A}{S/Exh} = \frac{AE}{h} = \frac{(3.14)(0.9^2-0.775^2)(5\times10^5)}{(0.06)(4)}$$

$$K_B = 1.38 \times 10^6 \text{ lb/in}$$

F.3.1.3 Load distribution - (see fig F-2)

The natural frequency of the deployer (thrust axis) is known to be 204 cps (see sect 3.2.1).

*"Formulas for Stress and Strain", Roack, third Ed., McGraw-Hill, Case 59, page 210

turn is attached to the outer housing frame structure via a frame spring of constant, K. The determination of these spring elements and the resulting load distribution follows:

F.3.1.1 Washer spring constant - K_W

$$* Y_{max} = \frac{-3W(m^2-1)}{2\pi E m^2 t^3}\left[\frac{(a^2-b^2)(3m+1)}{2(m+1)} - (b^2+r_o^2)\log\frac{a}{b} - \frac{r_o^2(a^2-b^2)(m-1)}{2a^2(m+1)}\right]$$

$$\frac{-6M(m^2-1)}{Emt^3}\left[\frac{b^2}{(m+1)} + \frac{2a^2b^2}{(a^2-b^2)(m-1)}\log\frac{a}{b}\right]$$

where $m = \frac{1}{\text{Poisons Ratio}} = 3.2$

E = Modulus of elasticity 5×10^5 psi

where $M = \frac{W}{8\pi m}\left[(m-1) + 2(m+1)\log\frac{a}{r_o} - (m-1)\frac{r_o^2}{a^2}\right]$

$$W/Y = K_W = 1.11 \times 10^5 \text{ lb/in}$$

F.3.1.2 Bushing spring constant - K_B (see fig F-1)

Assume washers never contact top of deployer pivot shaft

$F = S \times A \quad e = S/E \quad K = F/e \times h$

$$K_B = \frac{S \times A}{S/Exh} = \frac{AE}{h} = \frac{(3.14)(0.9^2-0.775^2)(5\times10^5)}{(0.06)(4)}$$

$$K_B = 1.38 \times 10^6 \text{ lb/in}$$

F.3.1.3 Load distribution - (see fig F-2)

The natural frequency of the deployer (thrust axis) is known to be 204 cps (see sect 3.2.1).

*"Formulas for Stress and Strain", Roack, third Ed., McGraw-Hill, Case 39, page 210

$$f_n = \frac{1}{2\pi}\sqrt{\frac{K_{total}}{Mass}}$$

$$K\ total = K_T = (200)^2(6.28)^2\frac{(7.25)}{(386)} = \underline{29600\ lb/in}$$

but K_T also equals $K_{eg1} + K_{eg2}$

$$\text{and } K_{eg1} = \frac{KK_B}{K+K_B}\ ,\quad K_{eg2} = \frac{KK_W}{K+K_W}$$

The quadratic solution for K gives $\underline{1.61 \times 10^4\ lb/in}$

$$K_{eg1} = 1.59 \times 10^4\ lb/in\ ,\quad K_{eg2} = 1.41 \times 10^4\ lb/in$$

$$\text{Per cent load carried by washers} = \frac{K_{eg1}}{K_{eg1}+K_{eg2}} = (\%)_W$$

$$(\%)_W = \frac{1.41}{1.61+1.4.} = 46.7\%$$

$$\text{Per cent load carried by bushing} = \frac{K_{eg2}}{K_{eg1}+K_{eg2}} = (\%)_B$$

$$(\%)_B = \frac{1.61}{1.6.x1.41} = 53.3\%$$

F.3.2 Dynamic Plus Preload Load Stresses

$$Load = (0.467)(470) + 87.2 = \underline{306.2\ lb}$$

$$*S_t = \frac{-3W}{2\pi\ mt^2}\left[\frac{2a^2(m+1)}{a^2-b^2}\log\frac{c}{d} + (m-1)\frac{(c^2-d^2)}{(a^2-b^2)}\right]$$

$$\boxed{S_t = 96{,}700\ psi}$$

*"Formulas for Stress and Strain", Roark, 3rd Ed., McGraw-Hill, case 15 page 198

turn is attached to the outer housing frame structure via a frame spring of constant, K. The determination of these spring elements and the resulting load distribution follows:

F.3.1.1 Washer spring constant = K_W

$$* Y_{max} = \frac{-3W(m^2-1)}{2\pi E m^2 t^3}\left[\frac{(a^2-b^2)(3m+1)}{2(m+1)} - (b^2+r_o^2)\log\frac{a}{b} - \frac{r_o^2(a^2-b^2)(m-1)}{2a^2(m+1)}\right]$$

$$\frac{-6M(m^2-1)}{Emt^3}\left[\frac{b^2}{(m+1)} + \frac{2a^2b^2}{(a^2-b^2)(m-1)}\log\frac{a}{b}\right]$$

where: $m = \frac{}{\text{Poison's Ratio}} = 3.2$

E = Modulus of elasticity 5×10^7 psi

where $M = \frac{W}{8\pi m}\left[(m-1) + 2(m+1)\log\frac{a}{r_o} - (m-1)\frac{r_o^2}{a^2}\right]$

$W/Y = K_W = 1.11 \times 10^5$ lb/in

F.3.1.2 Bushing spring constant - K_B

Assume washers never contact top of deployer pivot shaft

$F = S \times A \quad e = S/E \quad K = F/e \times h$

$$K_B = \frac{S \times A}{S/Exh} = \frac{AE}{h} = \frac{(3.14)(0.9^2-0.775^2)(5\times10^5)}{(0.06)(4)}$$

$$\therefore K_B = 1.38 \times 10^6 \text{ lb/in}$$

F.3.1.3 Load distribution - (see fig F-2)

The natural frequency of the deployer (thrust axis) is known to be 204 cps (see sect 3.2.1).

*"Formulas for Stress and Strain", Roack, third Ed., McGraw-Hill, Case 59, page 210

This stress is theoretically concentrated on the bottom edge of the inner diameter. The magnitude of the stress initially creates concern because it is about the same as the ultimate tensil strength of 303 SST (95,000 psi). In reality, however, this stress can never be obtained because local yielding begins at a stress level of 35,000 psi and spreads over a very small radial increment until the local tensil stresses fall below the yield stress (35,000 psi). Although the exact radial stress distribution is not known, it is felt that this washer will certainly be able to allow the localized inner radius theoretical stress to exceed the ultimate by 50% with ample margin for safely redistributing the stress elsewhere within the washer. This ascertion is backed up by the fact that a rectangular cross section beam can allow the maximum theoretical bending stress to exceed the ultimate by 50% before failure will occur. In the case of the washer, the margin should be greater than 50% because the stress will redistribute in two modes ((1) along a circumferential plane, tranverse to the plane of the washer and (2) radially away from the inner radius) whereas the stress on the beam in bending can only redistribute along a plane transverse to the netural plane of bending. Thus, a factor of safety of 1.5 minimum exists for this washer.

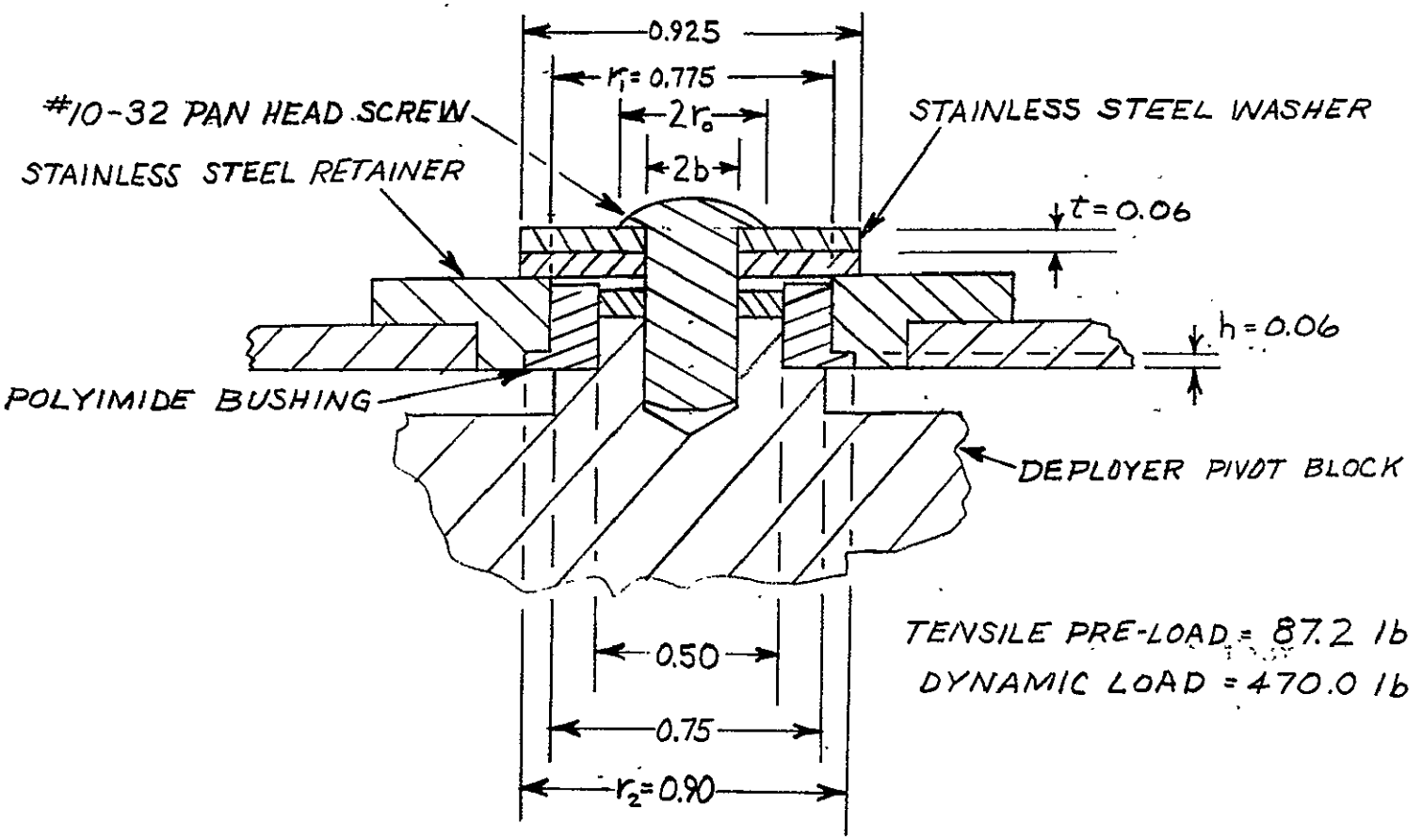

DEPLOYER PIVOT BEARING

FIG F-1

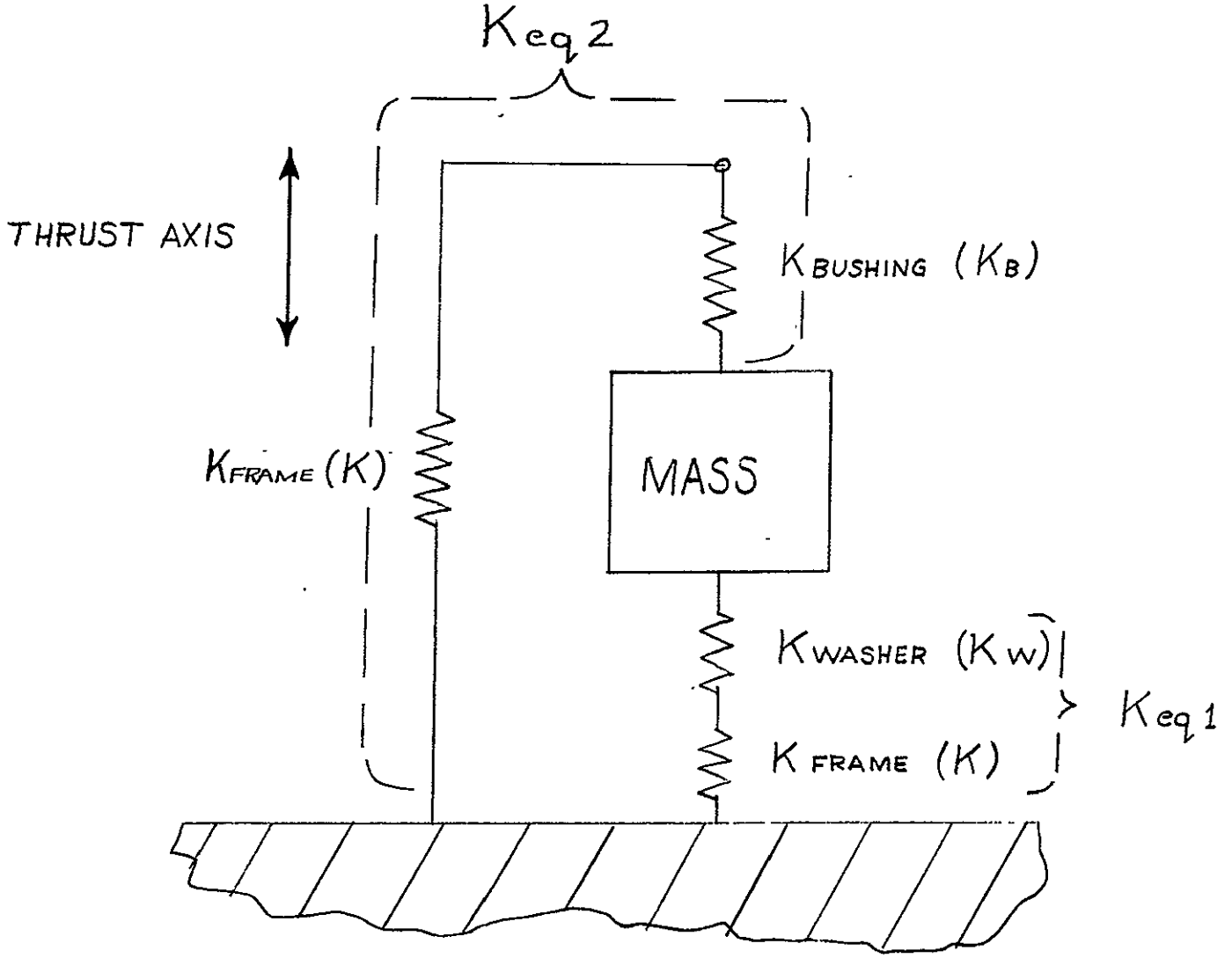

MODEL OF DEPLOYER PIVOT BEARING

FIG F-2

APPENDIX G

Determination of Maximum Outer Housing Plate Stresses - Vibration Loading

G.1 Scope of Analysis

The outer housing side plate (see fig G-1) is symmetrically loaded and supported, therefore only half of the side plate will be analyzed and the results will be considered applicable to the entire plate. The loading comes from deflection of Point "A" (into the plane of the paper) relative to support structure located along the perimeter of the plate (0-1-2-3-4). The plate to be analyzed will be assumed to be circular in shape rather than polygonal as shown above. The outer dia of radius "a" will be considered fixed while the inner hole of radius "b" is uniformly loaded around its circumference. This assumed shape is conservative in that the maximum stresses generated @ the outer edge will be higher than actual for a given deflection @ the perphery of the inner hole. This is true because the distance from the force to the clamped edge of the plate is on the average greater for the actual plate then for the assumed plate. To make the analysis even more conservative, it will be assumed that the support @ the outer periphery (r = a) is absolutely rigid; i.e., there is no flexibility in the outer housing framework between the "3" mounting points and the periphery of the plate in question. The analysis proceeds as follows:

G.2 Determination of maximum plate stress

For $a/b > 2.4$, the maximum stress* occurs at the inner edge and is given by

$$\text{Max } S_t = \frac{3W}{2\pi Mt^2}\left[1 + \frac{Ma^2(M-1) - Mb^2(M+1) - 2(M^2-1)a^2\ln\left(\frac{a}{b}\right)}{a^2(M-1) + b^2(M+1)}\right]$$

*"Formula for Stress and Strain", Roark, Third Ed., page 199, case 18

$$\text{Max } Y = \frac{-3W(M^2-1)}{4\pi M^2 E t^3} \left[a^2-b^2 + \frac{2Mb^2(a^2-b^2)-8Ma^2b^2 \ln\left(\frac{a}{b}\right) + 4a^2b^2(M+1)\left(\ln\frac{a}{b}\right)^2}{a^2(M-1)+b^2(M+1)} \right]$$

For aluminum

$$E = 1.06 \times 10^7 \text{ psi}$$

$$t = 2.50 \times 10^{-1} \text{ in}$$

$$M = \frac{1}{\nu} = \frac{1}{.334} = 3 \quad , \nu = \text{Poisson's Ratio}$$

$$\text{Max } S = 2.55W \left[1 + \frac{3a^2-6b^2-8a^2 \ln \frac{a}{b}}{a^2+2b^2} \right]$$

$$\text{Max } Y = -1.36 \times 10^{-6} W \left[a^2-b^2 + \frac{3b^2(a^2-b^2)-12a^2b^2 \ln \frac{a}{b} + 8a^2b^2\left(\ln \frac{a}{b}\right)^2}{a^2+2b^2} \right]$$

assume $a = 3.31$ $\qquad a^2 = 1.095 \times 10^1$

$b = 5.31 \times 10^{-1}$ $\qquad b^2 = 2.83 \times 10^{-1}$

$\frac{a}{b} = 6.23 > 2.4$

$\ln \frac{a}{b} = 1.83$ $\qquad \left(\ln \frac{a}{b}\right)^2 = 3.36$

$\text{Max } S = -26W$

$\text{Max } Y = -1.75 \times 10^{-5} W$

$S_{Max} = 1.43 \times 10^6 Y_{Max}$

From the results of the vibration analysis, table 3-3, it is seen that Y Max is .015 in

$S_{Max} = 1.43 \times 1.5 \times 10^4$

$S_{Max} = 21{,}500 \text{ psi}$

The aluminum used is 6061-T6 having an ultimate strength of 42,000 psi. Thus there is a factor of safety of 2:1 for the outer housing side plate (max dynamic deflection applied statically).

The minimum fatigue life for 6061-T6 aluminum @ a stress level of 21,500 psi is 3×10^6 cycles.* The total number of cycles for the entire vibration spectrum (3 axis sine plus random) is 700,000 cycles, only a small number of which occur at a stress level of 21,500 psi. This coupled with the conservative nature of the max stress analysis indicates that there will be no fatigue problem with the outer housing side plate.

*"Stress Strain and Strength", Robert C. Juvinall, McGraw-Hill, page 216

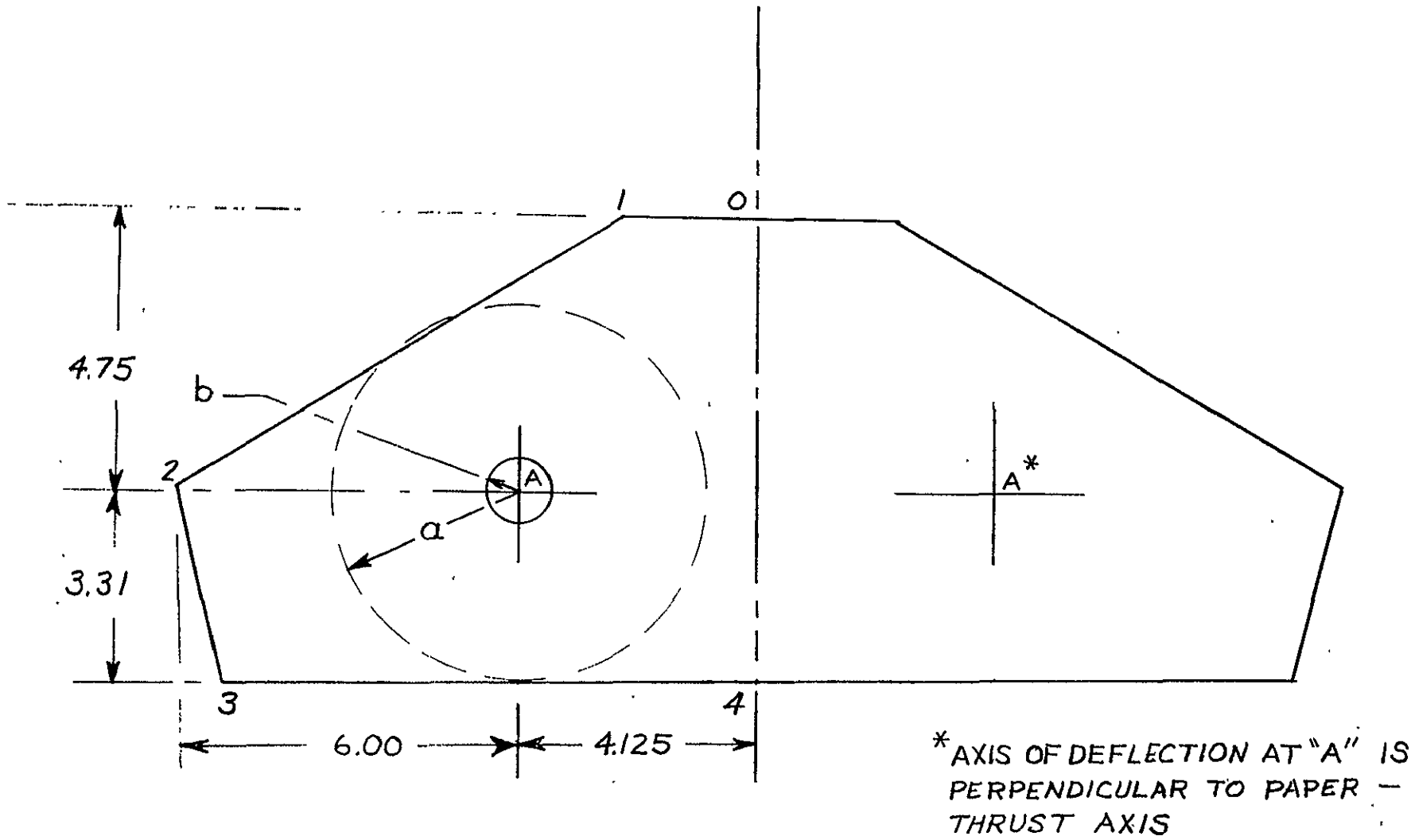

OUTER HOUSING SIDE PLATE

FIG G-1

APPENDIX-H

Analysis of Boom Isolation Ass'y - Vibration Loading

H.1 Scope of Analysis

This analysis determines the maximum bending stresses created in the boom isolation assembly and evaluates the assembly from the standpoint of fatigue life. The boom isolation assembly is shown in fig H-1. The relative displacement between the deployer guide support and the tip mass creates bending stresses in the spring wire and the coil spring. For the sake of this analysis it will be assumed that the coil spring does not exist and therefore the tip mass is attached to the boom via the spring wire only (a conservative assumption). It will be assumed that during vibration the ends of the .0317 dia SST wire remain perfectly clamped and normal to the direction of the relative deflection. This can be seen in fig H-2a.

H.2 Derivation of Stress Equation

The equation for the stress in the wire is found as follows: (refer to fig H-2b)

At X = 1/2 there is a point of inflection in the deflection curve - $\frac{d^2y}{dX^2} = 0$. Since $M = EI \frac{d^2y}{dX^2}$ we see that the moment @ X = 1/2 is zero.

X = 1/2 can be considered to be the free end of a cantilever beam of length 1/2 which has undergone a deflection of y = $\delta/2$. Thus the beam can be drawn as the equivalent beam shown in fig H-2c.

$$\delta/2 = \frac{F(1/2)^3}{3EI} = F1/2 = \frac{\delta}{2} \cdot \frac{3EI}{1^2/4}$$

or $$\frac{F1}{2} = \frac{6\delta EI}{1^2}$$

also, $\sigma = \frac{MC}{I}$ where $M = \frac{Fl}{2} = \frac{6\,\delta\,EI}{l^2}$

$$\boxed{\sigma = \frac{6\,\delta\,CE}{l^2}}$$

H.3 Static and Fatigue Analysis

for .0317 dia SST wire $E = 30 \times 10^6$ psi

$C = .0158$ in

$l = .74$ in

$$\sigma = \frac{6 \times 30 \times 10^6 \times .0158 \times \delta}{(.74)^2}$$

$$\sigma = 5.2 \times 10^6\,\delta$$

From table 3-3 we find that $\delta = .0277$ in.

$$\sigma = 5.2 \times 2.77 \times 10^4$$

$$\boxed{\sigma = 144{,}000 \text{ psi}}$$

The ultimate strength for this stainless steel wire (W PDS 6359-1) is 278,000 psi. Thus, it is apparent that there is a sufficient factor of safety (1.93) for the spring wire to undergo the anticipated relative deflection during vibration. This factor of safety is conservative in that the ends of the spring are not perfectly clamped and the stresses will be lower for a given deflection. Furthermore, the vibration model for the ATS boom system assumed that the boom isolation ass'y did not exist. Consequently, the value of $\delta = .0277$ in is somewhat higher than the relative deflection which will occur with the additional coupling between the deployer and the tip mass.

The above analysis considers the ability of the wire to withstand the maximum relative deflection statically. Since the stress in the wire is an alternating stress, fatigue must also be considered as a potential failure mode.

For ASTM-A313 stainless steel spring wire undergoing an alternating maximum stress of 144,000 psi the number of cycles to failure is 5000 cycles. The results of the vibration analysis indicate that the stress level of 144,000 psi is maintained for $<$ 10 cps; i.e., between 194 & 204 cps. During this interval @ a 2 octave per minute sweep rate (qual test spec), there will be 1000 cycles. Thus there appears to be an ample factor of safety - 5:1. Furthermore, the conservative aspects of the static analysis, previously mentioned, apply to the fatigue analysis as well. For instance if the maximum stress is actually 112,000 psi instead of the conservative 144,000 psi the number of fatigue cycles is increased to 10^7 cycles for this material.

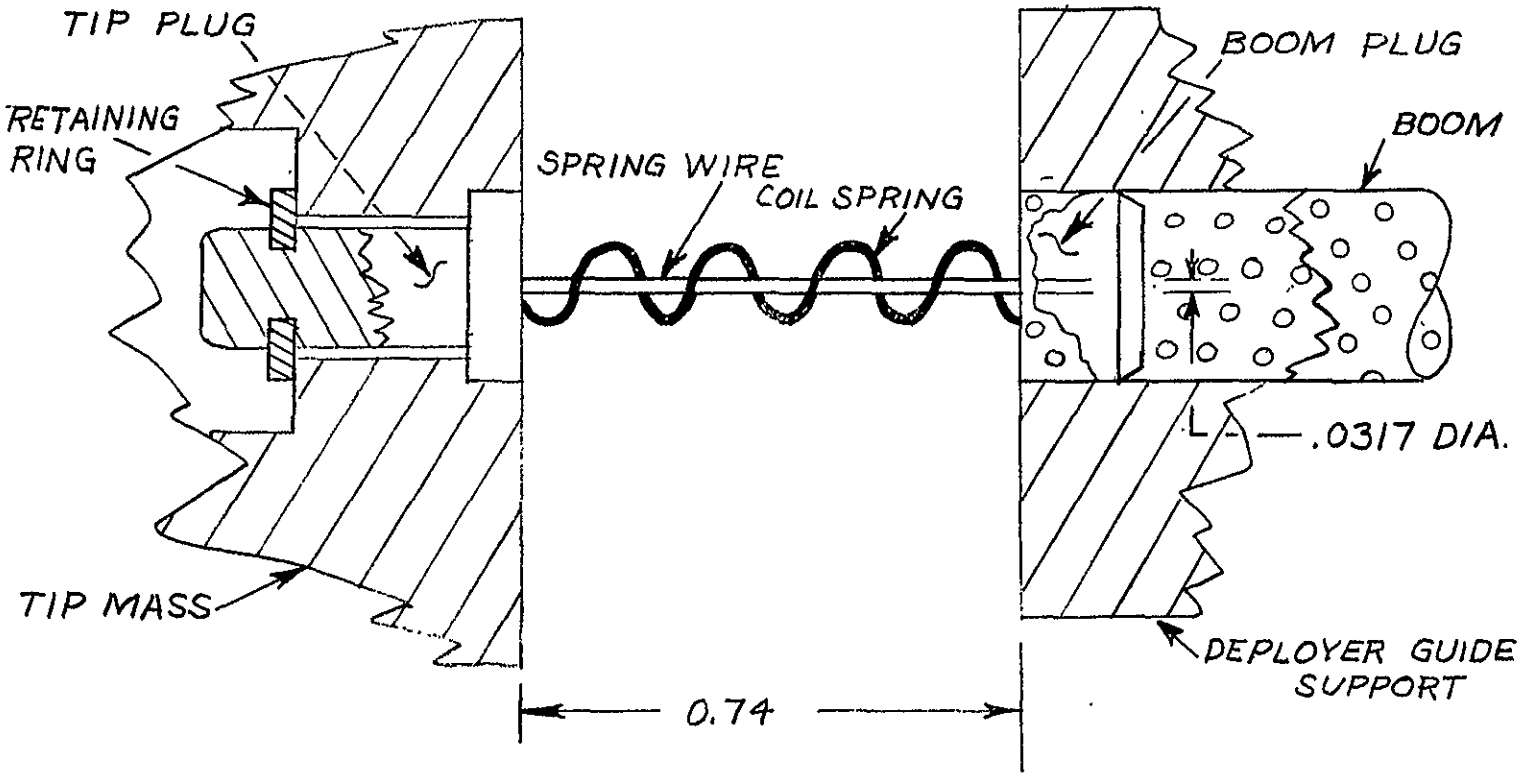

BOOM ISOLATION ASSEMBLY

FIG H-1

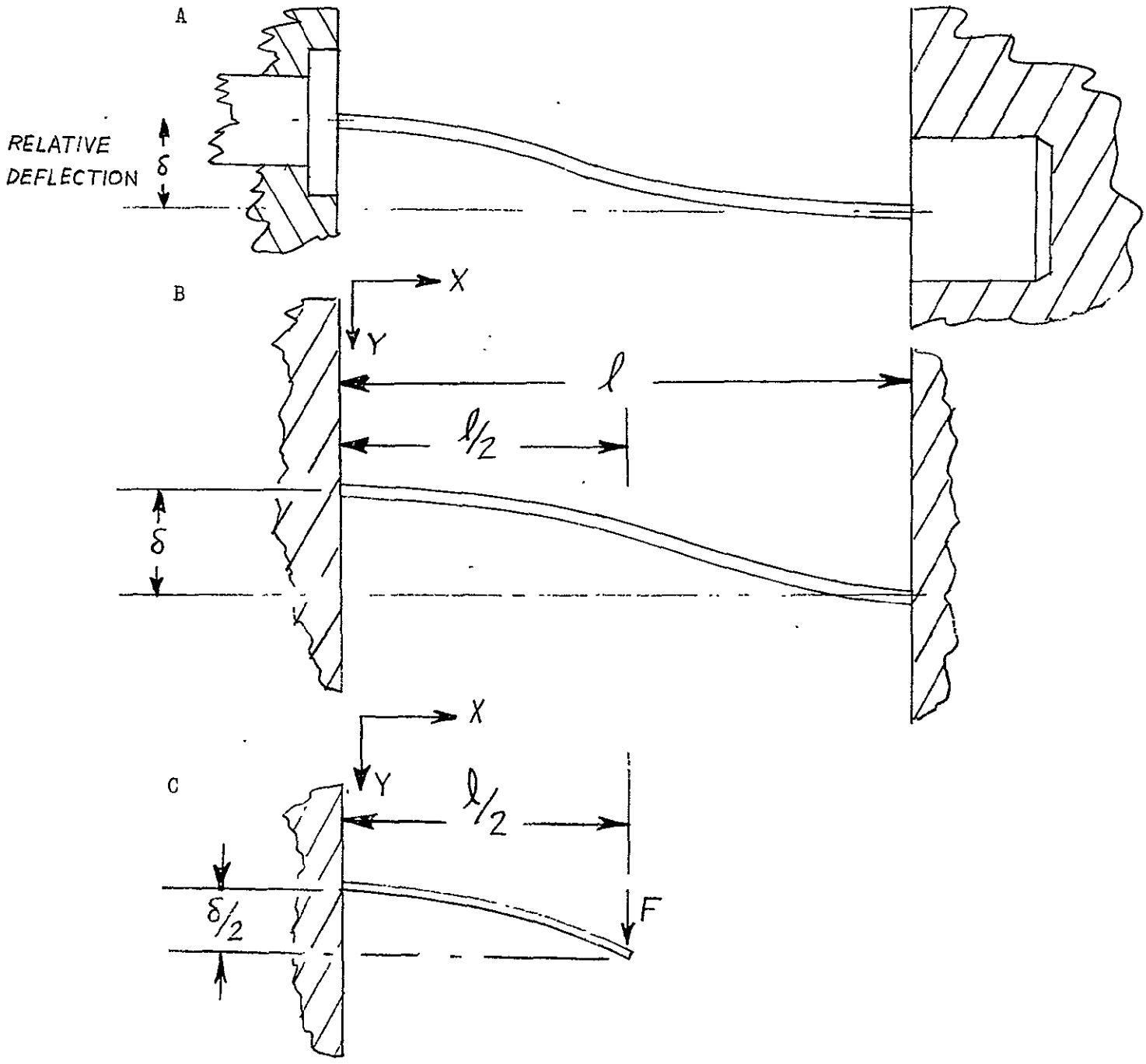

MODELS OF BOOM ISOLATION ASSEMBLY

FIG H-2

APPENDIX-I

Structural Analysis of Tip Mass Release Mechanism - Vibration Loading

I.1 Scope of analysis: (refer to fig 2-3)

This analysis determines the structural integrity, under qualification level vibration loadings, of the clamping lever, arm support, end plate posts, the cable, clamping lever and arm support pivot pins and the arm support wheel pivot pin. These elements are the most severely loaded and critically important of the various elements comprising the assembly and consequently they are the only elements being considered. The dynamic load for this analysis is taken as the maximum "g" loading on the 8 lb tip mass determined from the thrust axis dynamic analysis (see sect 3.2.1). The thrust axis load is the only load considered because the highest input levels and lowest system natural frequencies occur in this axis. The analysis will proceed as follows. First, the static forces, due to pre load, @ the clamping lever - tip mass interface will be determined. Next, the dynamic force acting on the clamping lever will be determined. To accomplish this, the spring constant of the series elements comprising the clamping mechanism (clamping lever, support, cable) must be determined and compared with the spring constant of the adjustment screw. These spring constants will be evaluated at the same point; i.e. the point where the clamping screw contacts the tip mass. The total force in the clamping lever elements will then be determined by superimposing the static (pre load) forces onto the dynamic forces. Finally the stresses resulting from these forces will be determined. It is assumed in this analysis that the peak dynamic forces can be treated as statically applied forces.

I.2 Pre-load analysis:

The pre-load in the tip mass release mechanism elements is obtained by alternately tightening the clamping lever screw and the cable tension adjustment with the tip mass supported on the support posts and held against the adjustment screw until the clamping lever beam gap (see fig I-1) closes by .008 $\pm$ .0005 in.

A detail of the pre-load clamping lever is shown in fig I-1. The relationship between the closing of the clamping lever beam gap (Δ d) and the force F_1 can be found as follows:

Δd is defined as the deflection at point B (fig I-1) transverse to the portion of the beam lying between points B and A. By applying a ficticious force, F_3, in the direction of Δ d the deflection @ B can be determined by use of Castigliano's Method.* The bending moments between C & B and B & A are given by:

$$M_{CB} = F_1 X$$

$$M_{BA} = F_1 h + F_1 Y \cos X + F_3 Y$$

Then Δ d is given by:

$$\Delta d = \int_0^h \frac{M_{CB}}{(EI)} x \frac{\partial}{\partial F_3} (M_{CB}) \cdot dX + \int_0^l \frac{M_{BA}}{(EI)} x \frac{\partial}{\partial F_3} (F_1 h + F_1 Y \cos X + F_3 g)\, dy$$

*"Stress, Strain and Strength", R. C. Juvinall, McGraw-Hill 1967, page 150

but $\int_0^h \frac{F_1 X}{EI} \frac{\partial (M_{CB})}{\partial F_3} dX = 0$ since M_{CB} is not a function of F_3

$$\therefore \Delta d = \frac{1}{EI} \int_0^l \left[F_1 h + (F_1 \cos X + F_3) Y\right] (Y)\, dy$$

but $F_3 = 0$

Thus $\Delta d = \frac{1}{EI} \int_0^l (F_1 h + F_1 [\cos \alpha] Y)(Y) dy = \frac{1}{EI} \int_0^l F_1 (hy + [\cos \alpha] Y^2)\, dy$

$$\Delta d = \frac{F_1}{EI} \left[\frac{hy^2}{2} + \frac{y^3 \cos \alpha}{3}\right]_0^l$$

or $$\boxed{\Delta d = \frac{F_1 l^2}{EI} \left[\frac{h}{2} + \frac{l \cos \alpha}{3}\right]}$$

The relationship between F_1 and F_2 is found by requiring that the moments about point A be zero.

Thus $$F_2 = \frac{l_1}{l_2} F_1$$

(1) or $$\boxed{F_2 = \frac{l_1}{l_2} \left[\frac{EI \Delta d}{l^2 \left[\frac{h}{2} + \frac{1}{3} \cos \alpha\right]}\right]}$$

I is found from section 2-2 of fig I-1 to be $.71 \times 10^{-4}$ in.^{4}

$l = .50$ in.

$h = .40$ in.

$l_1 = 1.20$ in.

$l_2 = .38$ in.

$E = 3 \times 10^7$ psi (steel)

$\alpha = 55°$

$\Delta d = .008$ in.

Thus, the value of the pre-load force acting at the clamping lever-tip mass interface is:

$$F_2 = \frac{1.2}{.38}\left[\frac{3 \times 10^7 \times .71 \times 10^{-4} \times .008}{(.50)^2\left[.20 + \frac{.5}{3}\cos 55°\right]}\right]$$

$$\boxed{F_2 = 730 \text{ lb}}$$

I.3 Dynamic load analysis:

In addition to the pre-load forces present in the assembly, there are dynamic loads arrising from the qualification vibration test which must be considered in analyzing the critical structural elements. A direct analogy can be drawn between the pre-loaded tip mass assembly and the pre-loaded assembly shown in fig I-2. Provided there is enough pre-load to present the "part" from separating from the "rigid support", the external force "P" does not add directly to the tension pre-load in the bolt. The relationship between the total tensil force, "F_b", the pre-load, "F_1", and the external load "P" is given by:

$$F_b = \left[\frac{K_b}{K_b + K_p} \right] P + F_o$$

where:

K_b = spring const. of bolt

K_p = spring const. of the part

If K_b is significantly less than K_p, the external force has very little affect on the initial pre-load. The bolt in the above example is equivalent to the elements comprising the clamping mechanism (clamping lever, support arm, cable, etc.). The "part" in the above example is equivalent to the support structure (support posts, and adjustment screw). The point of application of the force "P" in the above example is equivalent to the c.g. of the tip mass. Considering the vibration load to be acting as shown in fig I-3 (thrust axis) the total (dynamic plus pre-load) force acting on the clamping elements is found as follows:

The line of action of reaction forces f_1 & f_2 will pass thru point A as shown in fig I-3. Thus by summing moments about A and equating the sum to zero, we will eliminate f_1 & f_2 to give:

$$F \times A = -F_C \times C + F_B \times b$$

but $F_C = K_C \Delta L_C$

& $F_B = K_B \Delta L_B$

where: F = peak amplitude of dynamic load acting so as to increase the load on the clamping elements

K_C = spring constant of adjustment screw evaluated @ point "C"

K_B = spring constant of clamping elements evaluated @ point "B"

ΔL_C = deflection of tip mass at point "C" in the direction of F_C

ΔL_B = deflection of tip mass @ point "B" in the direction of F_B

It will now be assumed that the tip mass tends to rotate about point "A" under the action of forces F, F_B, & F_C. Thus the angular rotation of points "B" and "C" can be equated as follows:

$$\theta_C = \theta_B \qquad \text{where } \theta_C = -\frac{\Delta L_C}{C}$$

$$\theta_B = \frac{\Delta L_B}{b}$$

$$\therefore \dot{L}_C = -\Delta L_B \left(\frac{C}{b}\right)$$

$$\text{Thus, } F \times a = K_C \Delta L_B \left(\frac{C}{b}\right) C + K_B \Delta L_B b$$

$$F \times a = \Delta L_B \left[\frac{K_C \times C^2 + K_B \times b^2}{b}\right]$$

$$\Rightarrow \Delta L_B = \frac{F \times a \times b}{K_C \times C^2 + K_B \times b^2}$$

$$\text{but } F_b = K_B \Delta \dot{L}_B$$

$$\therefore (2) \quad \boxed{F_b = \frac{K_B F a b}{K_C C^2 + K_B b^2}}$$

The total load acting @ point "B" will be the dynamic load F_b (equation (2)) plus the static pre-load (equation (1))

$$(3)\quad F_{BT} = \left[\frac{K_B \cdot a\, b}{K_C^2 C + K_B b^2}\right] F + \left(\frac{1}{2}\right)\left[\frac{E I \Delta d}{l^2 \left(\frac{h}{2} + \frac{l}{3}\right) \cos\alpha}\right]$$

As with the pre-load bolt discussed above, if K_B is significantly less than K_C a very small portion of F (dynamic load) will be transmitted to point "B". It now remains to determine the values of K_B and K_C. It is assumed in calculating the spring constants that no yielding occurs.

I.3.1 K_C - Spring Constant of Support Structure

Referring to view A of fig 2-3 the support structure* will be considered to consist of the adjustment screw and the post into which the adjustment screw is threaded. The spring constant K_C consists of the series combination of two separate spring effects; i.e., the adjustment screw penetrating the tip mass and the cantilever effect of the screw support. The spring constant of the screw in contact with the mass is given as follows:

I.3.1.1 Spring Constant of Adjustment Screw

The screw has a spherical contour and the tip mass has a cylindrical cut out with the same radius as the spherical screw. It will be assumed that the tip mass will be considered to be a flat plate (simplifies calculations). This is a conservative assumption in that the calcuated spring constant will be lower than the actual spring constant.

*The "support" shown in view A has been neglected to simplify the analysis. Omitting the support makes the calculations conservative.

Thus $K_{C1} = \sqrt[3]{\frac{\bar{F}_C^2 \, E \, D}{1.55}}$ **

E = modulus of elasticity of steel = 30×10^6 psi

D = diameter of sphere

$\bar{F}_C$ = pre-load force acting on adjustment screw $\approx$ 400 lb

As can be seen from the above equation, the value of K_{C1} is not a constant but depends on the load level on the screw. For the purposes of this analysis, it will be assumed that K_{C1} depends only on the initial load level acting on the screw.

Thus $K_{C1} = 3.64 \times 10^5$ lb/in

I.3.1.2 Spring Constant of Adjustment Support

The spring constant of the screw support is given by:

$K_{C2} = \frac{3EI}{L^3}$

where:

I = moment of inertia of support cross section = 2.7×10^{-2} in.^{4}

E = modulus of elasticity of support material = 10^7 psi

L = distance between the point of application of force and fixed end of "cantilever beam" = .15 in

$K_{C2} = 2.02 \times 10^7$ lb/in

**"Formulas for Stress and Strain", Roark, McGraw-Hill, 3rd Ed., page 287

Thus the spring constant of the support structure becomes:

$$K_C = \frac{K_{C1} K_{C2}}{K_{C1} + K_{C2}} = \frac{3.64 \times 10^{5} \times 2.02 \times 10^{7}}{2.056 \times 10^{7}}$$

$$\boxed{K_C = 3.6 \times 10^{5} \text{ lb/in}}$$

I.3.2 K_B - Spring constant of clamping elements

The value K_B will be the series combination of the clamping lever spring evaluated @ the tip mass-clamping screw interface; and the support cable spring evaluated @ the support arm-clamping lever interface. The spring constant of the clamping lever is determined as follows:

I.3.2.1 Spring constant of clamping lever

Referring to figure I-1 assume for the moment that point "D" is fixed and point "C" moves under the action of "F_1". We then get, by using Castigliano's Energy Method, the following relationship between the deflection at "C" and "F_1":

$$\delta_C = \frac{F_1}{E \bar{I}} \left(\frac{h^3}{3} + h^2 l_1 + l_1^2 h \cos X + \frac{l_1^3}{3} \cos^2 X \right)$$

where:

$\bar{I}$ = Average moment of inertia of section 2-2 $\approx .8 \times 10^{-4}$ in^4

but $F_1 = \frac{l_2}{l_1} F_2$ (comes from equating moments about point A to zero)

Also, point "C" must in reality be considered fixed. If we rotate the entire part about point "A" point "C" moves ($-\delta C$), we can

determine a relationship between the imagined deflection @ "C" and the actual deflection @ "D".

The angle of rotation $\theta = \frac{C}{l_1} = \frac{D}{l_2}$

$$\frac{l_2/l_1 \; F_2}{I_1/l_2 \; \delta_D} = \frac{E\bar{I}}{\frac{h^3}{3} + h^2 l_1 + l_1^2 h \cos\alpha + \frac{l_1^3}{3}\cos^2\alpha}$$

but $F_2 = K_{B1} = $ spring const. of clamping lever

δ_D

or $$K_{B1} = \left[\frac{l_1}{l_2}\right]^2 \frac{E\bar{I}}{h^3 + h^2 l_1 + l_1^2 \cos\alpha + \frac{l_1^3}{3}\cos^2\alpha}$$

$$K_{B1} = 1.4 \times 10^5 \text{ lb/in}$$

I.3.2.2 Spring constant of cable

The spring constant of the cable evaluated at the support arm clamping lever interface is found as follows:

Referring to fig I-4 we see that the cable which constrains the support arm consists of two segments of length L_1 & L_2. The spring constant of the cable evaluated at point "A" becomes:

$$K_A = \frac{K_{C1} \; K_{C2}}{K_{C1} + K_{C2}}$$

where: K_{C1}^{*} = spring const of cable segment L_1

K_{C2}^{*} = spring constant of cable segment L_2

E = modulus of elasticity of cable = 30×10^6 psi

A = cross sectional area of cable

D = diameter of cable $\approx .020$ in

L_1 = 2 in

L_2 = 4 in

also, $K_{C1} = \frac{EA}{L_1} = \frac{E \pi D^2}{4L_1}$

$$K_{C1} = \frac{3 \times 10^7 \times \pi \times 4 \times 10^{-4}}{4 \times 2}$$

$$K_{C1} = 4.7 \times 10^3 \text{ lb/in}$$

and $K_{C2} = \frac{EA}{L_2} = \frac{3 \times 10^7 \times \pi \times 4 \times 10^{-4}}{4 \times 4}$

$$K_{C2} = 2.35 \times 10^3 \text{ lb/in}$$

$$K_A = 7.05 \times 10^3 \text{ lb/in}$$

but $K_A = \frac{F_A}{\delta_A}$ and $F_A \times a = F_1 \; (B + bsm \; 5.5^{o})$, ($M_G = 0$)

also $\frac{\delta_A}{a} = \frac{\delta_D}{d}$

*It is assumed that all of the friction between the cable segments and the parts against which the cable rests is concentrated at the pulley to the extent that the cable pulley is locked.

$$\frac{F_1 \; (\beta + b\sin 5.5^{\circ}) \; d}{a^2 \; \delta_D} = K_A$$

or $$\frac{F_1}{\delta_D} = \frac{K_A \; a^2}{d \; (\beta + b\sin 5.5^{\circ})}$$

but $\frac{F_1}{\delta_D} = K_{B2}$ = spring constant of cable evaluated at the support arm - clamping lever interface

$$K_{B2} = \frac{K_A \; a^2}{d \; (\beta + b\sin 5.5^{\circ})}$$

where:

$a = .38$ in.

$b = .7$ in.

$d = .88$ in.

$\beta = .050$ in.

$$K_{B2} = \frac{7.05 \times 10^3 \times (.38)^2}{.88 \; (.05 + .7 \times .1)}$$

$$= \frac{7.05 \times 10^3 \times .144}{.88 \times .12} = \frac{8.45}{.88} \times 10^3$$

$$K_{B2} = .97 \times 10^4 \text{ lb/in}$$

Thus the combined spring constant of the clamping elements is found to be

$$K_B = \frac{K_{B1} \; K_{B2}}{K_{B1} + K_{B2}} = \frac{14 \times 10^4 \times .97 \times 10^4}{14.97 \times 10^4}$$

$$K_B = 9 \times 10^3 \text{ lb/in}$$

Finally returning to equation (3) we can now calculate the total force (dynamic plus pre-load) acting @ the tip mass - clamping lever interface, F_{BT}, as follows

$$F_{BT} = \left[\frac{9 \times 10^3 \times a \times b}{3.6 \times 10^5 \times C^2 + 9 \times 10^3 \times b^2} \right] F + 730$$

referring to fig I-3,

$$* \begin{cases} a = .924 \text{ in.} \\ b = .740 \text{ in.} \\ c = .656 \text{ in.} \\ F = 55 \text{ g's} \times 8 \text{ lb/g} = 440 \text{ lb} \quad ** \end{cases}$$

$$F_{BT} = .038F + 730 = .038 \times 440 + 730 = 16.5 + 730$$

$$F_{BT} = 746.5 \text{ lb}$$

---

*These numbers assume that angles α and β are equal to 50^o and that f_1 and f_2 are positive as shown. In reality f_1 goes to zero and f_2 carries the load at some angle other than 50^o. The above assumption however gives a higher calculated value of F_{BT} and is therefore conservative.

**determined from section 3.2.1

I.4 Stress Analysis - Clamping Elements

I.4.1 Clamping lever: Referring to fig I-1 we see that $F_2 = F_{BT} = 747$ lb

This causes F_1 to be:

$$F_1 = \frac{1}{\frac{2}{1}} \quad F_2 = \frac{.38}{1.20} \quad (747)$$

$$F_1 = 237 \text{ lb}$$

This force creates a bending stress in the spring arm at point "E" of

$$\sigma = \frac{F_1 \, l_3 \, C}{I}$$

where:

I = moment of inertia of section 2-2 = $.71 \times 10^{-4}$ in.^{4}

$C = \frac{.145}{2} = .0725$

$l_3 = .65$

$$\sigma = \frac{237 \times .7 \times .0725}{.71 \times 10^{-4}}$$

$$\boxed{\sigma = 157{,}000 \text{ psi}}$$

This stress level is safe because the yield strength of the hardened tool steel is 240,000 psi and the ultimate is 280,000 psi. There are no geometric stress concentrations at this point of maximum bending stress which could aggrevate the situation. In addition the surface of maximum tensil stress is machined to a 63 micro inch finish and coated with MOS_2 so as to reduce the danger of stress concentrations arrising from corrosion propagating from machine marks

I.4.2 Clamping lever pivot: Referring to fig I-5a there are two elements which are considered critical; i.e. the steel pivot pin and the aluminum pivot bosses. The steel pivot pin is loaded in pure shear and the shear stress is given as follows:

$$\tau_1 = \frac{F_a}{A} \qquad A = \frac{\pi}{4}(.156)^2 = .0191 \text{ in}^2$$

Referring to figure I-1 we find

$$\sum M_D = 0 = F_{ay}(l_4 - l_1) - F_{l_1} l_4 + F_a x_{l_5}$$

$$\sum F_X = 0 = F_2 \cos\phi - F_{ax}$$

$$F_{ax} = F_2 \cos\phi \quad , \quad F_2 = F_{BT} = 746.5 \text{ lb}$$

$$\phi = 45^\circ$$

$$\Rightarrow F_{ax} = 528 \text{ lb}$$

$$F_{ay} = \frac{F_{l_4} l_4 - F_a x_{l_5}}{l_4 - l_1}$$

$l_4 = 1.44$ in.

$l_1 = 1.20$ in.

$l_5 = .33$ in.

$F_{l_1} = 237$ lb

$$F_{a_y} = \frac{237 \times 1.44 - 528 \times .33}{.24} = \frac{166}{.24}$$

$$F_{ay} = 690 \text{ lb}$$

$$F_a = \sqrt{F_{ax}^2 + F_{ay}^2}$$

$$F_a = 870 \text{ lb}$$

$$\tau_1 = \frac{870}{.0191}$$

$$\boxed{\tau_1 = 45{,}500 \text{ psi}}$$

This stress level is quite safe for the hardened steel pivot pin which has a yield of 100,000 psi and an ultimate of 125,000 psi in shear.

The aluminum pivot bushing is also loaded in shear. The mode of failure will be for the pin to tear thru the aluminum pivot bosses. The shear stress in the two bosses is given by

$$\tau = \frac{F_a}{A}$$

where:

F_a = Load on pin = 870 lb

A = Shear area of both bosses

Referring to fig I-5a it can be seen that F_a is taken to act along the .15 dimension. In reality, F_a acts at an angle to the .15 dimension; however, this assumption minimizes the shear area and therefore is conservative.

$$A = (.15 \times .18)(2)(2) = .108 \text{ in}^2$$

$$\Rightarrow \quad \tau = \frac{870}{.108}$$

$$\boxed{\tau = 8{,}050 \text{ psi}}$$

The shear strength of the 2024-T4 aluminum pivot bosses is 30,000 psi (yield) and 41,000 psi (ultimate). Thus, the above stress level is quite safe.

I.4.3 Support Arm Pivots - Referring to fig I-5b the shear strength at points C and G of the pivot pins will be determined. The shear stresses in the aluminum pivot bosses (point G) and the steel support arm (points C & G) will not be presented because these stresses are very low. The shear stresses at points C and G will be equal since the loads and pin diameters are equal. Thus the shear stress in each pin is found to be:

$$\tau = \frac{F_b}{A} \qquad A = \frac{\pi}{4}(.094)^2 = .00695 \text{ in.}^2$$

$$F_b = 237 \text{ lb}$$

$$\boxed{\tau = 34{,}000 \text{ psi}}$$

The ultimate strength in shear for the hardened steel pins is 125,000 psi so the design is quite safe.

I.4.4 Cable: Referring to figures I-4 and I-5b we find that

$$F_A = (T_1 + T_2) \cos 12^\circ$$

also, $F_A = \dfrac{F_1 (b \sin 5.5^o + B)}{a}$

$F_1 = F_b = 237$ lb

$b = .7$ in.

$a = .38$ in.

$B = .050$ in.

$$F_A = \frac{F_1 (.7 \times .1 + .05)}{.38}$$

$$F_A = 74.5 \text{ lb}$$

$$\Rightarrow T_1 + T_2 = 76$$

but $T_1 = K_{C1} \delta_A \Rightarrow \dfrac{T_1}{T_2} = \dfrac{K_{C1}}{K_{C2}}$

$T_2 = K_{C2} \delta_A$

$$T_1 + T_1 \frac{K_{C2}}{K_{C1}} = 76$$

$$T_1 = \frac{76}{1 + \frac{2.35}{4.7}} = \frac{76}{1.5}$$

where

T_1 = tension in cable element L_1, Lb

T_2 = tension in cable element L_2, Lb

$K_{C1} = 4.7 \times 10^3$ lb/in

$K_{C2} = 2.35 \times 10^3$ lb/in

$$\boxed{T_1 = 51 \text{ lb} \quad , \quad T_2 = 25 \text{ lb}}$$

It should be noted that the above calculation assumes that the cable pulley is locked and the cable is in turn locked to the pulley. This is a conservative assumption which more than compensates for the effects of cable

friction elsewhere in the system.

The above maximum value of cable tension (T_1 = 51 lb) is safe since the cables have and ultimate breaking strength of 70 lb.

I.5 Stress Analysis - Support Elements: The only support elements considered to be critically loaded are the two support posts (see fig 2-3). Forces f_1 and f_2 act thru point "A" to produce bending stresses and compressive stresses. The largest values of f_1 and f_2 occur when the alternating force acts in the opposite direction from that used to determine the maximum load on the clamping elements (see "dashed" force in fig I-3). The dynamic force acting @ point C is given by:

(4) $$F_C = \frac{K_C F A C}{K_B b^2 + K_C C^2}$$

where -

$K_C = 36 \times 10^4$ lb/in

$K_B = .9 \times 10^4$ lb/in

a = .924 in

b = .740 in

C = .656 in

F = 440 lb

$\Rightarrow F_C = 600$ lb

The static preload acting at point "C" is given by:

$$F_{Cp} = \frac{b}{C} F_o$$

F_o = preload @ point "B" = 730 lb

$\Rightarrow F_{Cp} = 820$ lb

Thus, the total load acting @ point "C" is found to be

$\Rightarrow F_{CT} = F_C + F_{CP} = 1420$ Lb

The total load acting @ point "B" is found by using eq (3) with the dynamic load being negative instead of positive. Thus,

$$F_{BT} = -16.5 + 730$$

$$\Rightarrow F_{BT} = 713.5 \text{ lb}$$

The values of f_1 and f_2 can now be determined as follows:

$$\sum F_X = 0 = f_2 \cos 50^\circ - f_1 \cos 50^\circ + F_{CT} - F_{BT} \cos 45^\circ + F$$

$$.643 (f_1 - f_2) = 1420 + 440 - 713.5 \times .707$$

$$f_1 - f_2 = 1355/.643$$

(a) $f_1 - f_2 = 2110$ lb

also, $F_y = 0 = (f_1 + f_2) \text{Sin } 50^\circ - F_{BT} \text{ Sin } 45^\circ$

(b) $F_1 + f_2 = 660$ lb

Solving equations (a) and (b) gives the following values for f_1 and f_2

$$f_1 = 1385 \text{ lb}$$

$$f_2 = -785 \text{ lb}$$

A negative value of f_2 is not possible since the interface between the tip mass and the support posts can only react compressive loads. Thus f_1 carries the full load @ an angle β other than 50°. In this case the point A moves to A".

The dynamic load F_C then becomes

$$F_C = \frac{K_C F a C}{K_B b^2 + K_C C^2}$$

where

$a = .74$ in.
$b = .88$ in.
$c = .84$ in.

} apply @ point "A"

$$\Rightarrow F_C = 378 \text{ lb} \Rightarrow F_{CT} = \underline{1198 \text{ lb}}$$

$$F_B = \frac{-K_B F a b}{K_B b^2 + K_C C^2} = -10 \text{ lb} \Rightarrow F_{BT} = \underline{720 \text{ lb}}$$

Equations (a) and (b) above then become

(a) $f_1 \cos\beta = 1128$

(b) $f_1 \sin\beta = 510$

$f_1 = 1240$ lb

$\beta = 24.3^\circ$

The only potential flaw in the above analysis is the assumption that f_1 could act @ any angle β. The force f_1 must be capable of acting at an angle of 24.3° from the normal to the support post surface. If only friction were available to satisfy this condition, the required coefficient of friction

between the tungsten tip mass and the aluminum support post would have to be 0.50.* The coefficient of friction between these two metals is in reality about .60 so friction alone should allow β to be 24.3°. In addition to this, however, local penetration of the tungsten into the aluminum will also help to support a 24.3° value of β. Thus the two support posts share a load of 1240 lbs acting at an angle of 24.3° thru point A". The resulting bending stress in each post becomes:

$$\sigma = \frac{MC}{I}$$

$C = .25$ in.

$I = \frac{.50\ (.5)^3}{12} = .0052$ in

$M = f \cos 24.3^{\circ} \times d$

$d = .93$ in

$f = f_1/2 = 620$ lb

} See fig I-3

$$\boxed{\sigma = 25{,}200 \text{ psi}}$$

This value of stress is quite safe since the ultimate tensil strength of 2024-T4 aluminum is 62,000 and the yield is 42,000 psi. There are generous radii at the base of each support post which eliminate stress concentrations in a material as ductile as 2024-T4 aluminum. Fatigue will not be a problem since a fully alternating stress of 25,200 psi will guarantee 10^6 cycles of operation without a failure (for 2024-T4 aluminum). In reality the stress level one half cycle later is not 25,200 psi but approximately 10,600 psi (due to the difference in the spring constants of the clamping elements and the support elements) and consequently the fatigue life is even greater since the stress is not fully alternating.

*When the dynamic load is reversed, f_2 supports the tip mass at the support post at an angle of 45°. The minimum coeff. of friction required to support this is only .09 which is easily exceeded for the materials in question.

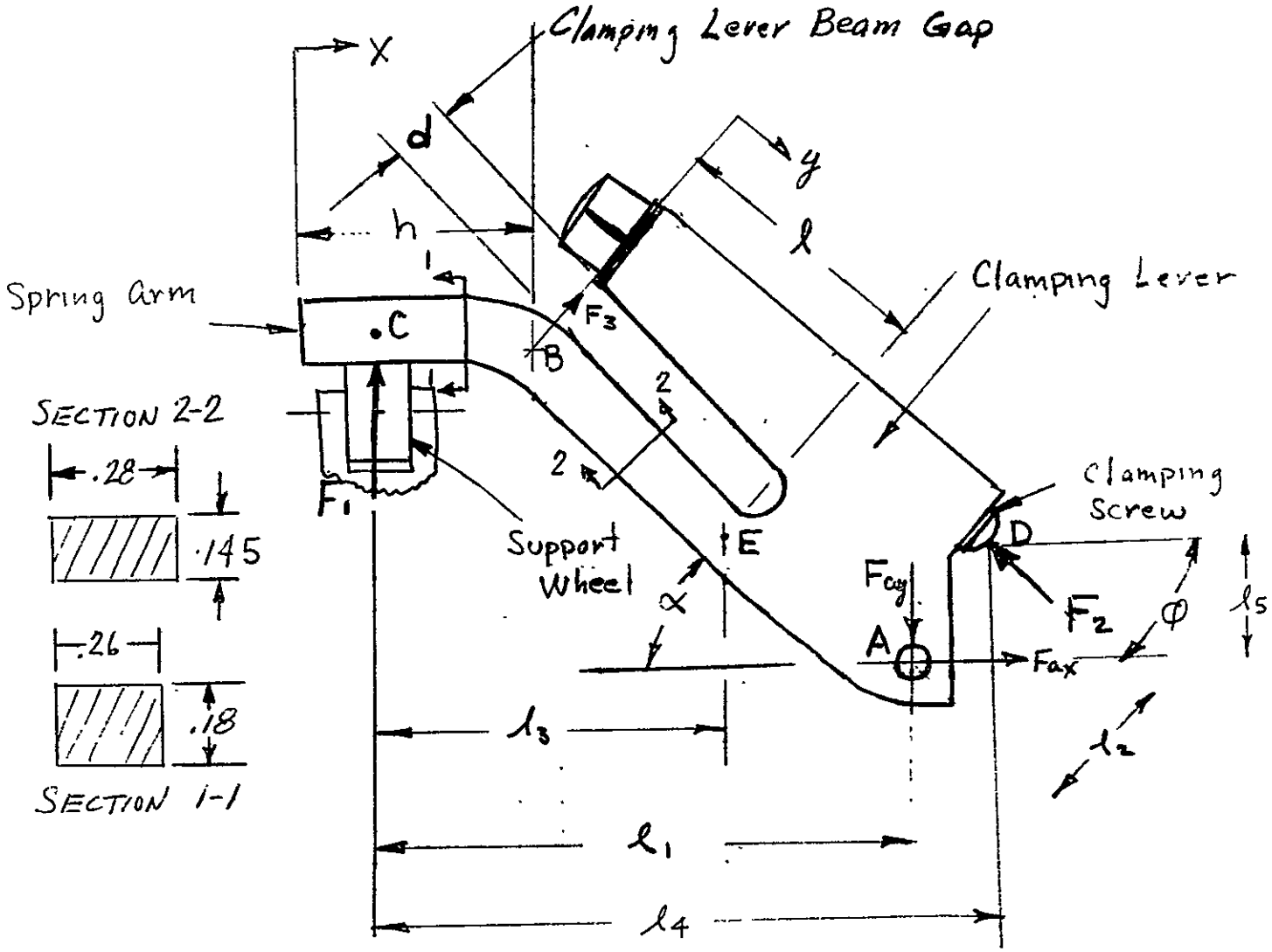

PRE-LOADED CLAMPING LEVER

FIG I-1

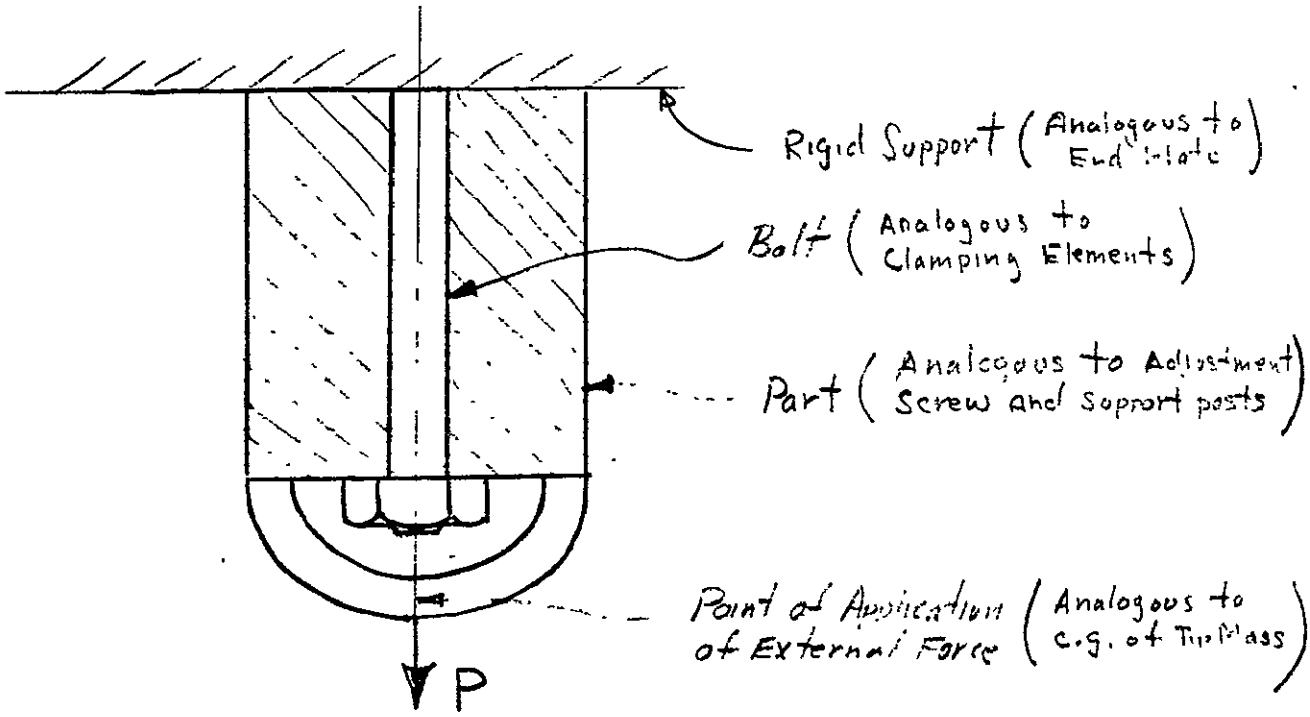

PRE-LOAD ANALOGY

FIG I-2

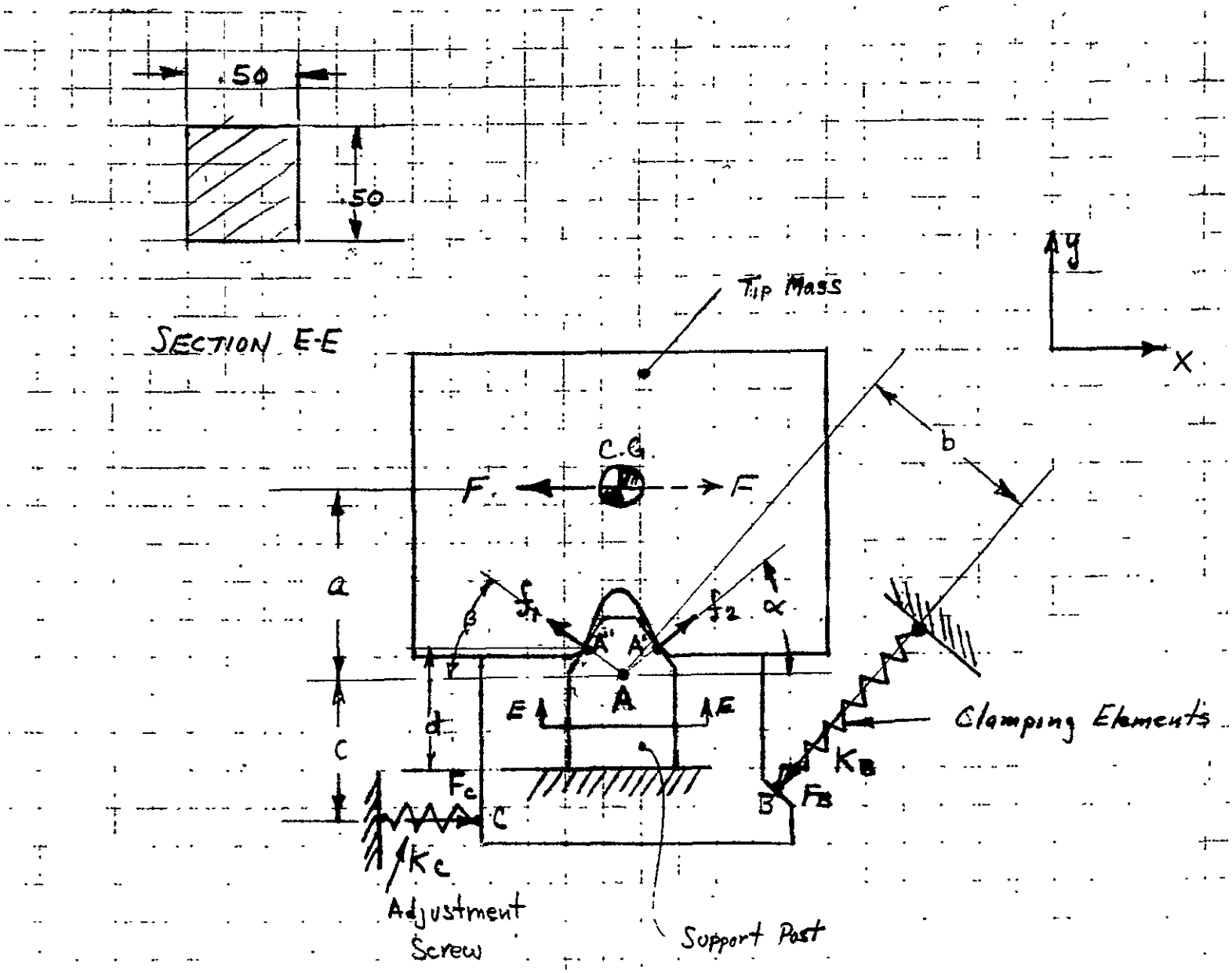

DYNAMIC MODEL OF TIP MASS RELEASE MECHANISM

FIG I-3

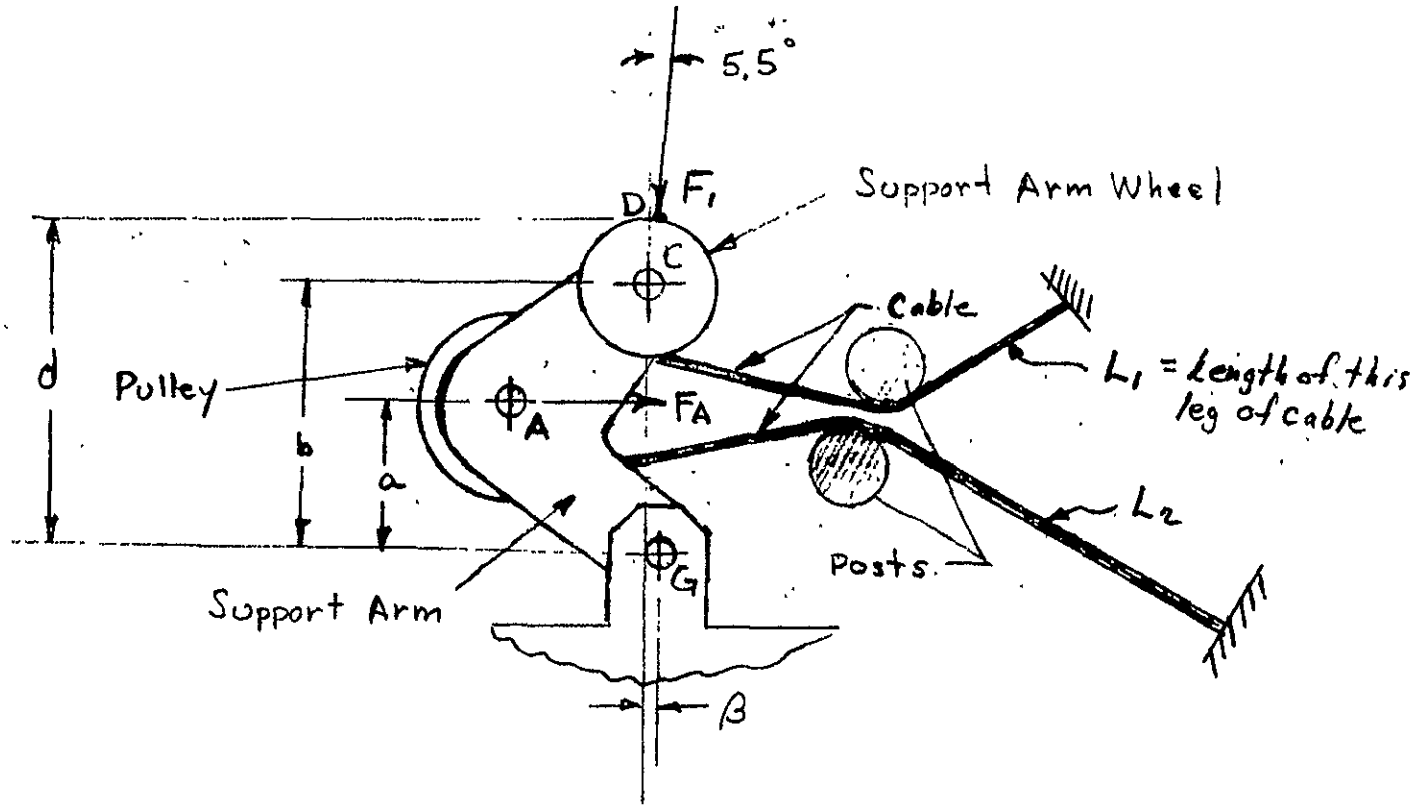

SUPPORT ARM AND CABLE UNDER LOAD

FIG I-4

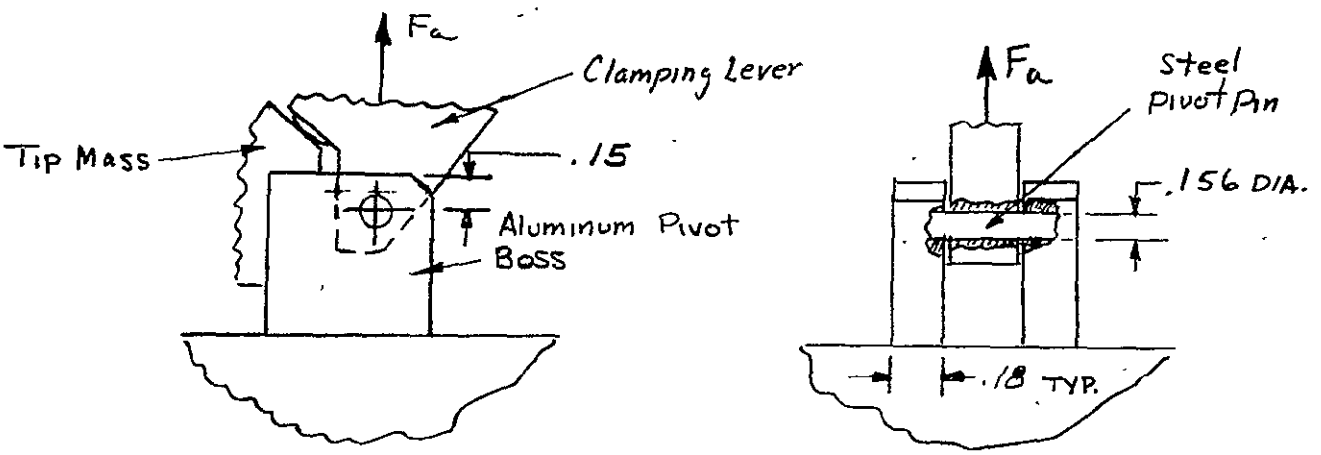

FIG I-5a Clamping Lever Pivot

CLAMPING LEVER PIVOT

FIG I-5A

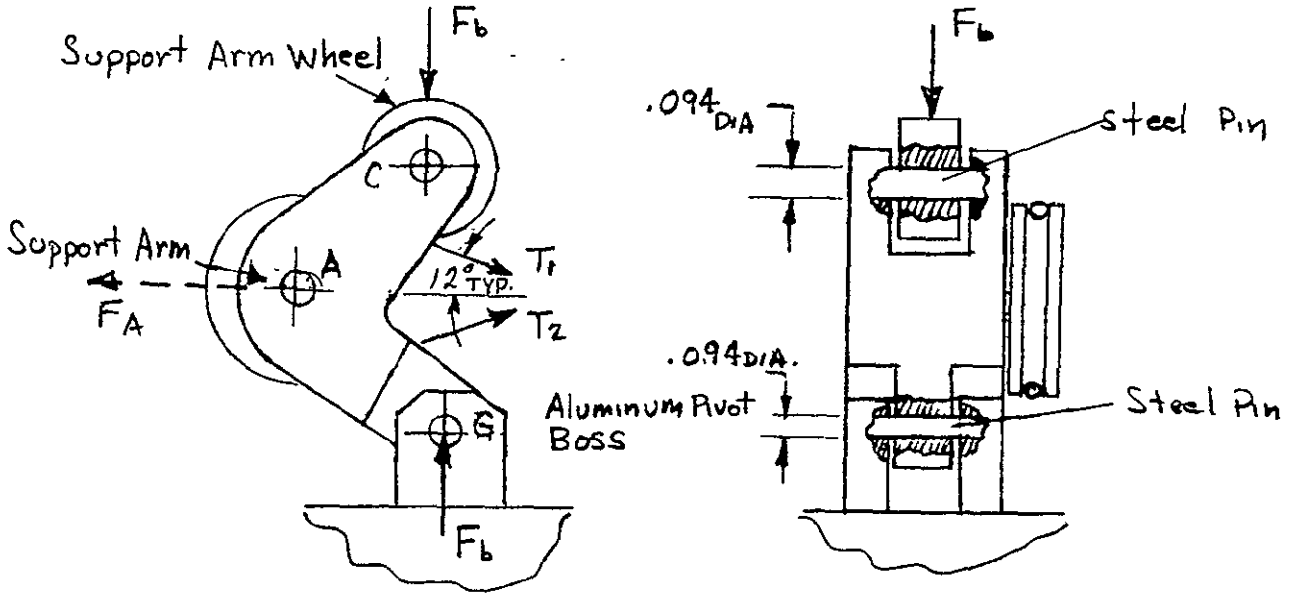

SUPPORT ARM PIVOTS

FIG I-5B

APPENDIX - J

DETERMINATION OF MAXIMUM DEPLOYER GEAR STRESSES - OPERATIONAL LOADING

J.1 Scope of Analysis

This analysis will consider the effects on the deployer gears of the deployment and retraction operation. Wherever possible, the gear loads equivalent to the motor stall torque will be used. In each case in which this assumption is made, a preliminary analysis was conducted (not included) to verify that stall conditions will not occur in the most extreme operating conditions. Consequently, the assumption of a stall condition is, at all times, conservative. No consideration is given to gear wear problems because of the short required life of the mechanism and the relatively low gear speeds and torques.

J.2 Determination of Gear Loads

Figure J-1 shows the deployer gear train. For the stall condition at the motor (motor torque = 5 oz.-in.), the gear loads are determined as follows:

J.2.1 Small Miter Gear - (F_1)

The force on the small miter gear which is appropriate for calculating the maximum gear tooth stress is the tangential force at the outside pitch diameter of the gear. The outside pitch diameter for this gear is .50 in. Thus:

$$F_1 = \frac{2T_1}{d_o}$$

T_1 = stall torque on motor = 5 oz.in.

d_o = outside pitch diameter of miter gear = .50 in.

$$\boxed{F_1 = 20 \text{ oz.} = 1.25 \text{ lb.}}$$

J.2.2 Large Miter Gear - (F_2)

The force on this gear is the same as for the small miter gear:

$$\boxed{F_2 = F_1 = 20 \text{ oz.} = 1.25 \text{ lb.}}$$

J.2.3 Harmonic Drive Gear - (F_3)

The torque on the harmonic drive gear in the stall condition will e 144 times the motor stall torque. Thus,

$$T_3 = 144\ T_1 = 720 \text{ oz.in.}$$

The force acting at the pitch diameter could come from the drive gear and/or the reel gear. For this analysis, it will be assumed that the tangential load is carried by one gear at one time, and the other gear at a different time. Thus, the maximum gear tooth load will be:

$$F_3 = \frac{2T_3}{D_3}$$

D_3 = pitch diameter of harmonic drive gear = 3.5 in.

$$\boxed{F_3 = 410 \text{ oz.} = 25.7 \text{ lb.}}$$

J.2.4 Drive Gear and Reel Drive Gear - (F_4), (F_5)

By virtue of the above assumption, each gear could be subjected to a tangential load equal to F_3. Thus,

$$\boxed{F_4 = F_5 = F_3 = 25.7 \text{ lb.}}$$

J.2.5 Reel Gear - (F_6)

This gear will be subjected to the same torque as the reel drive gear. Thus,

$$T_6 = T_5 = T_3 \frac{D_5}{D_3}$$

D_5 = pitch diameter of reel drive gear = 2.75 in.

$$T_6 = 720 \times \frac{2.75}{3.5}$$

$$T_6 = 565 \text{ oz.in.}$$

The tangential load which is required to react this torque is given by:

$$F_6 = \frac{2T_6}{D_6}$$

D_6 = pitch diameter of reel gear = 3.00

$$= \frac{2 \times 565}{3}$$

$$\boxed{F_6 = 377 \text{ oz.} = 23.5 \text{ lb.}}$$

J.2.6 Drag Gear - (F_7)

$$\boxed{F_7 = F_6 = 23.5 \text{ lb.}}$$

J.2.7 Potentiometer Worm Gear and Worm - (F_8)

For the motor stall torque to be reacted completely by the potentiometer worm gear, the resulting stress is far in excess of the allowable ultimate stress value of 24,000 psi (for phosphur bronze). Thus, the actual load will be determined based on an internal potentiometer friction torque of 5 oz.in. (max. torque value specified on vendor part drawing). Thus, the gear load becomes

$$F_8 = \frac{2T_8}{D_8}$$

$T_8 = 5$ oz.in.

D_8 = pitch dia. of worm gear = .78

$$= \frac{10}{.78}$$

$$\boxed{F_8 = 12.8 \text{ oz.}}$$

J.2.8 Limit Switch Worm Gear and Worm - (F_9)

As for the potentiometer worm, the assumption of stall torque cannot be used. Assuming that the limit switch friction torque is 10 oz.in. (conservative, based on measurements made on prototype unit), the worm gear-worm force is given by:

$$F_9 = \frac{2T_9}{D_9}$$

T_9 = 10 oz.in.

D_9 = pitch dia. of worm gear = .625

$$\boxed{F_9 = 32 \text{ oz.}}$$

J.3 Determination of Gear Stresses

J.3.1 Miter Gears - (Refer to J.2)

The maximum gear tooth stress (bending stress at base of gear tooth) is given by:

$$*_S = \frac{(F)(DP)}{\beta \text{ by } \pi} \times \frac{d_o}{d_i}$$

where:

F = tangential force acting at outer pitch diameter

DP = diametral pitch evaluated at the outer pitch diameter

β = stress concentration based on the virtual number of teeth

y = Lewis factor based on the virtual number of teeth

b = face width

d_o = outer pitch diameter

d_i = inner pitch diameter

small miter gear:

F_1 = 1.25 lb. DP = 72

d_i = .312

d_o = .500

b = .12

---

* - "Design of Machine Elements," M. F. Spotts, 2nd Edition, Prentice Hall, Pg. 343

The value of y and β must be determined on the basis of the virtual number of teeth N'. But, $N' = \frac{N}{\cos\alpha}$

where: $N = 36$ = actual number of teeth

α = pitch cone angle = 45°

Thus, $N' = 51$ teeth. The values of y and β are then found to be

$y = .130$

$\beta = .725$

Thus, the gear stress is found to be

$\boxed{S_1 = 4{,}230 \text{ psi}}$

Since the gear is #303 stainless steel with an ultimate strength of 95,000 psi, the above stress is quite safe.

<u>large miter gear</u>

$F_1' = 1.25$ lb. DP = 72

$d_i = .83$ in.

$d_o = 1.0$ in.

$N = 72$ teeth, $\alpha = 45°$) $N' = 102$ teeth $\Rightarrow \beta = .67$, & $y = .142$

Thus, the gear stress becomes

$\boxed{S_2 = 3{,}020 \text{ psi}}$

Since this gear is 2024-T4 aluminum with an ultimate strength of 60,000 psi, the above stress is quite safe.

J.3.2 <u>Spur Gears</u>

All spur gears can be examined for maximum tooth stresses using the following equation:

$$S = \frac{F\ DP}{\beta \text{ by } \pi}$$

<u>where:</u>
F, DP, b are defined the same as above, and β and y are the same except that they are evaluated for the actual number of teeth.

Table J-1 lists the values of F, DP, β, y, b, along with the resulting stress for each gear. (Refer to fig. J-1)

Table J-1

Gear Number (-)	F (lb.)	DP (teeth) (in.dia.)	β (-)	y (-)	b (in)	S (psi)
3	25.7	24	.69	.1395	.188	10,850
4	25.7	24	.735	.125	.188	11,400
5	25.7	24	.71	.1356	.188	10,850
6	23.5	32	.685	.1413	.125	19,700
7	23.5	32	.72	.1324	.125	20,000

Gears 3 and 7 are made of 303 stainless steel with an ultimate strength of 95,000 psi. Gears 4, 5, and 6 are made of 2024-T4 aluminum; S_{ult} = 60,000 psi. It is obvious, therefore, that the teeth of all of the deployer gears are adequately strong to withstand the full stall torque of the motor which is the most severe load condition that could be encountered.

J.3.3 Worm Gears and Worms

The following equation is used to determine the maximum bending stress acting on worm gear tooth,

$$S = \frac{F}{b_2 y CP_2}$$

F = tangential load on worm gear

b_2 = face width of worm gear

y = factor for worm gears depending on number of teeth, N

CP_2 = circular pitch for worm gear

potentiometer worm gear

$F = F_8 = 12.8$ oz. = .8 lb.

$b_2 = .188$

$y = .100$ for $N \geq 40$

$$CP_2 = \frac{\pi D_8}{N} = \frac{\pi \times .78}{50} = .049$$

The maximum bending stress in the worm gear teeth is:

$\boxed{S_8 = 870 \text{ psi}}$

Since the ultimate strength of the phosphur bronze worm gear is 35,000 psi, the above stress level is quite safe.

limit switch worm gear

$F = F_9 = 2$ lb.

$b_2 = .188$

$y = .100$ (N = 40 teeth)

$$CP_2 = \frac{\pi D_9}{N} = \frac{\pi \times .625}{40} = .049$$

The maximum bending stress in the worm gear teeth is:

$\boxed{S_9 = 2{,}170 \text{ psi}}$

This is also a very safe stress level for the phosphur bronze worm gear.

The bending stress of the worm threads for both the potentiometer and limit switch worms will be no higher than the worm gear stresses, and the worms are made of stainless steel which is even stronger than phosphur bronze. Therefore, the worm threads will not fail in bending.

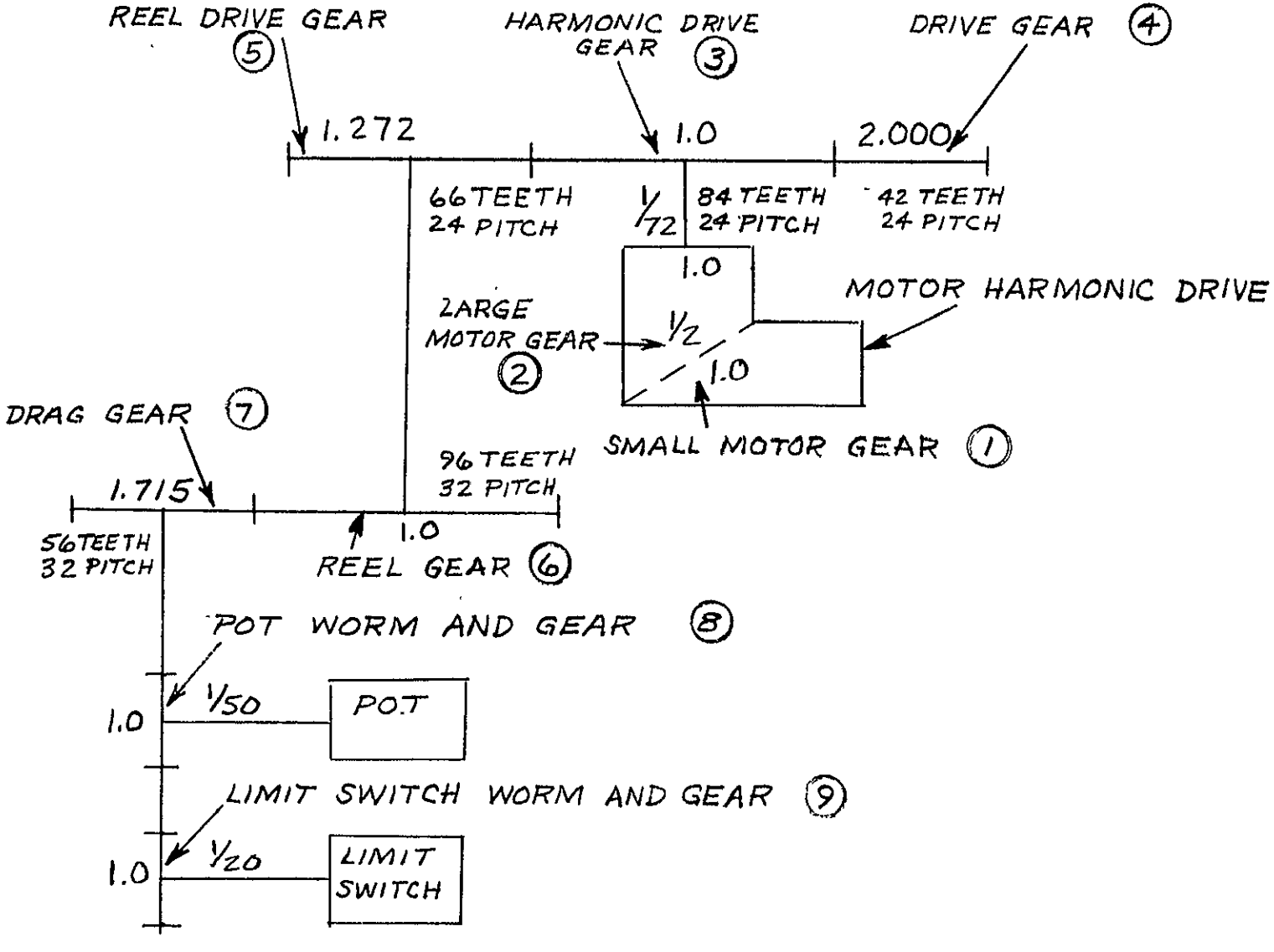

DEPLOYER GEAR TRAIN

FIG J-1

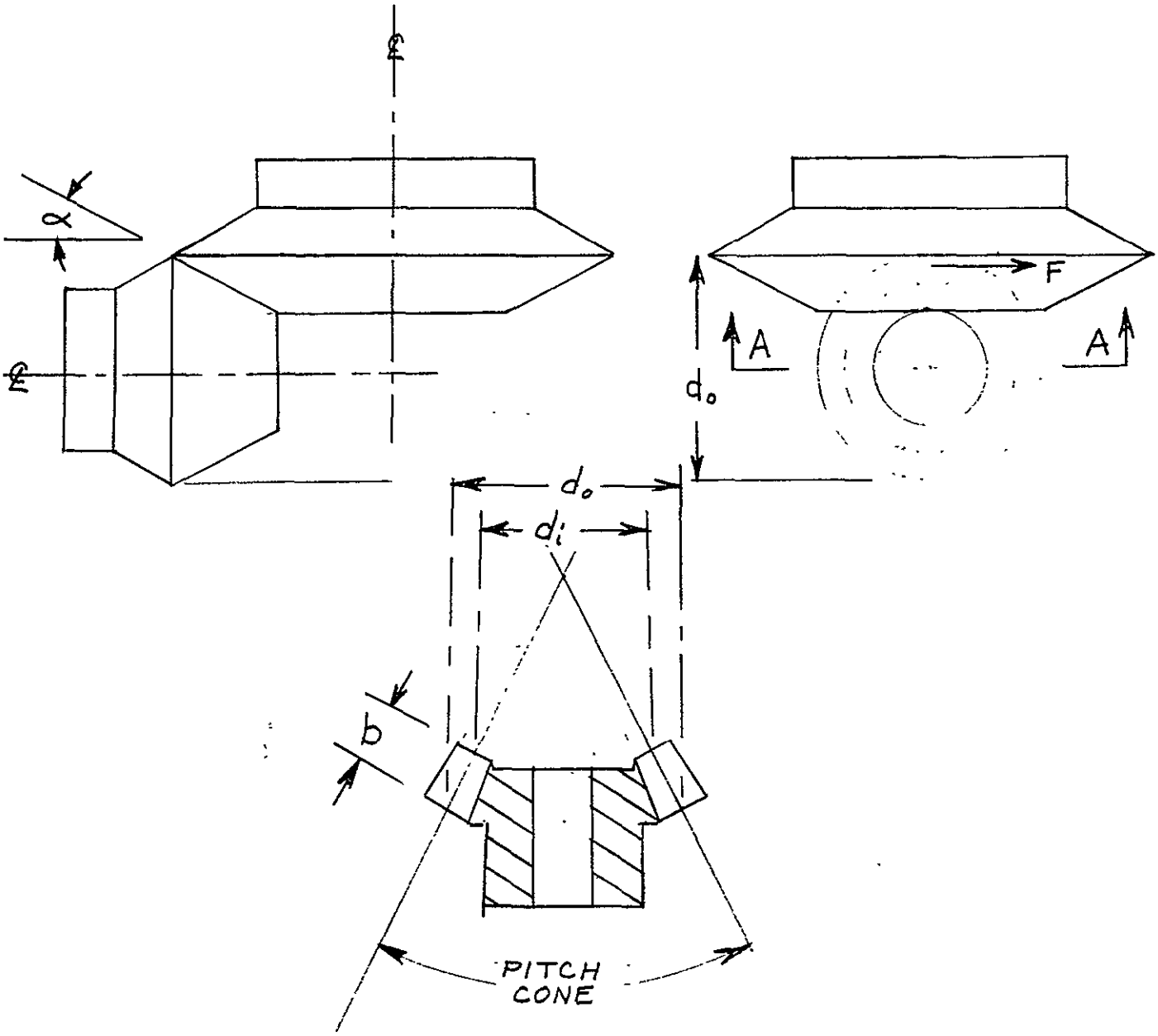

DEPLOYER MITER GEARS

FIG J-2

APPENDIX K

Determination of Scissor Mechanism Gear Stresses - Operational Loading

K.1 SCOPE OF ANALYSIS

This analysis will determine the stress on the scissor mechanism glass due to gear tooth loads generated during scissoring operation. The analysis is presented for room temperature operation (section K.2) and is then modified to include the effects of high and low temperatures (section K.3). The maximum stress values are presented in K.4. A mechanical schematic of the operation of the scissor mechanism is shown in figure 2-2.

K.2 Room Temperature Operation

Figure K-1 shows the mechanical elements of the scissor mechanism and its linkage arrangement with one of the two deployers controlled by the scissor mechanism (it is not necessary to show the other deployer linkage since it is identical to that shown). The gear tooth loads will be dictated by the torque required to turn the turnbuckles, T. This torque in turn must overcome friction in the deployer pivot, scissor leakage pivots and within the turnbuckle itself. The analysis will first determine the torque required to rotate the deployer within the deployer pivot. The axial force on the turnbuckle screw (scissor arm) required to overcome the friction in the deployer pivot and scissor linkage pivots will then be determined. Next the torque required to turn the turnbuckle in the presence of this axial load will be calculated. Finally, the resulting gear loads will be determined.

K.2.1 Deployer Pivot Torque

The deployer pivot is shown in detail in section A-A of figure K-1. The torque required to turn the "deployer pivot shaft" within the deployer pivot elements depends on the axial pre-load forces generated by torquing the #10-32 pivot screw

to 10 lb. in. of torque. This pre-load force is determined as follows:

Referring to figure K-1 a torque T_1 on the #10-32 screw will result in an axial load F given by:

* $$F_1 = 2T_1 \div \frac{dm\ l + dm\ \text{Sec}}{dm - l\ \text{Sec}} + {}_c\, dc$$

where: ds = major dia. of screw
d_{min} = minor dia. of screw
= coeff. of friction between screw and thread
$_c$ = coeff. of friction between screw head and washer
l = thread pitch
dc = dia. of screw head
dm = mean thread dia.
= $\frac{1}{2}$ thread angle

For #10-32 UNC-2A screws we find that:

dm = (ds + d_{min})/2
dm = .1645 in
= 30°
l = .03125 in/thread
dc = .373 in

Also, = $_c$ = .5 (SST against SST)

$$F = \frac{2 \times 10}{\frac{.1645}{\frac{.03125 + 3.14 \times .5 \times .1645 \times 1.155}{\times .1645 - .5 \times .03125 \times 1.155}} + .5 \times .287}$$

$$F = \frac{20}{\frac{.1645}{\frac{.03125 + .3}{.516 - .018}} + .143} = \frac{20}{.2525}$$

$$F = \boxed{79.2 \text{ lb}}$$

The friction torque (T_2) required to rotate the deployer about one deployer pivot due to pre-load is now found as follows:

* "Mechanical Engineering Design", J. E. Shigley, McGraw Hill, page 237

T_2 = (T_a) torque due to SST spacer slipping on polyimide insulator

+ (T_b) torque due to aluminum pivot block slipping on polyimide insert

+ (T_c) torque of deployer shaft slipping against the polyimide insert

$T_a = \mu F (.925 + .200)/4$

$T_a = \mu F \frac{(.563)}{2} = \frac{(.563)F}{2}$, $\mu = .30$ = coeff. of friction of metals against polyimide

$T_a = 6.66$ lb in This value is in excess of the torque required to turn the head of the #10-32 screw on the SST spacer. Thus the value of T_a should be calculated for the screw head sliding against the SST spacer.

$\therefore T_a = \mu F (.373 + .2)/4 = \frac{.287 F\mu}{2} = .143 \times 79.5 \times .5 = \underline{5.75 \text{ lb in}}$ *

$T_b = \mu F (.750 + .500)/4$, $\mu = .3$

$T_b = \underline{7.45 \text{ lb in}}$

*Note: Although this value of torque (5.75 oz in) is greater than the friction torque in the screw threads (4.25 oz in), there is no danger that the screw will turn in the helicoil insert before it can generate at least 5.75 oz in since the insert is a locking insert requiring $\approx$ 10 oz in to screw into.

$$\therefore \quad T_2^{**} = T_a + T_b = 5.75 + 7.45$$

$$T_2 = \underline{13.2 \text{ lb in}}$$

K.2.2. Axial load on turnbuckle

The axial load on the turnbuckle is determined as follows: (Referring to fig K-2).

$$\sum M_c = 0$$

$$F_a^1 \, 1.25 \sin 27^\circ + 13.2 - T_a = F_a \, 1.25 \sin 63^\circ$$

$$F_a - .51(F_a^1) = \frac{13.2 + .075 F_a - T_a}{1.11}$$

Assume $T_a \approx T_b$

and, $T_a \approx \mu F_a r_a = .019 F_a$

$$\sum F_{a,b} = 0 = F_a - F_b$$

$$\sum F_{a,b}^1 = 0 = F_a^1 - F_b^1$$

**This value of torque neglects the torque load due to scissoring forces. (T_c). These forces are reacted by the frictional forces within the pivot assembly due to preloading.

$$\sum_a M = 0 = T_a + T_b + F_b^1 (1.06)$$

$$\Rightarrow F_b^1 = -2\,T_a/1.06 = -1.89\,T_a = -.036\,F_a$$

$$F_a - .51\,(F_a^1) = \frac{13.2 - T_a}{1.11} \quad \text{but } F_a^1 = F_b^1 = -.036\,F_a$$

$$F_a - .51\,(.036\,F_a) = 11.9 - .019\,F_a$$

$$F_a - (.0184 - .0190)\,F_a = 11.9$$

$$1.0006\,F_a = 11.9$$

$$\boxed{F_a = 12.0 \text{ lbs}}$$

and

$$\boxed{\begin{array}{l} F_b = 12.0 \text{ lbs} \\ (F_b^1) = .036\,F_b = .43 \text{ lb} \end{array}}$$

Now F_b & F_b^1 have components in the "X" direction as shown in fig K2C

$$F_{bx} = F_b^1 \sin 27^\circ + F_b \cos 27^\circ$$

$$= .44 \times .57 + 12 \times .89$$

$F_{bx} = 11.95$ lb

This force is that required to overcome the friction in one pivot. Since each deployer has two pivots, the total force in one scissor arm in the "X" direction is twice the above value.

$F_{bT} = 23.9$ lb Axial load on scissor arm & turnbuckle threads

K.2.3 Determination of turnbuckle torque

The turnbuckle torque, T_T, is now determined as follows: (Refer to fig K-2d).

The torque required to turn a screw thread under an axial load is given by:

$$T = \frac{F_{bT}}{2}\left[dm\,\frac{(l + \pi\mu dm \sec\alpha)}{\pi dm - \mu l \sec\alpha} + (u)(d_c)\right]$$ not applicable

for $\frac{1}{4}$-32-UNEF thread,

$dm = .2308$
$l = .0313$
$\alpha = 30^\circ$

} also for BeCu against Al with a medium grease, $\mu \approx .15$

$$T = \frac{23.9}{2}(.2308)\left(\frac{.0313 + 3.14 \times .15 \times .2308 \times 1.155}{3.14 \times .2308 - .15 \times .0313 \times 1.1.55}\right)$$

$$T = 11.95 \times .2308\left(\frac{.0313 + .125}{.725 - .005}\right) = \frac{.1563}{.72} \times 2.76$$

$T = .6$ lb in But there are two deployers which the turnbuckle must scissor. ∴ the total torque (T_T) is twice the above value.

$T_T = 1.2$ lb in

K.2.4 Determination of loads on each scissor mehcanism gears

The loads on each gear are given as follows: (Refer to fig K-3). (All gears are 24 pitch)

$$F_1 = F_2 = \frac{1.2 \text{ lb/in}}{.41} = 2.9 \text{ lbs}$$

$$F_3 = F_2 = 2.9 \text{ lbs} \quad \text{from pot.}$$

$$F_4 = F_5 = \frac{5 \text{ oz in}}{.625} = 8 \text{ oz} = .5 \text{ lbs}$$

$$F_6 = \frac{F_3 r_3 + F_4 r_4}{r_6} = \frac{2.9 \times .33 + .5 \times .33}{.5} = \frac{3.4 \times .33}{.5}$$

$$F_6 = 2.3 \text{ lb} = F_7$$

K.3 Effect of temperature on scissoring torque values

The major scissoring torque contributions determined above for room temperature will be modified to reflect the high and low temperature environments. The high temperature is $+140^{o}$ F and the low temperature is -20^{o} F.

K.3.1 High temperature

K.3.1.1 Deployer pivot torque - high temperature

The deployer pivot torque will change due to changes in the pre-load forces caused by difference in thermal expansion among the various pivot bearing elements. The surfaces which slip against each other will be identical to those in the room temperature case. The change in pre-load is determined

as follows:

Fig K-4 shows a cross section view of the pivot bearing. Due to the $+70^{o}$ F temperature change surface [-C-] moves relative to surface [-A-] as follows

ΔX_c = motion of [-B-] relative to [-A-] + motion of [-C-] relative to [-B-]

$$\Delta X_c = (.085 \times \alpha_s \times \Delta t + .06 \alpha_p \times \Delta t) + (-.2 \times \alpha_a \times \Delta t)$$

where: α_s = coefficient of thermal expansion for SST $7 \times 10^{-6} \frac{in}{in^{o}F}$

α_p = coefficient of thermal expansion for polyimide 35×10^{-6}

α_a = coefficient of thermal expansion for aluminum 12×10^{-6}

Δt = temperature change = 70^{o} F

$$\Delta X_c = .206 \times 10^{-4} \text{ in}$$

Surface [-f-] tends to move relative to surface [-A-] as follows:

ΔX_f = motion of [-D-] relative to [-A-] + motion of [-E-] relative to [-D-] + motion of [-f-] relative to [-E-]

$$= -.1 \times \alpha_s \Delta t - (.06 \alpha_s + .06 \alpha_p) \Delta t + .165 \alpha_s \Delta t$$

$$\Delta X_f = -1.45 \times 10^{-4} \text{ in}$$

Surfaces [-C-] and [-f-] however must in reality coincide since by definition they are the same surface. Forcing these surfaces to remain coincident results in an increased tensil force in the pivot screw.

Fig K-5 shows the elements of the pivot as a series of springs. By bringing K_1 and K_3 together the resulting increase in tensil force can be determined as follows:

$$F_1 = \left(\frac{K_1 K_2}{K_1 + K_2} \right) \Delta_1$$

where:

F_1 = force in pivot screw

Δ_1 = theoretical deflection of screw (surface [-f-]) if unrestrained during +70°F temperature change, relative to restrained equilibrium position

also $F_3 = \left(\frac{K_3 K_4}{K_3 + K_4} \right) \Delta_3$

F_3 = force in pivot shaft

Δ_3 = theoretical deflection of pivot shaft (surface [-C-]), if unrestrained during +70°F temperature change, relative to restrained equilibrium

but $\Delta_1 + \Delta_3 = \Delta_T$

and $F_1 = F_3$

$$\Delta_3 = \frac{\Delta_T}{1 + \frac{K_3 K_4}{K_1 K_2} \left(\frac{K_1 + K_2}{K_3 + K_4} \right)}$$

and $F_3 = F_1 = \left(\frac{K_3 K_4}{K_3 + K_4} \right) \Delta_3$

$$F_3 = F_1 = \frac{K_1 K_2 K_3 K_4 \Delta T}{K_1 K_2 (K_3 + K_4) + K_3 K_4 (K_1 + K_2)}$$

The various values of K_1, K_2, K_3, K_4 must now be determined:

K_1 : $K_1 = \frac{AE}{l}$ where A = mean cross sectional area of pivot screw = .0226 in^2

E = modulus of elasticity of steel = 30×10^6 psi

l = length of screw between surface -f- and surface -D- = .2 in

$$K_1 = 3.4 \times 10^6 \text{ lb/in}$$

K_2 : (Refer to figure K-6a)

$$K_2 = \left[\frac{4\pi Em^2 t^3}{3(m^2-1)\left[\frac{(a^2-b^2)(3m+1)}{m+1} + \frac{4a^2 b^2 (m+1)}{(m-1)(a^2-b^2)} \left(\log_e \frac{a}{b}\right)^2 \right]} \right] \text{SST}$$

$$+ \left[\frac{4\pi Em^2 t^3}{3(m^2-1)\left[\frac{(a^2-b^2)(3m+1)}{m+1} + \frac{4a^2 b^2 (m+1)}{(m-1)(a^2+b^2)} \left(\log \frac{a}{b}\right)^2 \right]} \right] \text{Polyimide}$$

E = modulus of elasticity; 3×10^7 psi SST & 450,000 psi polyimide

m = inverse poisson's ratio; 1/.3 SST, 1/.45 polyimide

t = plate thickness; .06 for SST & polyimide

a = radius of support = .388

b = radius of clearance hole = .1

$$K_2 = \frac{4 \times 3.14 \times 3 \times 10^{7} \times 11.1 \times .216 \times 10^{-3}}{3(11.1-1)\left[\frac{(.15-.01)(11)}{4.3} + \frac{4(.15)(.01)(4.3)(\ln 3.88)^2}{2.3\ (.15-.01)}\right]}$$

$$+ \frac{4 \times 3.14 \times 4.5 \times 10^{5} \times .216 \times 10^{-3}}{3\ (3.93)\left[\frac{(.15-.01)(7.66)}{3.22} + \frac{4\ (.15)(.01)(3.22)}{1.22\ (.15-.01)}\ (\ln 3.88)^2\right]}$$

$$K_2 = 5.85 \times 10^{4} + 1.9 \times 10^{2}$$

$$\boxed{K_2 = 5.87 \times 10^{4}\ \text{lb/in}}$$

K_3 : where: A = cross sectional area of pivot shaft = .196 in^2

E = modulus of elasticity of aluminum shaft = 10^7 psi

$K_3 = \frac{AE}{l}$

l = length of shaft between surface [-B-] and surface [-C-]

$$\boxed{K_3 = 9.8 \times 10^{6}\ \text{lb/in}}$$

K_4 : (Refer to fig K-6b)

$K_{4_s} = \frac{AG}{l}$

A = shear area $\approx .06x \quad x.75 = .141\ in^2$

G = shear modulus $\approx$ 150,000 psi

l = .012 in

K_{4_s} = contribution to K_4 due to shear

$$K_{4_s} = \frac{.141 \times 150{,}000}{.012} = 1.76 \times 10^{6}\ \text{lb/in}$$

$K_{4_c} = \frac{AE}{t}$ $\quad t =$ thickness of piece in compression $\approx .06$

$A = \frac{\pi}{4}\left[(.75)^2 - (.50)^2\right]$

$E =$ modulus of elasticity $\approx 4.5 \times 10^5$ psi

$K_{4_c} =$ contribution to K_4 due to compression

$$K_{4_c} = \frac{.245 \times 4.5}{.06} \times 10^5$$

$$K_{4_c} = \underline{1.83 \times 10^6 \text{ lb/in}}$$

now, $K_4 = \frac{K_{4s} K_{4c}}{K_{4s} + K_{4c}} = \frac{1.76 \times 1.83}{1.76+1.83} 10^6$

$$\therefore \boxed{K_4 = 9 \times 10^5 \text{ lb/in}}$$

The value of F due to ΔT can now be determined.

$$\Delta T = \Delta X_c - \Delta X_f$$

$$\Delta T = .206 \times 10^{-4} + 1.45 \times 10^{-4}$$

$$\Delta T = 1.65 \times 10^{-4} \text{ in}$$

$$\Rightarrow F_3 = \frac{3.4 \times .0587 \times 9.8 \times .9 \times 1.656 \times 10^{-4} \times 10^{24}}{\left[3.4 \times .0587\ (9.8+.9) + 9.8 \times .9\ (3.4+.0587)\right] \times 10^{18}}$$

$$F_3 = \frac{1.76 \times 1.656 \times 10^2}{2.14 + 30.5} = \frac{29.2}{3.26}$$

$$\boxed{F_3 = 9.0 \text{ lb}}$$

The initial pre-load force @ room temperature has been determined to be 79.2 lbs. The total pre-load @ high temperature .°. becomes:

$$\boxed{(F)_H = 88.2 \text{ lb}}$$ @ high temperature

The resulting pivot friction torque will be proportionally higher than the room temperature pivot torque by the ratio of the pre-load forces at high and low temperature

$$\therefore (T_2)_H = T_2 \frac{(F)_H}{F}$$

where:

T_2 = pivot torque for one pivot bearing at room temperature = 13.2 oz in

F = pre-load force at room temperature

$$\boxed{(T_2)_H = 14.7 \text{ oz in}}$$

K.3.1.2 Determination of axial load on turnbuckle

High temperature will not change the nature of the friction action of the scissor linkage from the room temperature condition. The only change will be the higher pivot torque, determined above, which must now be transmitted thru the linkage. Thus, the axial load on the turnbuckle will be proportionally greater than the room temperature axial load by the ratio of the high temperature and room temperature pivot torques.

$$\therefore (F_{bT})_H = F_{bT} \times \frac{(T_2)_H}{T_2}$$

$$\boxed{(F_{bT})_H = 26.7 \text{ lbs}}$$

K.3.1.3 Determination of turnbuckle torque

Since the turnbuckle torque is directly proportional to the axial load on the turnbuckle, the high temperature value of torque is given by:

$$(T_T)_H = T_T \left(\frac{F_{bT}}{F_{bT_H}}\right) = 1.1\, T_T$$

$$\boxed{(T_T)_H = 1.32 \text{ lb in}}$$

This represents a 10% increase over the room temperature turnbuckle torque

K.3.1.4 Determination of loads on scissor mechanism gears

In like manner, the gear loads at high temperature are 10% higher than those at room temperature. Thus,

$$F_1 = F_2 = F_3 = 3.2 \text{ lb}$$

$$*F_4 = F_5 = .5 \text{ lb}$$

$$F_6 = F_7 = 2.5 \text{ lb}$$

K.3.2 Cold temperature

K.3.2.1 Deployer pivot torque

As with the high temperature case, the low temperature deployer pivot torque is proportional to the pre-load forces. In a like manner to that used to determine the high temperature pre-load it can be shown that the low temperature pre-load force is different from the room temperature value. The pertinent results of the low temperature analysis are as follows:

$$\Delta_T = -1.91 \times 10^{-4} \text{ in}$$

* F_4 & F_5 are independent of the turnbuckle torque

This value indicates that the head of the pivot screw will move away from surface [-D-] by 1.91×10^{-4} inches. The initial deflection of surface [-E-] relative to surface [-D-] is only 1.21×10^{-4} inches. Therefore the initial pre-load applied at room temperature will be completely lost at cold temperature.

Thus the pre-load is reduced to zero and consequently the pivot torque is reduced to zero.

K.3.2.2 Determination of turnbuckle axial load

Based on the above results the turnbuckle axial load will be reduced to zero.

K.3.2.3 Determination of turnbuckle torque

The turnbuckle torque due to axial loading will be zero. At the low temperature, however, the increased friction due to changes in the lubricating ability of the aprezon H grease and relative thermal expansions within the turnbuckle must be considered. The grease is applied to the scissor arm and turnbuckle threads and becomes very viscous at low temperatures. The torque required to turn one scissor arm into the turnbuckle was measured on the prototype unit and was found to be 6 oz in after a 3 hour soak at -20° F. This value includes the effects of the increase in the apparent viscosity of the grease as well as differential thermal expansion within the turnbuckle assembly. Since there are two scissor arms within the turnbuckle, the total turnbuckle torque at low temperature is:

$$(T_T)_L = 12 \text{ oz in}$$

K.3.2.4 Determination of loads on scissor mechanism gears

Since the turnbuckle torque @ low temperature is less than it is at room temperature and high temperature the resulting lower scissor mechanism gear loads will not be presented.

K.4 Determination of maximum scissor mechanism gear stresses

The stresses for each gear are found as follows:

$$*S = \frac{DP\ F}{B\ b\ \pi\ Y}$$

where DP = diametral pitch = 24

F = load normal to gear tooth, lb

b = gear face width, = .188 in

Y = Lewis factor

B = stress concentration factor

S = maximum tooth stress, (bending), psi

The value of F will be the load as calculated above and thus will not be corrected for dynamic effects because of the slow velocities ($\approx$ 3 rpm). Table K-1 lists the values of F, B, and Y for each gear. The resulting stresses are also shown in table K-1.

TABLE K-1

Gear Number	F (lb)	B (-)	Y (-)	S (psi)
1	3.2	.82	.102	1560
2	3.2	.82	.102	1560
3	3.2	.85	.094	1630
4	0.5	.85	.094	255
5	0.5	.77	.107	232
6	2.5	.79	.107	1200
7	2.5	.75	.120	1130

Since all of these gears are made of 2024-T4 aluminum with an ultimate strength of 60,000 psi, these are no stress problems.

*"Design of Machine Elements", M. F. Spotts, 2nd Edit., Prentice Hall, page 308

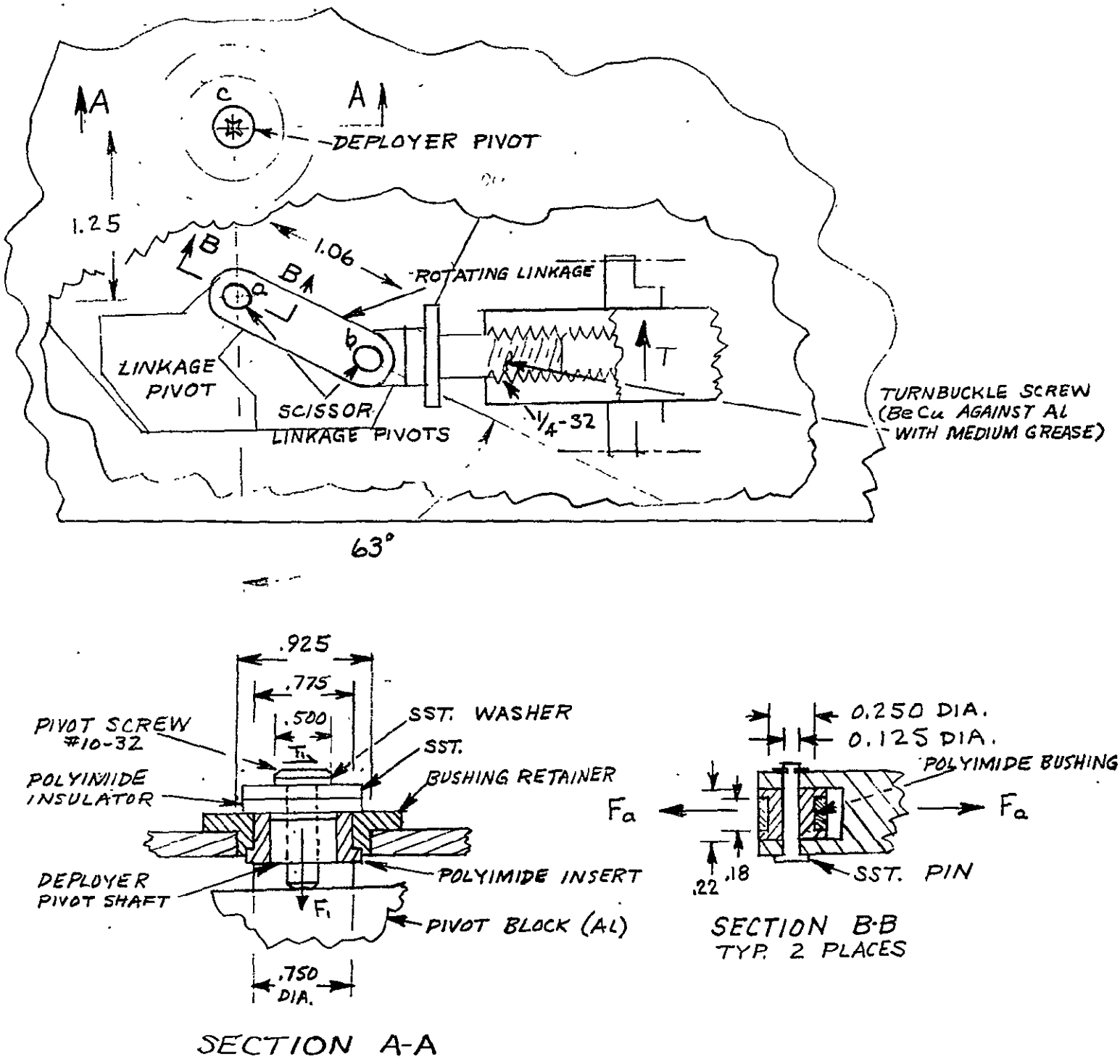

SCISSORING DRIVE TRAIN

FIG K-1

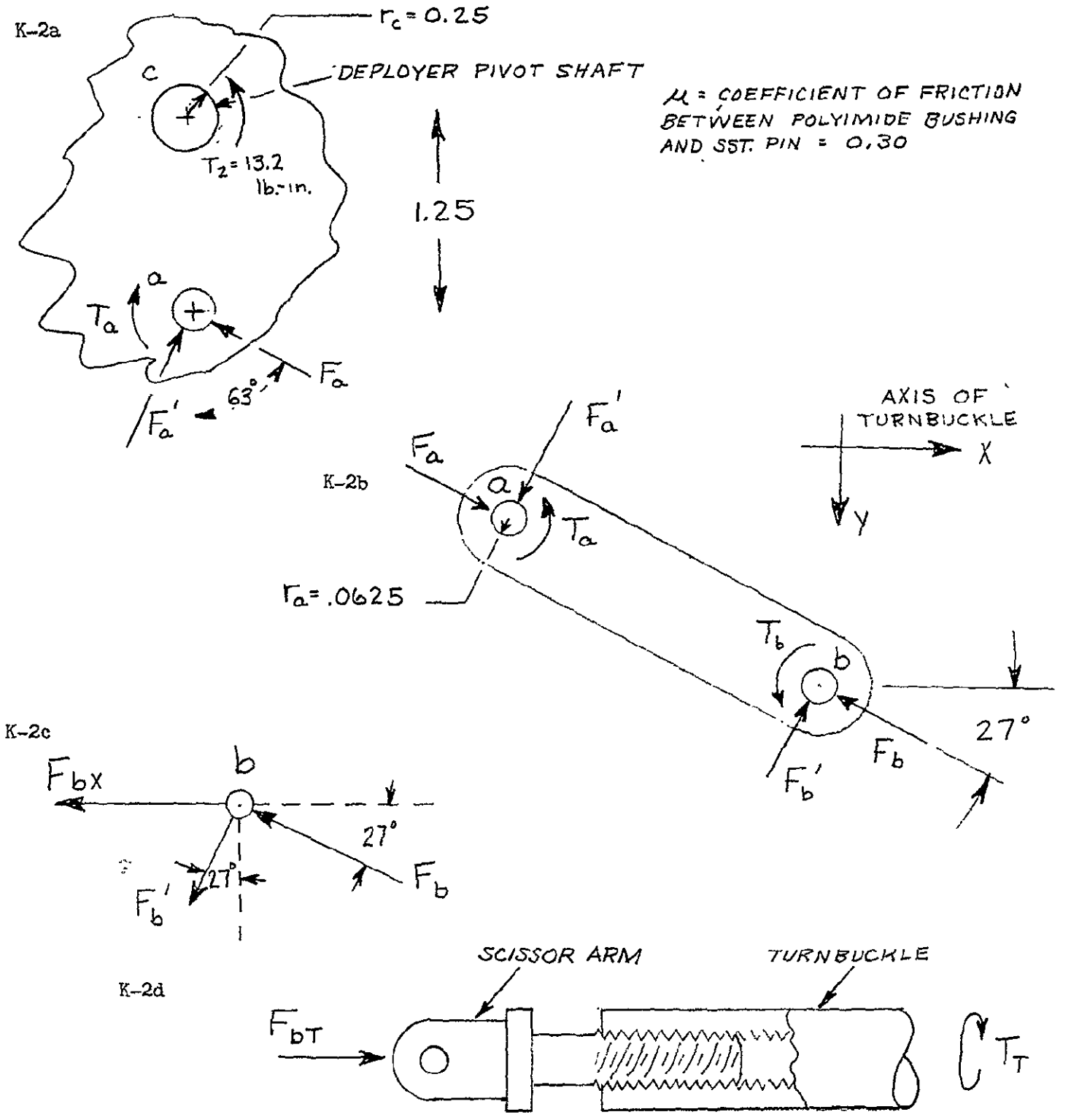

FREE BODY DIAGRAMS SCISSORING DRIVE TRAIN

FIG K-2

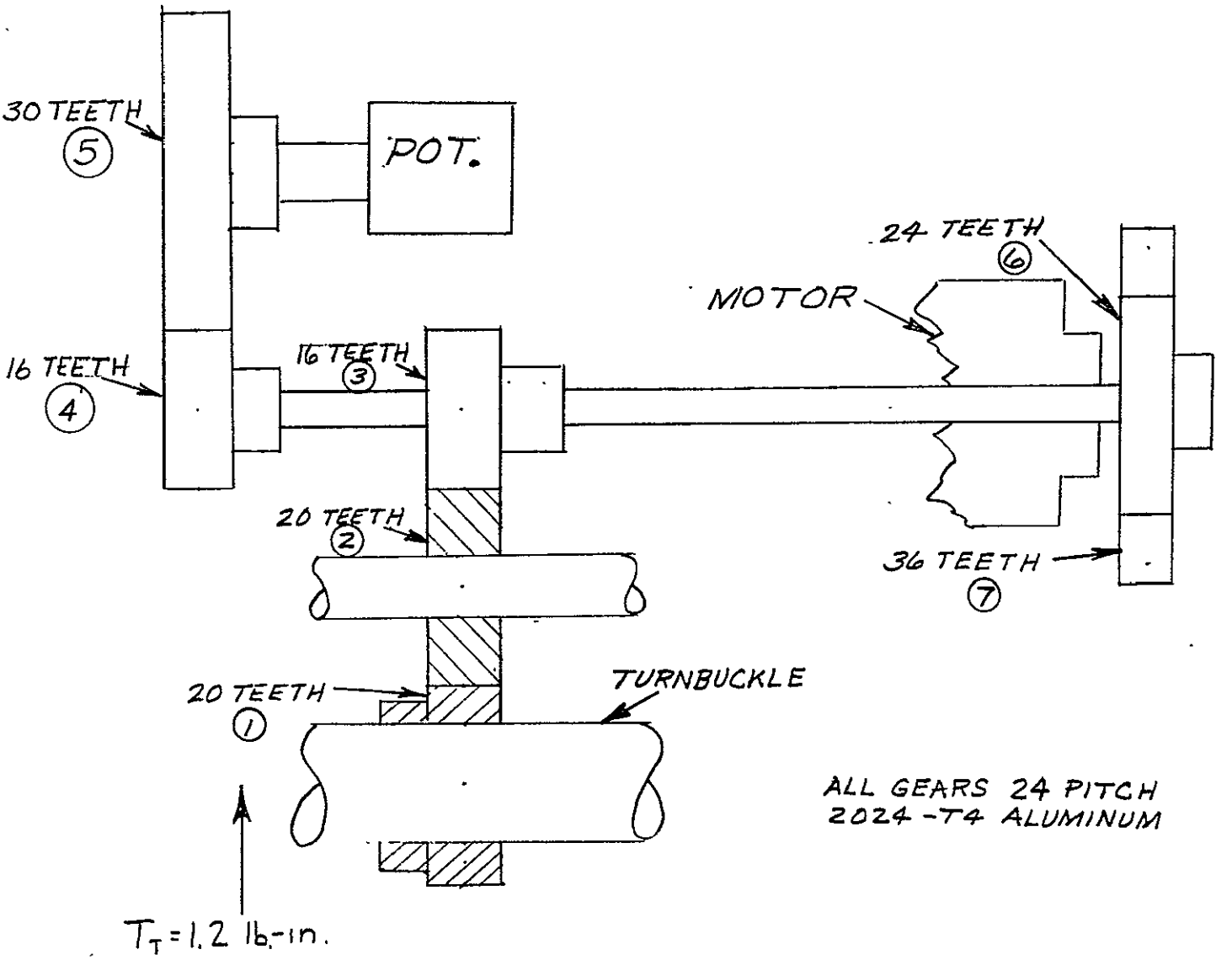

SCISSOR MECHANISM GEAR TRAIN

FIG K-3

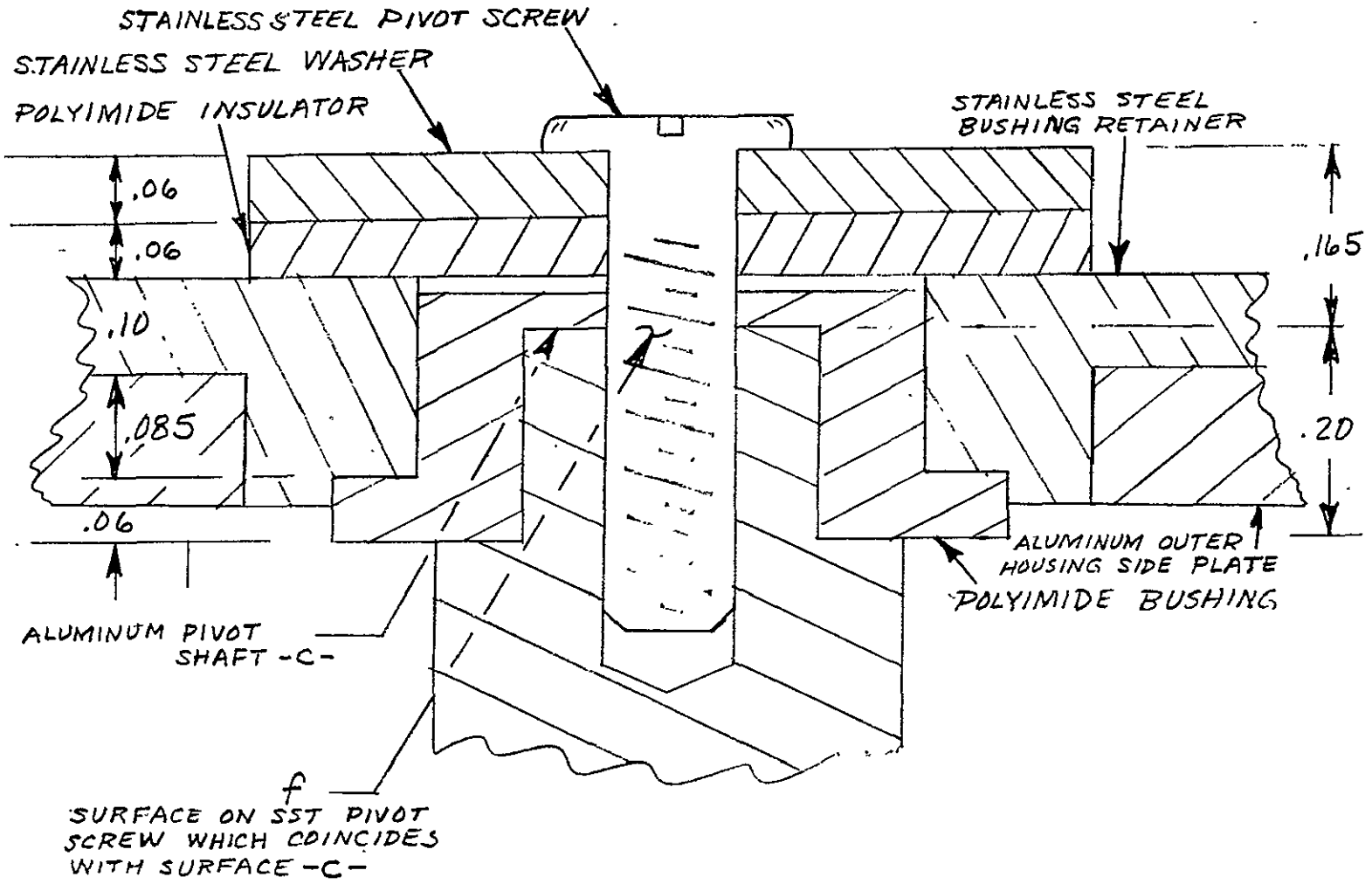

DEPLOYER PIVOT BEARING - THERMAL EXPANSION ANALYSIS

FIG K-4

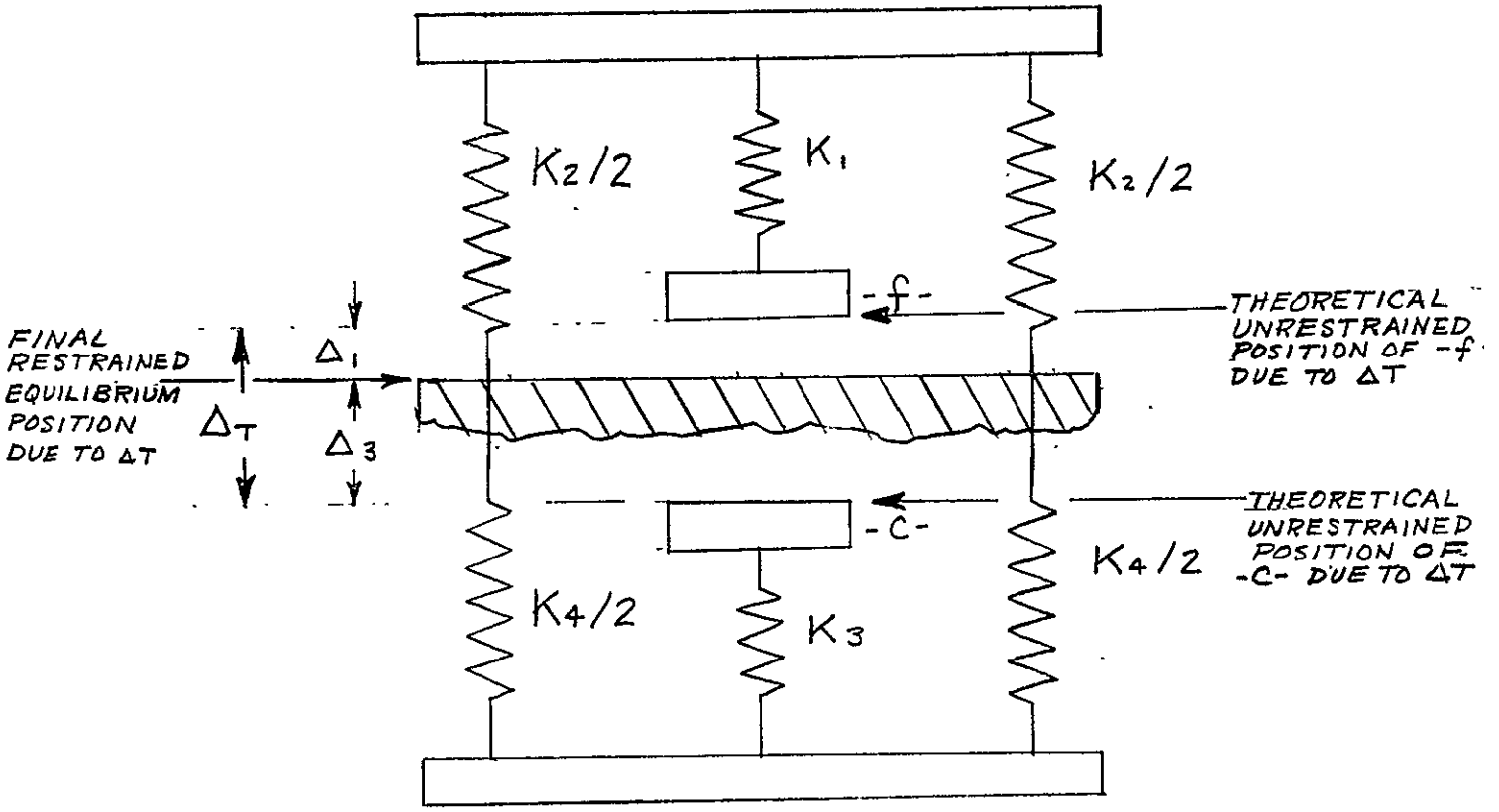

K_1 = SPRING CONSTANT OF PIVOT SCREW
K_2 = SPRING CONSTANT OF SST. SPACER AND POLYIMIDE INSERT
K_3 = SPRING CONSTANT OF PIVOT SHAFT
K_4 = SPRING CONSTANT OF POLYIMIDE BUSHING

MODEL OF DEPLOYER PIVOT BEARING -
THERMAL EXPANSION ANALYSIS

FIG K-5

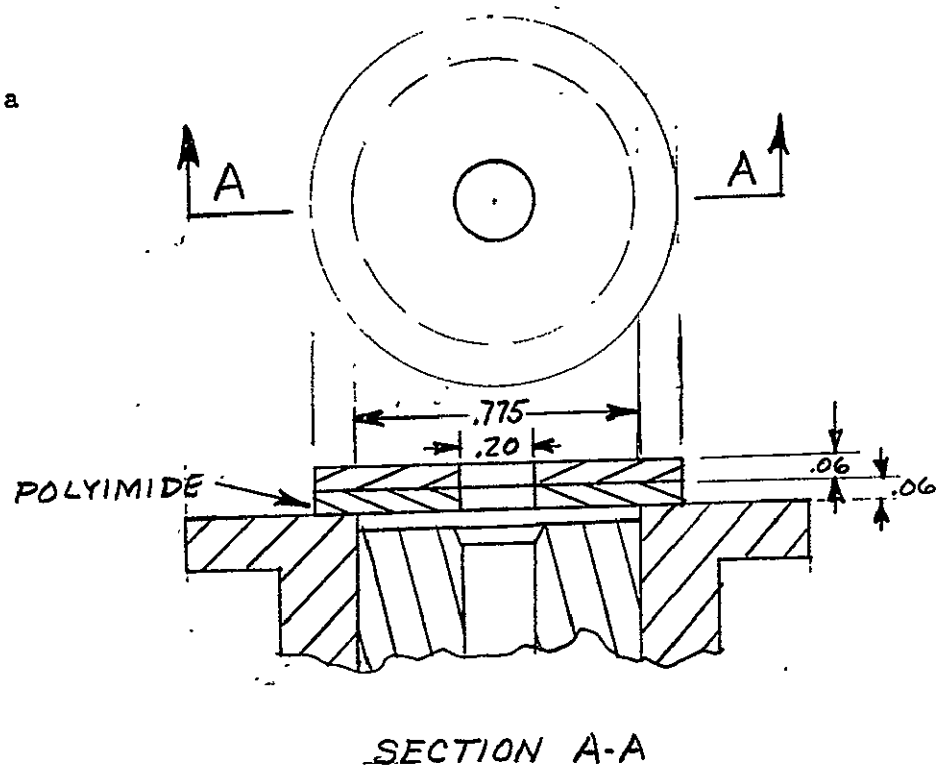

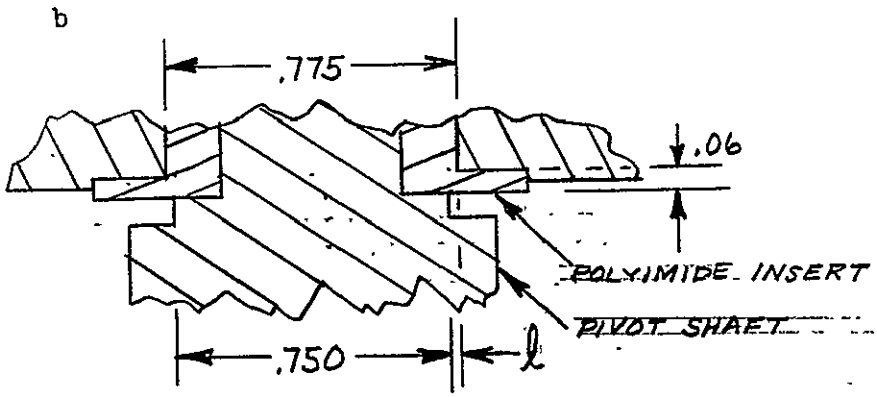

DEPLOYER PIVOT BEARING - SPRING CONSTANT ANALYSIS

FIG K-6

APPENDIX L

Determination of Structural Integrity of The Deployer Drive Roller Spring Arms - Operational Loading

L.1 Scope of Analysis

This analysis will determine the maximum bending stress on the drive roller spring arms (see Figure C-1a) due to the arm deflection required to produce the drive roller friction drive force. Of main concern is the maximum bending stress level and the degree of the resulting long term stress relaxation in the arms, which could lead to a loss of a significant part of the drive roller friction drive force.

L.2 Derivation of the Maximum Bending Stress Equation

Referring to Figure C-1c, the moment for $0 \leq F \leq 1$ due to load F can be written as:

$$M = F(1 + 1' - X)$$

but

$$M = \frac{d^2y}{dx^2} = \left[F(1 + 1') - FX\right] EI$$

$$\frac{dy}{dx} = \left[F(1 + 1')X - \frac{FX^2}{2} + C\right] EI$$

but for $X = 0$, $dy/dx = 0 \Rightarrow C = 0$

$$\therefore \quad (1) \quad \frac{dy}{dx} = \left[F(1 + 1')X - \frac{FX^2}{2}\right] EI$$

At $x = 1$,

$$\left(\frac{dy}{dx}\right)_1 = \left[F(1 + 1')1 - \frac{F1^2}{2}\right] EI = \left[\frac{F1^2}{2} + F11'\right] EI$$

Further integration of Equation (1) gives

$$y = \left[\frac{F(1 + 1')X^2}{2} - \frac{FX^3}{6} + C\right] EI$$

but at $X = 0$ $y + 0 \Rightarrow C = 0$

$$\therefore \quad y = \left[\frac{F(1 + 1')X^2}{2} - \frac{FX^3}{6}\right] EI$$

At $X = l$,

$$y_l = \left[\frac{F(l + l')l^2}{2} - \frac{Fl^3}{6}\right] EI = \left[\frac{Fl^3}{3} + \frac{Fl'l^2}{2}\right] EI$$

Now the deflection at point "A" is given by

δA = deflection at point "A" due to load "F"

$$\delta A = y_l + l' \left(\frac{dy}{dx}\right)_l$$

This equation assumes that there is no bending of portion of the beam of length "l" and height "d". Thus

$$\delta A = \left[\frac{Fl^3}{3} + \frac{Fl'l^2}{2} + \left(\frac{Fl^2}{2} + Fll'\right) l'\right] EI$$

$$\delta A = F\left[\frac{l^3}{3} + l'l^2 + l^2l'\right] EI$$

or (2)

$$\boxed{F = \frac{\delta AEI}{\frac{l^3}{3} + l'l^2 + l^2l'}}$$

But the equation of maximum bending stress is given by:

$$\sigma = \frac{MC}{I} K$$

Where: $M = F(l + l')$

$C = h/2$

K = Stress concentration factor

(3)

$$\boxed{\sigma = \frac{KF(l + l')h}{2I}}$$

Substituting Eq. (2) into Eq. (3) we get

(4)

$$\boxed{\sigma = \frac{\delta A(l + l')hEK}{2\left(l^3/3 + l'l^2 + ll'^2\right)}}$$

L.3 Determination of Maximum Bending Stress

For both spring arms, the length "l" is taken to be "R/2" less than the measured length to compensate for the changing cross section in the area of the fillet. Thus,

l = 1.075 in (gear side plate spring arm); .92 in (motor side plate spring arm)

Also, $l' = .39$ in (both arms)

h = .189 in (gear side), .154 in (motor side)

and $E = 10^7$ psi (both sides)

$\delta A = .012$ in (both sides)

The value of K is found to be

K = 1.19* (gear side), 1.15* (motor side)

Using the above values and equation (4), the maximum bending stress in each spring arm is given by:

σ(gear) = 19,300 psi

σ(motor) = 19,100 psi

These stress levels are quite safe if fracturing or immediate yielding of the spring arms are considered as potential failure modes. The yield strength for 7075-773 aluminum is 60,000 psi and the ultimate strength is 80,000 psi.

L.4 Determination of Long Term Stress Relaxation

Data just generated by Alcoa Aluminum Corporation Research Division indicates that a maximum stress relaxation of 2000 psi would occur over a three year period for temperatures in the same range anticipated for the deployer. If it is assumed that all bending stresses throughout the beam are reduced by the same percentage, 10%, (this is a very conservative assumption since the percent change of a given stress due to stress relaxation is greatest for the highest stress and smaller for lower stresses, and the 10% relaxation, obtained for the highest stress level, has been applied to the remaining lower stresses as well) the drive roller friction force would

be reduced by 10% likewise. This change is quite acceptable for normal deployer operation.

* "Formulas for Stress and Strain", R. J. Roark, 3rd Edit., McGraw Hill, Page 346

APPENDIX M

Analysis of Overrunning Clutch Elements - Operational Loading

M.1 Scope of Analysis

This analysis is concerned with determining the load carrying capability of the tape reel overrunning clutch in both the deploy (free wheeling) and retract (maximum clutch resistance) modes. The maximum stress in the clutch coil for a stall condition will also be determined.

M.2 Clutch Operation

The tape reel overrunning clutch consists of a coil spring, a clutch collar and a clutch hub (see figure E-1), the diameters of which are slightly larger than the inner diameter of the coil. The clutch collar is directly attached to the tape reel and the clutch hub is directly attached to the reel shaft which is isolated from the tape reel by bearings. The coil is sprung over the two cylinders thus coupling the tape reel to the shaft. The relative velocity between the tape reel and the shaft tends to unwind the coil and thus produces a slipping torque in one direction and tends to tighten the coil against the cylinder and thus produce a large drive torque in the other direction. Thus in the deploy mode the clutch is uncoupled from the drive train by slipping at a certain slip torque (must be less than 5 oz. in.) and in the retract mode the tape reel is driven directly thru the clutch (clutch should be capable of transmitting the stall torque without slipping).

M.3 Derivation of Equation of Retract Drive Torque

Figure M-1a shows a differential element of the coil and the forces acting on the element when the direction of rotation of the clutch shaft is such as to wind the coil tighter. The symbols used in the derivation are summarized in the "Symbols List" (section M-7). The torque to be determined is the torque at which slipping between the coil and the cylinders occurs.

Equilibrium Equations (Neglect bending due to $\mu dF_N r_w$)

$\sum$(Tangential Forces) = 0

$$(T + dT)\cos\left(\frac{d\theta}{2}\right) - T\cos\left(\frac{d\theta}{2}\right) = \mu dF_N$$

$$dT\cos\left(\frac{d\theta}{2}\right) = \mu dF_N$$

Assume $d\theta \longrightarrow 0$; $\cos\left(\frac{d\theta}{2}\right) = 1$

$$\boxed{dT = \mu dF_N} \qquad \text{Eq. (1)}$$

$\sum$(Normal Forces) = 0

$$dF_N = (T + dT)\sin\left(\frac{d\theta}{2}\right) + T\sin\left(\frac{d\theta}{2}\right)$$

$$dF_N = 2T\sin\left(\frac{d\theta}{2}\right) + dT\sin\left(\frac{d\theta}{2}\right)$$

Assume $d\theta \longrightarrow 0$; $\sin\left(\frac{d\theta}{2}\right) \longrightarrow \frac{d\theta}{2}$

Neglecting 2nd order differentials

$$\boxed{dF_N = Td\theta} \qquad \text{Eq. 2}$$

Define:

f = Normal force per unit length of circumference
r = coil radius
R = Shaft radius

$$dF_N = frd\theta \qquad \text{Eq. 3}$$

Combine eqs. (2) and (3)

$$frd\theta = Td\theta$$

$$fr = T$$

$$rdf = dT \qquad \text{Eq. 4}$$

Substitute into Eq. (1)

$$dT = \mu f r d\theta = r df \qquad \text{Eq. 4a}$$

$$df = \mu f d\theta \qquad \text{Eq. 5}$$

$$\int_{f_o}^{f} \frac{df}{f} = \int_{0}^{\theta} \mu d\theta$$

$$N\,(f/f_o) = \mu\theta$$

$$\boxed{f = f_o e^{\mu\theta}} \qquad \text{Eq. 6}$$

Substituting Eq. 6 into Eq. 4a and integrating

$$\int_{0}^{T} dT = \int_{0}^{\theta} \mu f_o r e^{\mu\theta} d\theta$$

$$\boxed{T = r f_o \left(e^{\mu\theta} - 1\right)} \qquad \text{Eq. 7}$$

By definition:

$$f_o = \frac{F_o}{\theta r}$$

and

$$F_o = K\theta$$

$$f_o = \frac{K}{r} \qquad \text{Eq. 8}$$

Therefore

$$\boxed{T = K\left(e^{\mu\theta} - 1\right)} \qquad \text{Eq. 9}$$

Consequently:

$$M = TR$$

$$\boxed{M = KR\left(e^{\mu\theta} - 1\right)} \qquad \text{Eq. 10}$$

The expression for K can be determined as follows:

Consider figure M-2, which shows one full turn of the clutch coil (open at point O). When the clutch is subjected to a uniform force distribution "f" lb. per inch of circumference, the coil can be thought of as being built in at point "A". Under this condition, the moment at any point "B" can be found as follows:

$$dM_B = frd\alpha \times \Delta L$$

but $\Delta L = r \sin(\theta - \alpha)$

$$\therefore M_B = \int_o^\theta fr^2 \sin(\theta - \alpha)d$$

or

$$\boxed{M_B = fr^2 \left[1 - \cos\theta\right]} \qquad \text{Eq. 11}$$

By applying a fictitious force "F" at point "O" in the "X" direction, we can determine the deflect. at point "O" in the "X" direction by using Castigliano's method.

$$\Delta X = \int_o^\pi \frac{M\,(\partial M/\partial F)}{EI}\, rd\theta$$

$$M = M_B + Fr \sin\theta$$

$$\Delta X = \int_o^\pi \frac{(M_B + Fr \sin\theta)(r \sin\theta)\, rd\theta}{EI}$$

But $F = 0$

$$\therefore \quad \Delta X = \int_o^\pi \frac{fr^4}{EI}\left(1 - \cos\theta\right) \sin\theta d\theta$$

$$\boxed{\Delta X = \frac{2fr^4}{EI}} \qquad \text{Eq. 12a}$$

In a like manner, a fictitious force "Q" at point "O" in the "Y" direction can be used to determine " ΔY".

$$\Delta Y = \int_o^{\pi} \frac{M(\partial M/\partial Q)}{EI}\, r d\theta$$

$$M = M_B + Qr\,(1 - \cos\theta)$$

$$\Delta Y = \int_o^{\pi} \frac{\left[M_B + Qr\,(1 - \cos\theta)\right]}{EI}\, r\,(1 - \cos\theta)\, d\theta$$

But $Q = 0$

$$\Delta Y = \int_o^{\pi} \frac{fr^4}{EI}\,(1 - \cos\theta)^2\, d\theta$$

$$\therefore \qquad \boxed{\Delta Y = \frac{3\pi}{2}\,\frac{fr^4}{EI}} \qquad \text{Eq. 12b}$$

Now, referring to figure M-2, we find the following relationship between "R", "ΔX", "ΔY" due to point "O" moving to $\bar{O}$ and the coil center, "C", moving to "C'".

$$R^2 = \left(r + \frac{\Delta X}{2}\right)^2 + \Delta Y^2$$

$$R = \sqrt{\left(r + \frac{\Delta X}{2}\right)^2 + \Delta Y^2}$$

We will now define $\Delta r = R - r$

$$\therefore \qquad (r + \Delta r) = \sqrt{\left(r + \frac{\Delta X}{2}\right)^2 + \Delta Y^2}$$

$$r + \Delta r = r + \frac{\Delta X}{2} + \tfrac{1}{2}\left(r + \frac{\Delta X}{2}\right)^{-1} \Delta Y^2$$

$$\Delta r = \frac{\Delta X}{2} + \frac{\Delta Y^2}{2\left(r + \frac{\Delta X}{2}\right)}$$

But $\frac{\Delta X}{2} << r$

Then, $\Delta r = \frac{\Delta X}{2} + \frac{\Delta Y^2}{2r}$

$$\Delta r = \frac{fr^4}{EI} + \frac{\left(\frac{3\pi}{2}\right)^2 f^2 r^8 / E^2 I^2}{2r}$$

$$\Delta r = \frac{fr^4}{EI} + \frac{11.1f^2r^7}{E^2I^2}$$

$$f^2\left(\frac{11.1r^7}{E^2I^2}\right) + f\left(\frac{r^4}{EI}\right) - \Delta r = 0$$

$$f^2 + f\left(\frac{.09EI}{r^3}\right) - .09\Delta r\ \frac{E^2I^2}{r^7} = 0$$

$$f = \frac{-.045EI}{r^3} + \frac{1}{2}\sqrt{\left(\frac{.09EI}{r^3}\right)^2 + \frac{.36\Delta rE^2I^2}{r^7}}$$

$$f = -.045EI + \sqrt{.002\ \frac{E^2I^2}{r^6} + .36\frac{\Delta r}{4r}\ \frac{E^2I^2}{r^6}}$$

let $f = f_o$

$$\therefore\ f_o = \frac{EI}{r^3}\left[-.045 + \sqrt{.002 + \frac{.09\ \Delta r}{r}}\right]$$

by definition $K = rf_o$

$$\therefore\ (13)\quad \boxed{K = \frac{EI}{r^2}\left[-.045 + \sqrt{.002 + \frac{.09\Delta r}{r}}\right]}$$

Thus equations (10) and (13) define the available driving torque of the clutch in the retract mode.

M.4 Derivation of Equation of Deploy Clutch Torque

Figure M-1b shows a differential element of the coil and the forces acting on the element when the direction of rotation of the clutch shaft is such as to unwind the coil. The slip torque in this mode is found as illustrated in Figure M-1b.

Applying the same method used in calculating the maximum clutch torque resistance, the following equations are generated:

$$dT = \mu\, dF_N \qquad \text{Eq. (14)}$$

$$dF_N = -\,T d\theta \qquad \text{Eq. (15)}$$

$$dF_N = f r d\theta \qquad \text{Eq. (16)}$$

Substitute Eq. (16) into Eq. (15):

$$f r d\theta = -\,T d\theta$$

$$f r = -\,T$$

In differential form:

$$r df = -\,dT \qquad \text{Eq. (4)}$$

Substitute Eq. (16) into Eq. (14) and substitute result into Eq. (4):

$$r df = -\mu f r d\theta$$

$$\int_{f_o}^{f} \frac{df}{f} = -\mu \int_{0}^{\theta} d\theta$$

$$\ln f/f_o = -\mu\theta$$

$$f = f_o e^{-\mu\theta} \qquad \text{Eq. (17)}$$

Also by substitution:

$$dT = \mu f_o e^{-\mu\theta} d\theta$$

Integrating gives:

$$T = r f_o (1 - e^{-\mu\theta}) \qquad \text{Eq. (18)}$$

Since $f_o = K/r$

And $M = TR$

$$M = KR\,(1 - e^{-\mu\theta}) \quad \text{Eq. (19)}$$

Note that as $\mu\theta$ becomes large, M approaches KR

Thus the free-wheeling torque of the clutch in the deploy mode is defined by Eq. (19) and Eq. (13).

M.5 Determination of Retract Drive Torque and Resulting Stresses

Referring to Eq. (10)

$$M = KR\,(e^{\mu\theta} - 1) \quad \text{where:} \quad \theta = (7)(2\pi) = 44 \text{ rad.}$$
$$\mu = .15 \text{ (conservative guess)}$$
$$R = .25 \text{ in.}$$

$$M = .25K\,(e^{6.6} - 1) = .25K\,(740 - 1)$$

$$M = 185K \text{ lb-in}$$

From Eq. (13)

$$K = \frac{EI}{r^2}\left[-.045 + \sqrt{.002 + \frac{.09\,\Delta r}{r}}\right]$$

where: $E = 3 \times 10^7$ psi
$r = .243$ in $\Rightarrow \frac{\Delta r}{r} = .0291$
$\Delta r = .007$ in
$dw = .031$in

Also, $$I = \frac{\pi dw^4}{64}$$

$$I = \frac{\pi}{64}(.031)^4 = 4.55 \times 10^{-8} \text{ in}^4$$

$$K = \frac{3 \times 10^7 \times 4.55 \times 10^{-8}}{(.243)^2}\left[-.045 + \sqrt{.002 + .0026}\right]$$

$$K = 23.1\left[-.045 + \sqrt{.0046}\right] = 23.1 \times \left[-.045 + .0678\right]$$

$$K = 23.1 \times .0228$$

$$K = .526 \text{ lb/}_{\text{rad}}$$

Finally we get

$$M = 97 \text{ lb-in}$$

For a condition of motor stall, the tape reel could only see 35 lb-in of torque. Thus the above torque indicates that the clutch will never slip during operation in the retract mode. It now remains to be shown t hat the coil can transmit the stall torque without breaking. Considering tension on the coil due to transmitting the torque plus tensile bending stresses due to opening the coil to slip over the clutch hub and collar, we get:

$$\sigma = \sigma_b + \frac{T}{A}$$

$$T = \frac{35.\ \text{lb-in}}{R} = \frac{35}{.25}$$

$$T = 140\ \text{lb}$$

now, $\sigma_b = \frac{MC}{I}$

but, $M = (M_B)_{max}$

where M_B is defines in Eq. 11. Thus,

$$M = 2f_o r^2 = 2Kr = 2 \times .526 \times .243$$

$$M = .255\ \text{lb-in}$$

$$\therefore \sigma_b = \frac{.255 \times .0155}{4.55} \times 10^8 = \frac{2.55 \times 1.55 \times 10^5}{4.55}$$

$$\sigma_b = 87{,}000\ \text{psi}$$

Thus, $\sigma = 87{,}000 + \frac{140{,}000}{.785} = 87{,}000 + 178{,}000\ \text{psi}$

where

σ_b = maximum tensile bending stress due to assembly of coil over shafts

T = maximum tension in cable for stall torque

A = cross-sectional area of coil = $.785 \times 10^{-3}$

M = maximum bending moment in coil due to assembly

C = $dm/_2$ = .0155

I = moment of inertia of coil = $4.55 \times 10^{-8}\ \text{in}^4$

$$\boxed{\sigma = 265{,}000\ \text{psi}}$$

This stress cannot be achieved in reality because the yield strength of the music wire being used is $\approx$ 200,000 psi. Thus, when the combined tensile and binding stresses reach 200,000 psi at the ID of the coil, yielding will propogate radially towards the OD of the coil until the local stresses fall below 200,000 psi. Yielding can continue as the load increases until the stress exceeds the ultimate strength of the music wire (250,000 psi) at the ID side of the coil. Because of this effect if has been established that for a wire of circular cross section

and subjected to pure benching, the calculated maximum bending stress can exceed the actual ultimate strength by≈33% without causing failure. Thus σ could be as large as 333,000 psi. The value of σ obtained therefore indicates that the coil can withstand the full stall torque.

M.6 Determination Clutch Torque in Deploy Mode

From Eq. 19 we have

$M = KR\,(1 - e^{-\mu\theta})$ Where:

$K = .526$ lb/in

$R = .25$ in

$\mu\theta = 6.6$

$M = .1315\,(1 - e^{-6.6})$

$M = .1315\,(1 - .0014) = .131$ lb in

or

$M = 2.1$ oz-in

The maximum acceptable value of the deploy slip torque is 5 oz-in. Thus, it is obvious that the clutch will provide a safe level of deployment slip torque.

M.7 Symbols List

M = Torque

T = Tension caused by friction force

R = Shaft Radius

F_N = Normal Force

f = Normal force per unit circumferential length

F_o = Initial normal force due to spring stretching

f_o = Uniform initial normal force per unit circumverential length

μ = Coefficient of static friction

θ = Total coil angle for portion of coil over hub or collar

Δr = Coil radial expansion

E = Modulus of elasticity

I = Moment of Inertia

r = Coil Radius

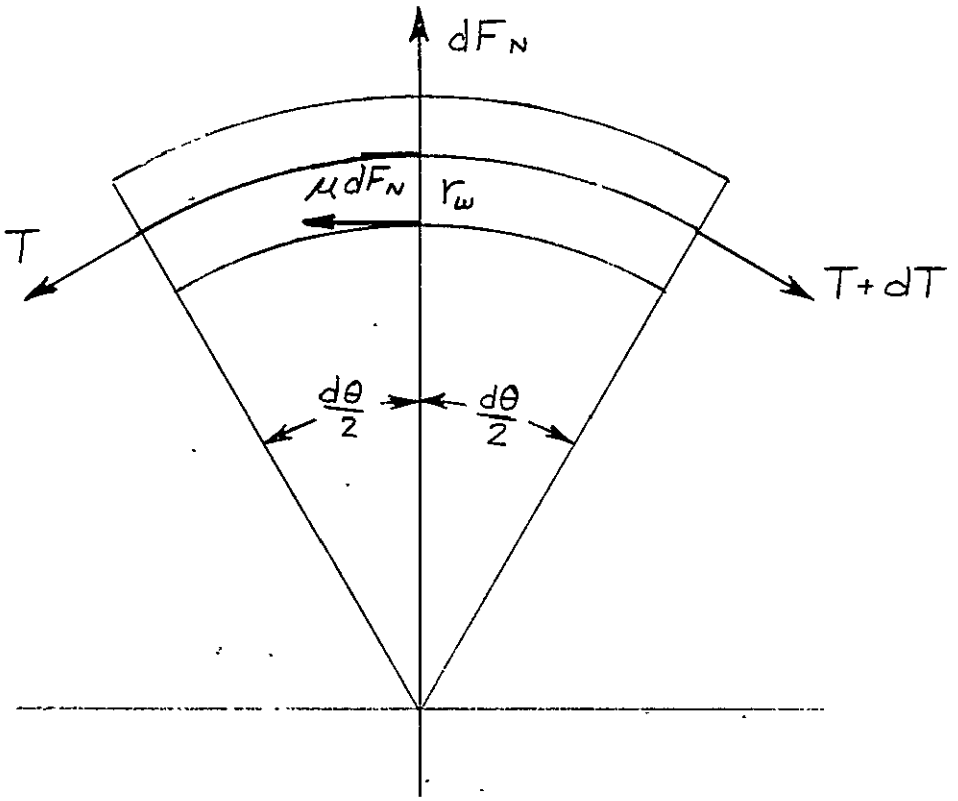

b

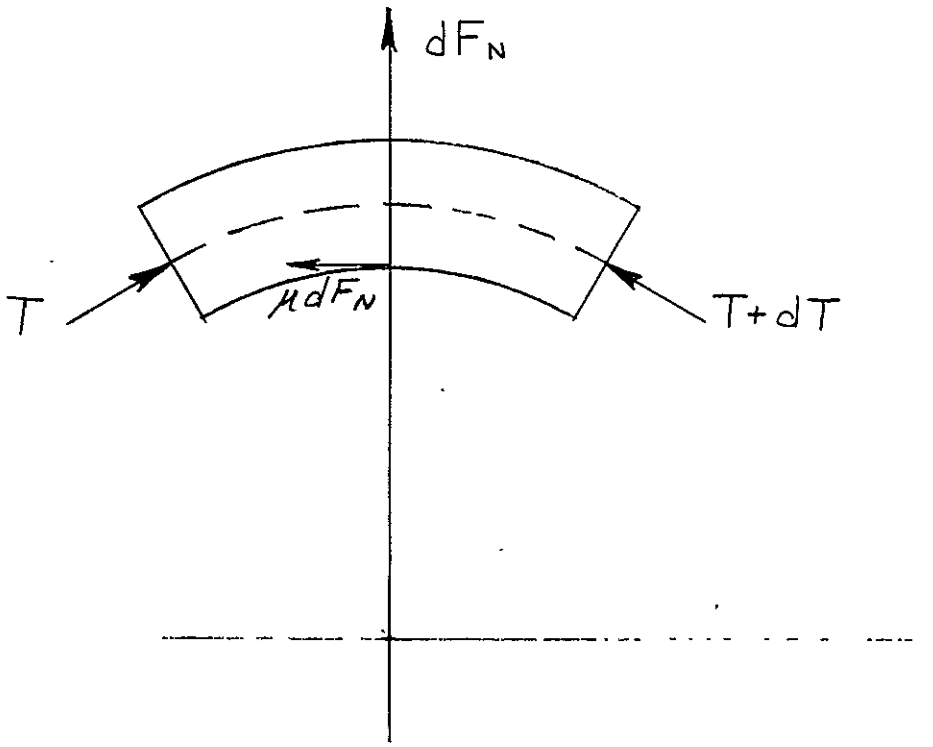

FREE BODY DIAGRAMS - DIFFERENTIAL COIL ELEMENT

FIG M-1

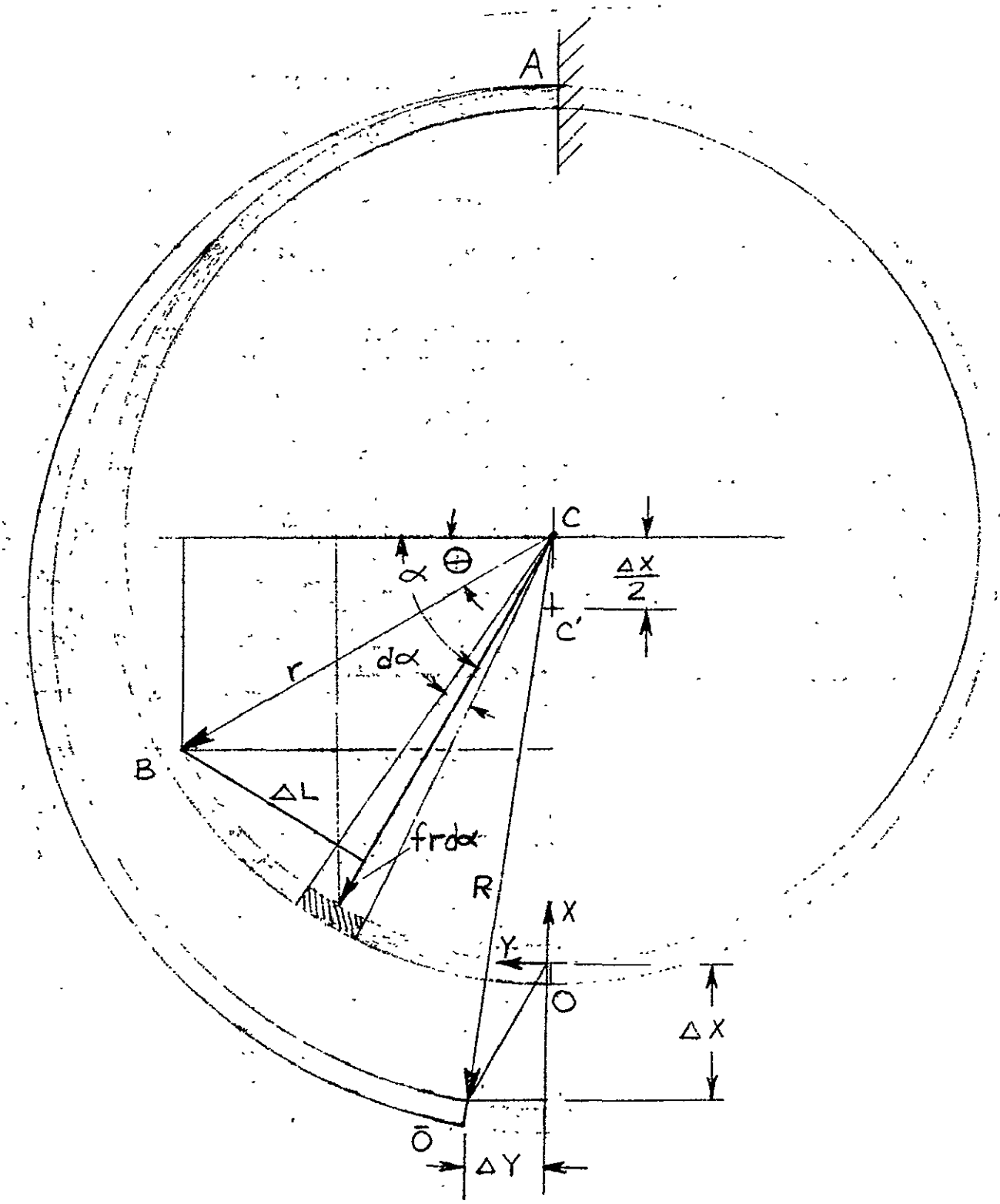

EXPANSION OF ONE TURN OF CLUTCH COIL

FIG M-2

APPENDIX N

Analysis of Belleville Washer for Drag Clutch

N.1 Scope of Analysis

This analysis is concerned with determining the maximum stress occuring in the belleville washers used in the drag clutch assembly (see figure 1a). This stress will be a compressive stress occuring at the convex edge of the inner diameter of the washer. This stress will be evaluated on the basis of initial yielding (acceptable, provided that the yielding occurs before final assembly into the clutch) and long term stress relaxation.

N.2 Effects on Washer of the Initial Deflection

Referring to figure N-1b we see that the total possible deflection of the washer is $(f)_{max}=h = .009 + .001 = .010$ in (including tolerances). Although the washers are not compressed to this value (nominal value of compression is .006 in per washer) in the assembled state, the assembly procedure is such that each spring washer could be totally flattened. Therefore, the stress calculation will be made assuming that the total possible deflection is achieved. Hence:

* $$S = \frac{Ef}{(1-\sigma^2)Ma^2}\left[C_1(h-f/2) + C_2 t\right]$$

Where:

S = Maximum washer stress (tangential occuring at I. D. of washer), psi

E = Modulus of elasticity of Beryllium Copper = 18×10^6 psi

σ = Poisson's ratio of Beryllium Copper = .285

f = deflection of washer, inches

M, C_1, C_2 = constants depending on the dimensions of the washer

h = total possible deflection of washer = .010 inches

$a = \frac{O.\ D.}{2}$

t = thickness of washer material, inches

* "Handbook of Mechanical Spring Design", Associated Spring Corporation, page 71

As with the deflection, f, the thickness, t, will be chosen as the maximum possible value including tolerances. Therefore t = .021 in. The maximum stress is therefore found to be: M = .625, C_1 = 1.16, C_2 = 1.27

$$S = \frac{18 \times 10^6 \times .010}{\left[1 - (.285)^2\right] \times .625 \times (.22)^2} \left[1.16\ (.010 - \frac{.010}{2}) + 1.26 \times 0.21\right]$$

$$S = \frac{18 \times 10^4}{.92 \times .625 \times .048} \times \left[.0058 + .0265\right]$$

$$\boxed{S = 210{,}000 \text{ psi}}$$

The yield strength of the beryllium copper alloy used (in its heat treated condition) is 130,000 psi and the ultimate is 200,000 psi. Although the value of stress is greater than both of these stresses, it is common knowledge that in belleville washer design, the stress calculated by the above equation (Alman-Laszlo equation) can exceed the material yield stress by 60% without any plastic setting of the washer occurring, provided the washer is not operating in a fatigue mode. Since this washer is deflected only a few times during assembly and once deflected, it is never again moved, the above calculated stress indicates that a very small amount of initial yielding will occur since (S) allowable = 1.6 x 130,000 = 208,000 psi. This yielding will slightly reduce the value of "h" after the first flexure is released. Subsequent flexure cycles (free height to flat condition to free height) will not produce any further change in "h". Hence, a new, effective yield stress for the washer of 208,000 psi has been created. The assembled deflection of only .006 in. produces a maximum stress of 120,000 psi which is well below this limit.

N.3 Effects on Washer of Long Term Deflection

The assembled deflection (.006 in. per washer) initially produces the nominal force needed to create the desired clutch slipping torque. The value of this

force could change by the process of stress relaxation. Stress relaxation is the reduction after a period of time of the initial stress value created in a part due to a fixed (for all time) deflection. A loss of the initial value of stress is accompanied by a corresponding reduction of the initial force required to produce the fixed deflection. This phenomenon is analogous to creep, which is a change in deflection with time under a constant load. Equations for the long term stress relaxation and the corresponding load relaxation have not been developed for belleville washers. Therefore, in lieu of a theoretical analysis, several tests were conducted on the washers and on the fully assembled clutch. Three clutches were assembled and their torque values measured in November, 1968. Two of these clutches were on the prototype half system and the other was on the take-up mechanism deployer (this deployer is used to take up and payout the half-system boom which is not deployed down the deployment track). After completing the qualification testing, these clutches were again examined in March, 1969. It was found that after four months in the assembled configuration and after being subjected to the full qualification test, the torque values had not changed. In addition, Mr. C. Staugaitis of NASA's (GSFC) materials branch examined and tested several randomly selected washers. He was unable to observe any stress relaxation of these washers in a time span of two weeks.

In light of the above, it can be concluded that there are no bad long term effects on the clutch belleville washers in the assembled configuration.

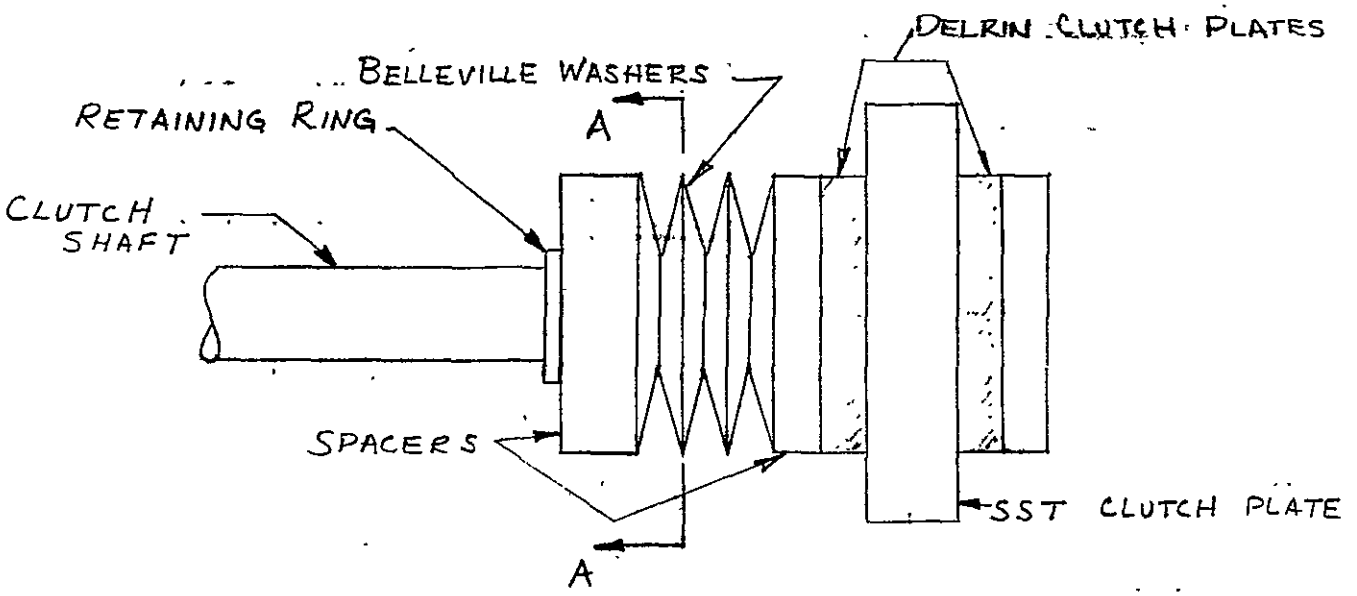

a

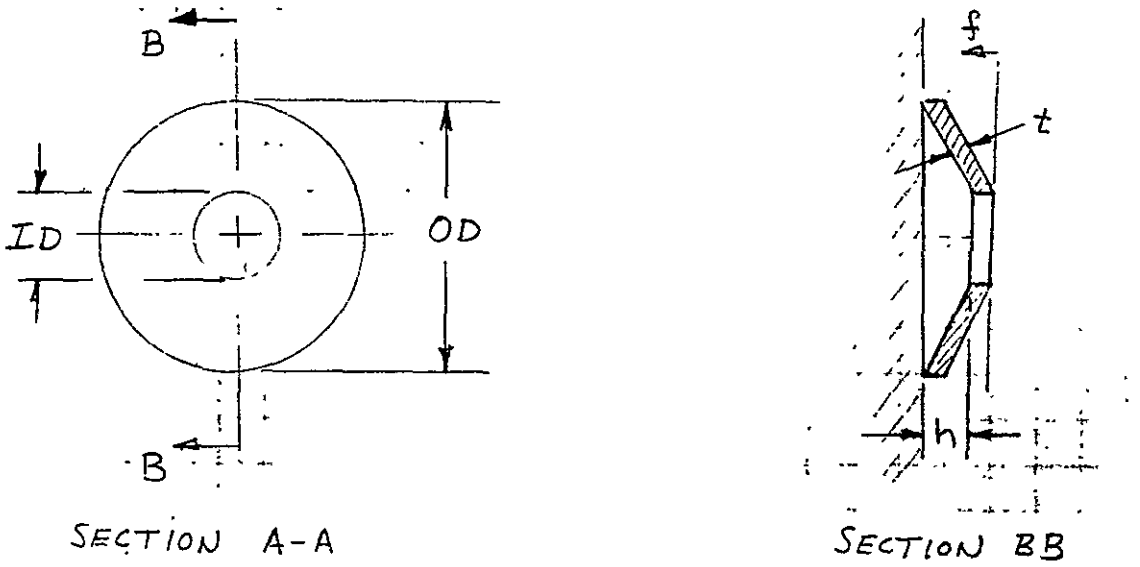

b

DRAG CLUTCH - BELLEVILLE WASHER ANALYSIS

FIG N-1

APPENDIX P

ASSEMBLY DRAWINGS OF MAJOR SYSTEM ASSEMBLIES

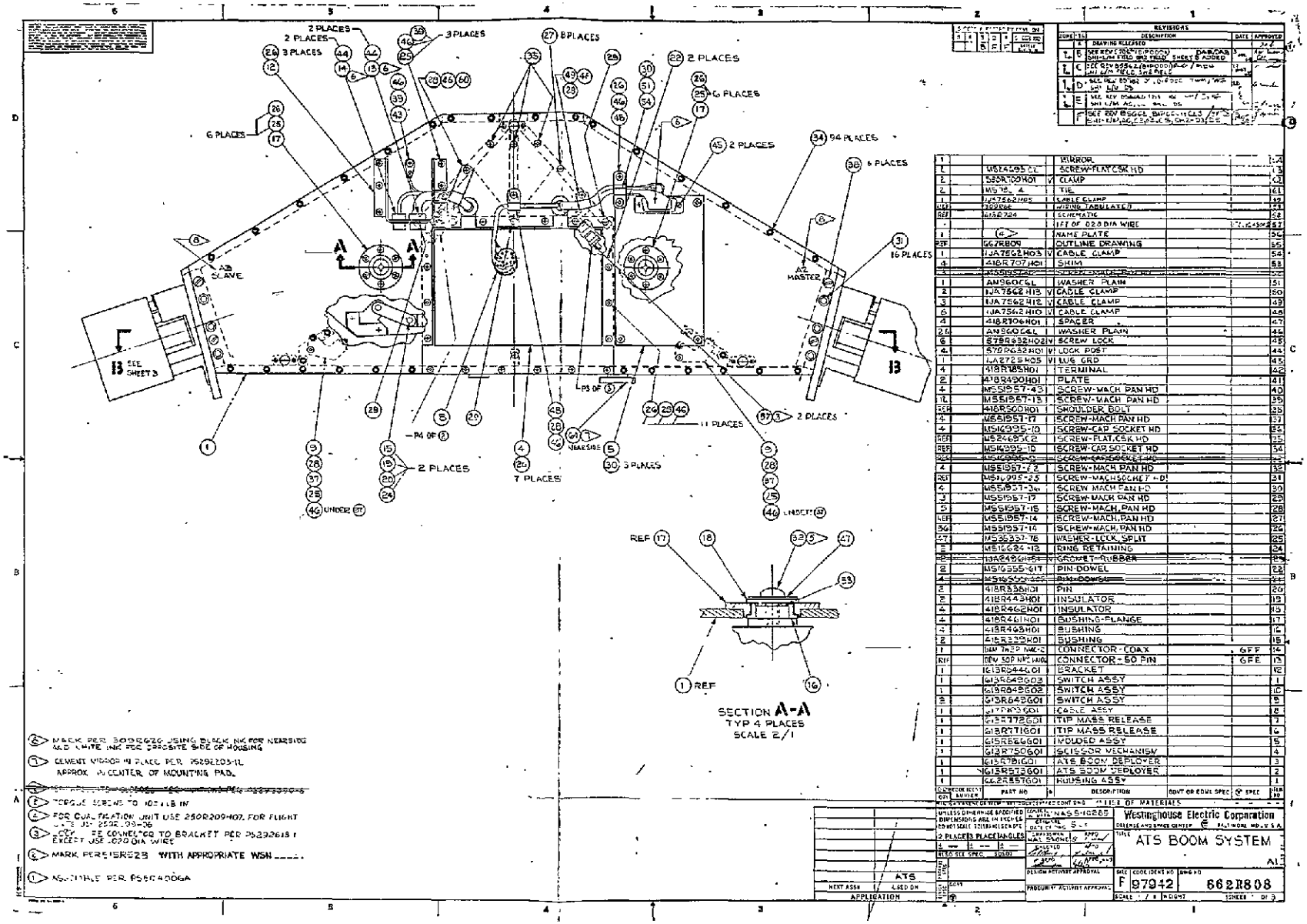

FOLDOUT FRAME 1

P-3/P-4

FOLDOUT FRAME 2

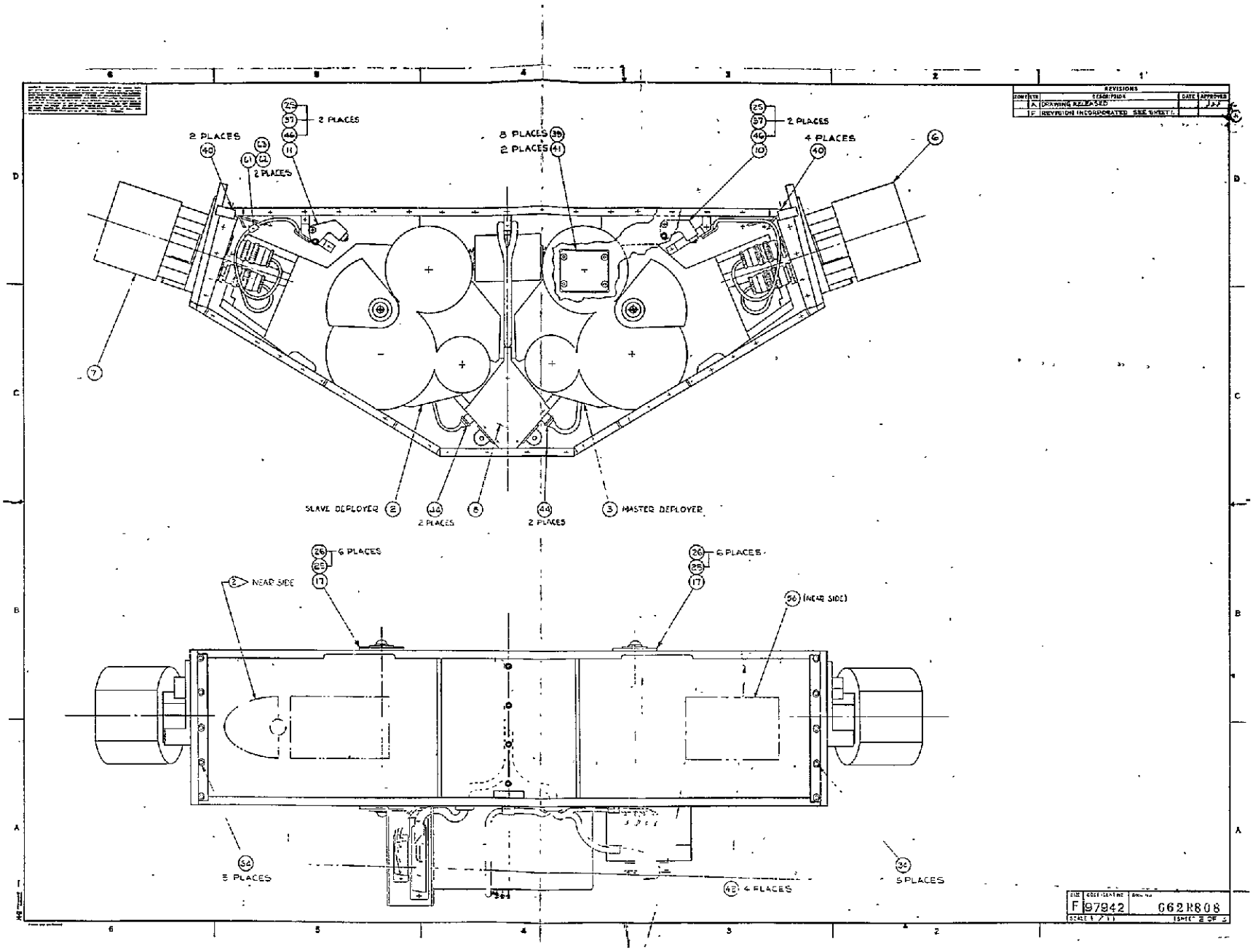

FOLDOUT FRAME 1

P-5/P-6

FOLDOUT FRAME 2

REVISIONS			
SYM	DESCRIPTION	DATE	APPROVED
B	THIS SHEET ADDED		

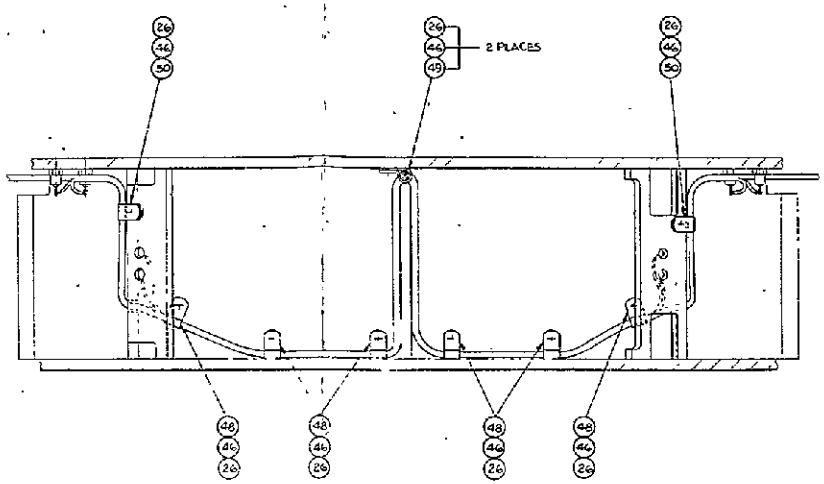

SECTION B-B
SEE SHEET 1

CAGE IDENT NO	SIZE	DWG NO
97942	F	662R808
SCALE		SHEET 2 OF 5

FOLDOUT FRAME 1

FOLDOUT FRAME 2

L/M CONTINUED ON SHEET 3

SHEETS AFFECTED BY REVISION					
5	4	3	2	1	SHEET NO
		J	J	J	LATEST REV LTR

REVISIONS

ZONE	LTR	DESCRIPTION	DATE	APPROVED
	A	DRAWING RELEASED		
	J	SEE REV B5623(BIP0001) JSJ/ SH1 L/M, B6; SH2 A2, C3, C4, C5; SH3 L/M	28 JAN 69	
	D	SEE REV E209 (BIP0001) RWC/GDS SH1 L/M; SH2 L/M, A5 B3 B6	24 OCT 68	
	C	SEE REV B555 (BIP0001) RAE/GDS SH1 L/M SH2 A5		
	F	SEE REV B5576 (BIP0001) RWC/GDS SH1 L/M, SH2 A1, A2, A3 B4 B5, B6		
	G	SEE REV B5586 (BIP0001) JSJ/HD SH1 L/M, SH3 C6	28 JAN 69	
	H	SEE REV B5594.03 (BIP0001) JSJ/HD SH1 L/M, SH2 A2, A3		

QTY	CODE IDENT NUMBER	PART NO	*	DESCRIPTION	GOVT OR COML SPEC	SPEC	ITEM NO
1		2JC2416H05	V	TERMINAL-PIN TYPE			92
1		418R682H01		BRUSH SHIM			91
2		MS51957-2		SCREW-MACH, PAN HD			90
1	56878	28702-98-C2B		SETSCREW			89
4		MS16555-627		PIN-DOWEL			88
(7) 5	08664	0906-03400		SET SCREW			87
1		MS18064-10		SET SCREW			86
2		MS51957-17		SCREW-MACH, PAN HD			85
1		MS21043-04		NUT-SELF LOCKING			84
1		MS24693-C4		SCREW-FLAT CSK HD			83
6		MS24693-C1		SCREW-FLAT CSK HD			82
1				WIRE, 12FT OF #22 WHT	MIL-W-16878/4	(9928-13)	81
1		579R504H01	V	CONNECTOR			80
8		MS17821-4		TIE			79
1		580R659H02	V	R.F. BRUSH ASSY			78
8		580R700H01		CLAMP			77
1		RG188U		1 FT OF COAX CABLE			76
1		575R136H03	V	TERMINAL			75
1		418R543H03		INSERT			74
2		418R543H02		INSERT			73
1		418R544H01		INSULATOR			72
3		418R543H01		INSERT			71
1		418R545H01		INSULATOR			70
1		418R548H01		SCISSOR INSULATOR			69
2		418R547H01		INSERT			68
2		418R302H04		SPACER			67
1		418R491H01		PLATE			66
2		1JA8683H04		TERMINAL			65
1		515R520G01		TRACKER			64
9		MS16555-625		PIN-DOWEL			63
9		MS15795-803		WASHER-FLAT			62
5		MS16995-10		SCREW-SOC HD CAP			61
2		MS51957-30		SCREW-MACH, PAN HD			60
13		MS18064-1		SETSCREW			59
5		MS21043-06		NUT-SELF LOCKING			58
6		AN960C6L		WASHER-FLAT			57
6		MS51957-32		SCREW-MACH, PAN HD			56
2		MS51957-31		SCREW-MACH, PAN HD			55
11		MS51957-29		SCREW-MACH, PAN HD			54
13		MS51957-28		SCREW-MACH, PAN HD			53
5		MS51957-16		SCREW-MACH, PAN HD			52
1		MS51957-15		SCREW-MACH; PAN HD			51
25		MS51957-14		SCREW-MACH, PAN HD			50
12		MS51957-13		SCREW-MACH, PAN HD			49
4		MS24693-C3		SCREW-FLAT, CSK HD			48
3		MS16624-4025		RING-RETAINING			47
1		MS16624-12		RING-RETAINING			46
1		418R677G01		BALANCE WEIGHT			45
1		418R678G01		BALANCE WEIGHT			44
1		515R519G01		RETAINER			43
1		515R515G01		SPACER			42
1		418R338H01		PIN			41

LIST OF MATERIALS

501 QTY	CODE IDENT NUMBER	PART NO	*	DESCRIPTION	GOVT OR COML SPEC	SPEC	ITEM NO.
1		418R339H01		BUSHING			40
(4) 10		1JB6277H27	V	BEARING			39
1		418R056H01		RETAINER			38
1		418R329H01		LINK			37
2		418R301G01		ARM SUPPORT			36
1		418R094H01		COLLAR			35
1		418R443H01		INSULATOR			34
1		418R302H03		SPACER			33
1		418R302H01		SPACER			32
5		309R593G01		SPACER			31
1		580R425H01	V	SLIP CLUTCH			30
1		579R301H02	V	GEAR-WORM WHEEL			29
1		579R300H05	V	GEAR			28
1		579R300H03	V	GEAR			27
1		418R399H01		GEAR			26
1		515R251H01		GEAR			25
1		515R245H01		GEAR			24
1		516R152G01		CONTROL SHAFT ASSY			23
1		418R044G01		SUPPORT			22
1		580R380H01	V	POTENTIOMETER			21
1		515R291H01		SHOE BRACKET			20
1		613R811G01		SHOE			19
1		515R531G02		SHOE BASE			18
1		617R066H01		BOOM			17
1		515R515G01		TRACKING GUIDE			16
1		418R719G01		ROLLER ASSY			15
1		515R265G01		DRIVE ROLLER ASSY			14
1		613R796G02		TAPE REEL			13
1		515R193H01		GUIDE SUPPORT			12
1		613R802G01		DRIVE UNIT			11
1		613R779G02		LIMIT SWITCH			10
1		515R217H01		PIVOT			9
1		515R171G01		PIVOT BLOCK			8
1		515R167G01		PIVOT BLOCK			7
1		515R126G01		CROSS FRAME			6
1		515R161G01		PLATE			5
1		515R136G01		PLATE			4
1		515R166G01		PLATE			3
1		613R556G01		GEAR FRAME			2
1		613R557G01		MOTOR FRAME			1

* V=VENDOR ITEM SEE SOURCE/SPEC CONT DWG — LIST OF MATERIALS

(10) AFTER ADDING ITEM (108) SO THAT IT JUST TOUCHES THE HUB OF GEAR (24), SECURE ITEM 24 GEAR TO THE TAPE REEL SHAFT USING SET SCREW (89) SO THAT THERE IS NO ALLOWABLE AXIAL MOTION OF THE TAPE REEL. AFTER THOROUGHLY MASKING THE DEPLOYER, MACHINE THE TAPE REEL SHAFT SO THAT THE .010 + .005 DIMENSION IS OBTAINED (BE CERTAIN TO USE A VACUUM SYSTEM DURING MACHINING). CHECK TO VERIFY THAT SET SCREW (89) IS TIGHTENED & SECURED PER PS 598213. ADD ITEM (106) BY TORQUING THE SCREW TO 5±1 LB-IN & LOCKTITE PER PS293013-1 USING LOCKTITE "E".

(9) MARK PART NO AND APPLICABLE 4 DIGIT SERIAL NO. APPROX AS SHOWN PER 309R626 USING BLACK INK.

(8) MARK P3 PER 309R626 USING BLACK INK.

(7) PURCHASE FROM BRISTOL SOCKET SCREW.

(6) CAUTION. DISCONNECT (10) AND (21) IF DEPLOYER IS OPERATED WITHOUT BOOM TO PREVENT DAMAGE TO THESE COMPONENTS.

(5) [illegible — struck through]

(4) BEARINGS ARE NOT TO BE EXPOSED TO ANY OIL, GREASE OR MORE THAN 65% HUMIDITY AT ANY TIME.

(3) [illegible — struck through]

(2) [illegible — struck through]

(1) ASSEMBLE PER PS 598213

NEXT ASSY	USED ON
662R808	ATS

APPLICATION

UNLESS OTHERWISE SPECIFIED DIMENSIONS ARE IN INCHES DO NOT SCALE. TOLERANCES ON DEC 2 PLACE ±.— 3 PLACE ±.— ANGLES ±—

ALSO SEE SPEC 90S01

CONTRACT NUMBER NAS 5-10285

DRAFTSMAN HAL STONE

DESIGN ACTIVITY APPROVAL

PROCURING ACTIVITY APPROVAL

Westinghouse Electric Corporation
DEFENSE AND SPACE CENTER BALTIMORE, MD., U.S.A.

TITLE ATS BOOM DEPLOYER
ATS BOOM SYSTEM A1

SIZE D | CODE IDENT NO 97942 | DWG NO 613R791

SCALE 1/1 | WEIGHT | SHEET 1 OF

FOLDOUT FRAME 1

FOLDOUT FRAME 2

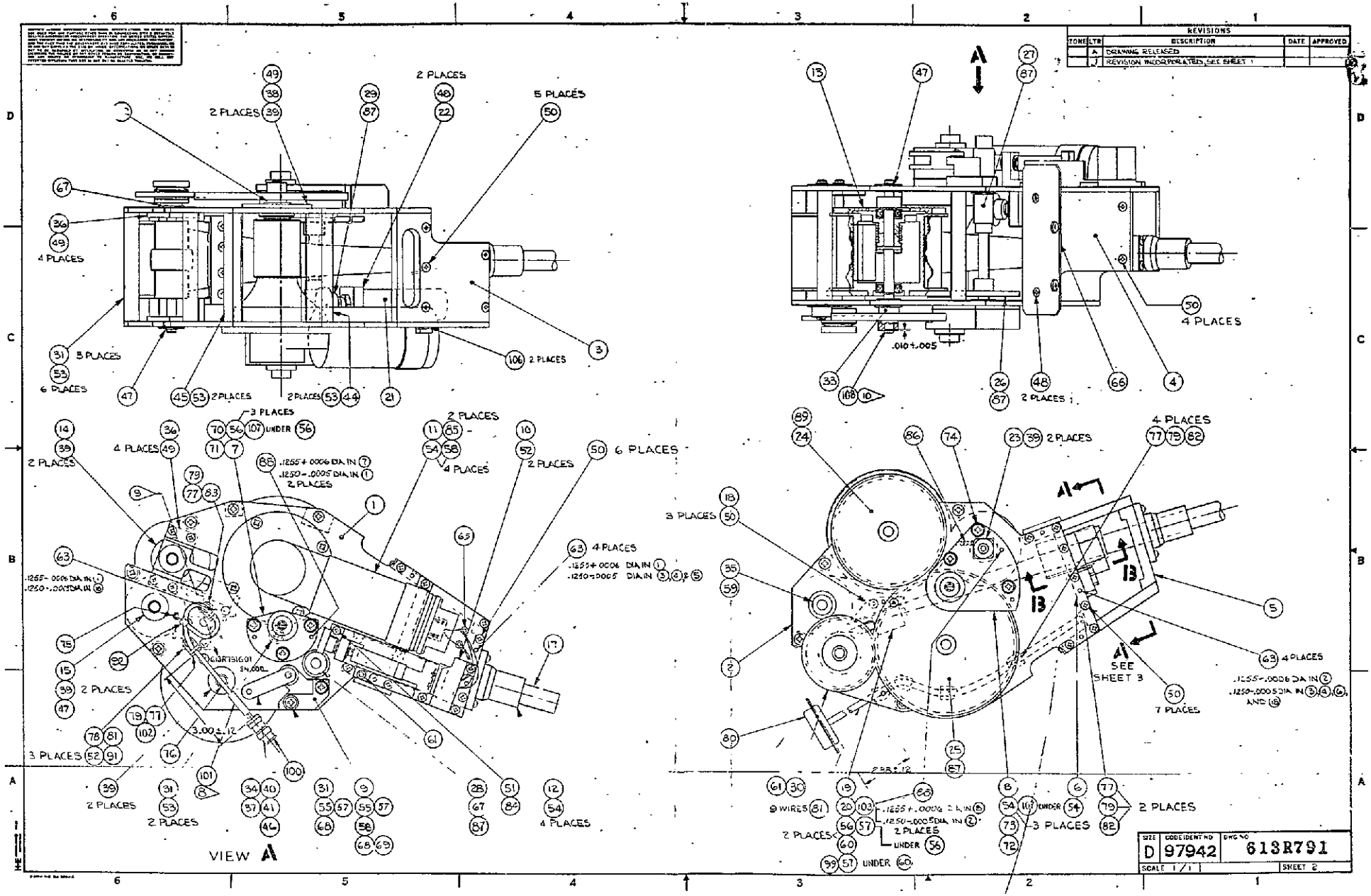

FOLDOUT FRAME 1

P-11/P-12

FOLDOUT FRAME 2

REVISIONS				
ZONE	LTR	DESCRIPTION	DATE	APPROVED
	C	THIS SHEET ADDED		
	J	REVISION INCORPORATED SEE SH 1		

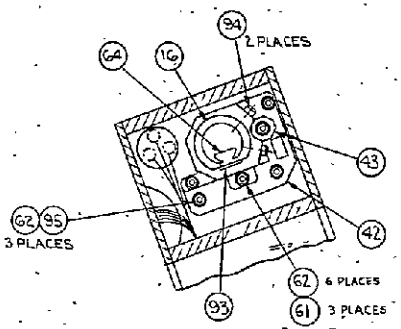

SECTION A-A
SEE SHEET 2

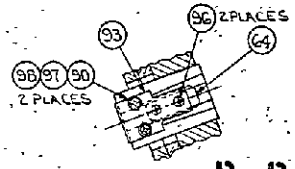

SECTION B-B
SEE SHEET 2

QTY	CODE IDENT NUMBER	PART NO.	* DESCRIPTION	GOVT OR COML SPEC	(W) SPEC	ITEM NO.
1		MS 51957-41	SCREW-MACHINE PAN HEAD			108
6		MS 15795-805	WASHER-FLAT			107
2		415R852H01	SHIM			106
2		415R848H02	SHIM (.010)			105
2		415R848H03	SHIM (.005)			104
1		515R530H01	SHOE PLATE			103
1		MS24693-C6	SCREW-CSK HD			102
1			TUBING-.50 OF-.18 ID TEFLON-WHITE	MIL-T-22129	(M44TB1K2)	101
1	95077	3006-0003	V CONNECTOR-COAX			100
2		MS35338-136	WASHER-SPLIT LOCK			99
2		MS35338-134	WASHER-SPLIT LOCK			98
2		MS15795-302	WASHER-FLAT			97
2		MS51957-3	SCREW-PAN HD			96
3		MS16995-11	SCREW-SOC HD CAP			95
2		MS16995-9	SCREW-SOC HD CAP			94
1		418RT02H01	PLATE-ADJUSTMENT			93

REF: VENDOR LIST, SEE SOURCE SPEC CONT DWG. LIST OF MATERIALS (CONT'D FROM SHEET 1)

SIZE	CODE IDENT NO	DWG NO
D	97942	613R791
SCALE 1/1		SHEET 3

FOLDOUT FRAME 1

FOLDOUT FRAME 2

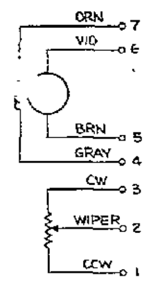

SCHEMATIC DIAGRAM

PIN ORIENTATION
SCALE 1/2

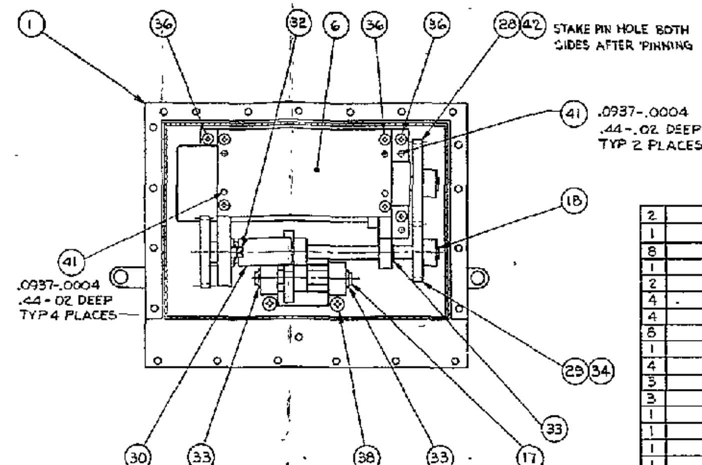

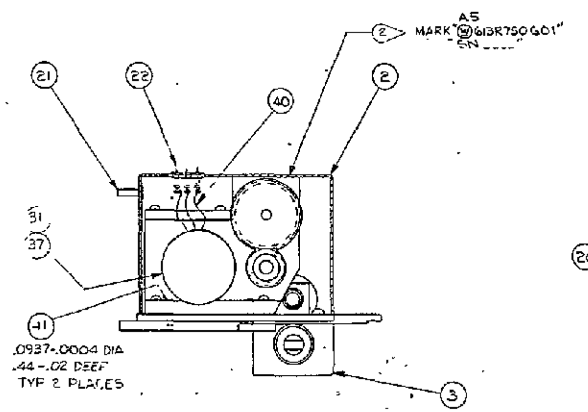

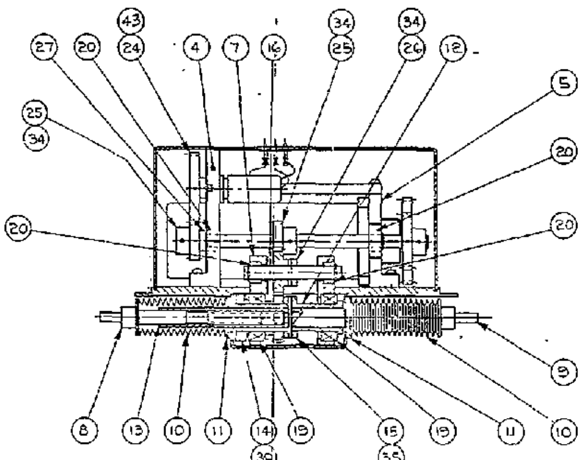

Rev	Zone	Ltr	Description	Date	Approved
		A	DRAWING RELEASED		
		B	SEE REV P1091 (BIP0001)		
		C	SEE REV P1117 (BIP0001)		
		D	SEE REV E2037 (BIP0001) A6, B4, B6, C5		
	A6	E	SEE REV B5593 (BIP0001)		
		F	SEE REV B5657 (BIP0001) L/M, D3		
		G	SEE REV B5659 (BIP0001) L/M, C4, C5	MAR 28	

QTY REQD	CODE IDENT NUMBER	PART NO.	*	DESCRIPTION	GOVT OR COML SPEC	SPEC	ITEM NO
2		MS18064-1		SETSCREW			43
1		MS16555-611		PIN DOWEL			42
8		MS16555-620		PIN-DOWEL			41
1		———		WIRE, 1FT OF #24, WHITE	MIL-W-16878/4	(FDS9928-B)	40
2		MS18064-5		SETSCREW			39
4		MS51957-27		SCREW-MACH, PAN HD			38
4		MS51957-15		SCREW-MACH, PAN HD			37
8		MS51957-16		SCREW-MACH, PAN HD			36
1		MS16562-216		PIN-SPRING			35
4		MS16562-194		PIN-SPRING			34
3		MS16624-4025		RING-RETAINING			33
3		MS17183-1		CLAMP			32
1		580R364H01	V	MOTOR			31
1		580R381H01	V	POTENTIOMETER			30
1		2JC3581H42	V	GEAR			29
1		2JC3581H43	V	GEAR			28
1		418R302H02		SPACER			27
1		2JC3581H41	V	GEAR			26
2		2JC3581H40	V	GEAR			25
1		2JC3581H38	V	GEAR			24
REF		T-789491		TEST SPEC			23
1		580R373H02	V	HEADER			22
1		418R330H01		PRESSURE TUBE			21
4		418R332H01		BEARING			20
2		580R607H01	V	BEARING			19
1		418R340H01		SHAFT			18
1		418R343H01		SHAFT			17
1		418R393H01		SPACER			16
1		418R410G01		GEAR ASSY			15
1		418R335H01		COLLAR			14
1		515R208H01		DRIVE SCREW			13
1		418R334H01		SLEEVE			12
2		418R328H01		BELLOWS SEAT			11
2		580R512H01		BELLOWS			10
1		515R207H02		SCISSOR ARM			9
1		515R207H01		SCISSOR ARM			8
1		515R209G01		HOUSING			7
1		418R331H01		PLATE			6
1		515R205G01		PLATE			5
1		515R213G01		SUPPORT			4
1		418R337H01		COVER			3
1		515R215H01		COVER			2
1		613R750H01		PLATE			1

* V = VENDOR ITEM SEE SOURCE/SPEC CONT DWG — LIST OF MATERIALS

3. MASK AND PAINT PER INSTRUCTIONS IN PS598209-1 (HOUSING ASSEMBLY)
2. AFTER PAINTING PER 3, MARK PER 309R626 USING WHITE INK.
1. ASSEMBLE PER PS597689-1

NEXT ASSY	USED ON
662R808	ATS

APPLICATION

UNLESS OTHERWISE SPECIFIED DIMENSIONS ARE IN INCHES DO NOT SCALE

CONTRACT NUMBER NAS 5-10285
ORIGINAL DATE OF DWG MAR 67
CRAFTSMAN HAL STONE

Westinghouse Electric Corporation
DEFENSE AND SPACE CENTER BALTIMORE MD., U.S.A.

TITLE SCISSOR MECHANISM ATS BOOM SYSTEM A1

SIZE D CODE IDENT NO 97942 DWG NO 613R750
SCALE 1/1 SHEET 1 OF 1

FOLDOUT FRAME 1

FOLDOUT FRAME 2

NOTICE — WHEN GOVERNMENT DRAWINGS, SPECIFICATIONS, OR OTHER DATA ARE USED FOR ANY PURPOSE OTHER THAN IN CONNECTION WITH A DEFINITELY RELATED GOVERNMENT PROCUREMENT OPERATION, THE UNITED STATES GOVERNMENT THEREBY INCURS NO RESPONSIBILITY NOR ANY OBLIGATION WHATSOEVER; AND THE FACT THAT THE GOVERNMENT MAY HAVE FORMULATED, FURNISHED, OR IN ANY WAY SUPPLIED THE SAID DRAWINGS, SPECIFICATIONS, OR OTHER DATA IS NOT TO BE REGARDED BY IMPLICATION, OR OTHERWISE AS IN ANY MANNER LICENSING THE HOLDER OR ANY OTHER PERSON OR CORPORATION, OR CONVEYING ANY RIGHTS OR PERMISSION TO MANUFACTURE, USE, OR SELL ANY PATENTED INVENTION THAT MAY IN ANY WAY BE RELATED THERETO.

REVISIONS			
LTR	DESCRIPTION	DATE	APPROVAL
A	DRAWING RELEASED		
B	SEE REV P1151.01(BIP0001)	13SEP67	
C	SEE REV P1256(BIP 0001)		

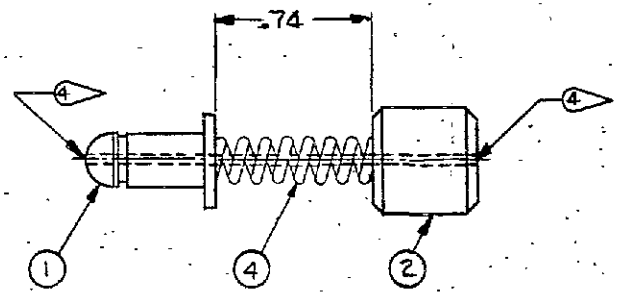

(5) TEST WITH 20 Lb. TENSION BETWEEN (1) AND (2) INSPECT FOR CRACKS AT SOLDERED AND BRAZED JOINTS AND DIMENSION CHANGES

(4) SOLDER FULL LENGTH OF (1) & (2) TO (3) PER MIL-STD-454, REQ 5, SOLDER COMP SN60, ACID FLUX (PS 292399-5)

(3) BEFORE (4), PASSIVATE PER QQ-P-35, TYPE II (PS294193-2) FOR A MAXIMUM OF 30 MIN

(2) BRAZE (1) AND (2) TO (4) PER MIL-B-7883 USING QQ-S-561, CL4 OR CL5 ALLOY

(1) QQ-W-423, FORM 1, COMP 302, COND B

GOVT REQD	CODE IDENT	PART NO.	*	DESCRIPTION	GOVT OR COML SPEC	⊗ SPEC	ITEM NO.
1		418R527H01		SPRING-ISOLATION			4
1				WIRE-3.00 OF.031 DIA SST	(1)	(PDS63594)	3
1		418R438H01		BOOM PLUG			2
1		418R436H01		BOOM PLUG			1

* V = VENDOR ITEM. SEE SOURCE/SPEC CONT DWG — LIST OF MATERIAL

613R791	ATS
613R573	ATS
NEXT ASSY	USED ON
APPLICATION	

PROCESS SPEC (1)
FINISH SPEC GOVT (⊗)

UNLESS OTHERWISE SPECIFIED DIMENSIONS ARE IN INCHES. DO NOT SCALE TOLERANCES OF SEC.
2 PLACE ±.05 | 3 PLACE ±.— | ANGLES ±—
ALSO SEE SPEC SQSD1

CONTRACT NAS5-10285
ORIGINAL DATE OF DWG 9FEB67
DRAFTSMAN N.SWIFT APPD
CHECKED APPD
APPD
DESIGN ACTIVITY APPROVAL
PROCURING ACTIVITY APPROVAL

Westinghouse Electric Corporation
DEFENSE AND SPACE CENTER ⓦ BALTO. MD. U.S.A.

TITLE BOOM ISOLATION ASSY
ATS BOOM DEPLOYER AB

SIZE B | CODE IDENT 97942 | DWG NO 418R439

SCALE 2/1 | WEIGHT | SHEET 1 OF 1

FORM NO. BA 8361-1

FOLDOUT FRAME 1

FOLDOUT FRAME 2

ZONE	LTR	REVISIONS DESCRIPTION	DATE	APPROVED
	A	DRAWING RELEASED		
	B	SEE REV P1107 (BIP 0001) HLS/HS ALL ZONES		
	C	SEE REV P1180 (BIP 0001) LVD/ SHT 1 - LM, A5, A6 SHT 2 A2, A3, B2, B3, B4, C3, C4, D2, D4		
	D	SEE REV E2031 (B-P0001) WES/ SHT 1 - L/M, A1-A6 SHT 2 A5, B1, B3, B4, D2, D4		
	E	SEE REV B5625 (B-P0001) SH 1 LM SH 2 A2 & C2 B3		
	F	SEE REV B5662 (B-P0001) LCW/P SH1 L/M, C5 - SH 2 A2, A3, B1, B3, C2 C3 D4		

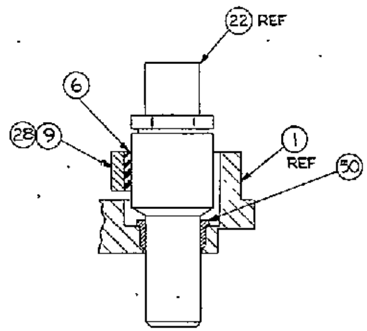

SECTION B-B
SCALE 2/1
SEE SHEET 2

QTY REQD	CODE IDENT NUMBER	PART NO	*	DESCRIPTION	GOVT OR COML SPEC	(W) SPEC	ITEM NO
1		MS21043-4		NUT-SELF LOCKING			53
1		418R879H01		ADJUSTMENT POST			52
1		418R874H01		INSERT			51
2		418R875H01		SLEEVE			50
1		418R881H01		STOP ANGLE			49
1		418R404H01		TORSION SPRING			48
1		418R861H01		HUB			47
~~1~~		~~[illegible]~~		~~[illegible]~~			~~46~~
1	08664	0506-03400	V	SETSCREW			45

QTY REQD	CODE IDENT NUMBER	PART NO.	*	DESCRIPTION	GOVT OR COML SPEC	(W) SPEC	ITEM NO
1		NAS620C2		WASHER-PLAIN			[illegible]
1		MS51957-2		SCREW-MACH PAN HD			[illegible]
1		AN960C4L		WASHER-PLAIN			[illegible]
1		MS16628-4025		RING-RETAINING			[illegible]
1		418R439G01		ISOLATION ASSY			[illegible]
1		418R877H01		RETAINER			[illegible]
4		418R471H01		CABLE RETAINER			[illegible]
1		418R469H01		SCREW-ADJUSTMENT			[illegible]
1		MS27216-2		SWITCH			[illegible]
1		515R301H01		CAM			[illegible]
1		418R683H01		LEVER-STOP			[illegible]
2		MS51957-6		SCREW-MACH, PAN HD			[illegible]
1		MS21043-04		NUT-SELF LOCKING			[illegible]
3		AN960C2L		WASHER-PLAIN			[illegible]
1		AN340C4		NUT			[illegible]
10		MS35337-77		WASHER-SPLIT LOCK			[illegible]
2		MS16995-28		SCREW-SOC HD			[illegible]
~~1~~		~~MS16995-25~~		~~SCREW-SOC HD~~			[illegible]
7		MS16995-1		SCREW-SOC HD			[illegible]
1		418R470H02		PIN-DOWEL			[illegible]
1		418R470H01		PIN-DOWEL			[illegible]
1		MS16629-4075		RING-RETAINING			[illegible]
(5) 2		(1)		GUILLOTINE			[illegible]
1		580R531H03	V	CABLE			[illegible]
1		309R631H01		INSULATOR			[illegible]
1		418R404H02		TORSION SPRING			[illegible]
3		418R403H01		SPRING			[illegible]
1		418R402H01		PIN			[illegible]
1		418R860H01		PIN-PIVOT			[illegible]
1		418R400H01		PIN			[illegible]
1		418R377H01		SCREW-CLAMPING			[illegible]
1		MS21043-3		NUT-SELF LOCKING			[illegible]
1		418R876H01		POST			[illegible]
1		418R370H01		PULLEY			[illegible]
1		418R878H01		PULLEY-SHAFT			[illegible]
1		418R367H01		CLAMP			[illegible]
1		418R366H01		RETAINER			[illegible]
1		418R365H02		RETAINER			[illegible]
2		418R359H01		PAD			[illegible]
1		418R356H01		WHEEL			[illegible]
1		515R260H01		LEVER-CLAMPING			[illegible]
1		515R259H01		SUPPORT			[illegible]
1		515R258G01		TIP MASS			[illegible]
1		662R857H08		END PLATE			[illegible]

*V=VENDOR ITEM SEE SOURCE/SPEC CONT DWG — LIST OF MATERIALS

(6) MARK PER 309R626 USING BLACK INK "(W) 618R771G01" & "SN____".

(5) CAUTION! (22) HAVE ELECTRO-EXPLOSIVE CARTRIDGES (CLASS "C" EXPLOSIVES) AND ROUGH HANDLING MUST BE PREVENTED. PRIOR TO ASSEMBLY THE LEAD WIRES MUST BE KEPT SHUNTED AS THEY ARE DURING SHIPMENT, TO PREVENT ACCIDENTAL FIRING BY STRAY CURRENTS. TEMPERATURE BELOW 450°F ARE SAFE.

(4) RELEASE PER PS597694

(3) ASSEMBLE PER PS597694

~~(2) [illegible] FOR THIS ASSEMBLY. REMOVE [illegible] FROM [illegible] ASSEMBLY (662R857) AFTER ASSEMBLY MACHINING.~~

(1) PURCHASE FROM HOLEX INCORPORATED PER GENERAL ELECTRIC P/N 115C7516

NEXT ASSY	USED ON
662R808	ATS
APPLICATION	

UNLESS OTHERWISE SPECIFIED DIMENSIONS ARE IN INCHES DO NOT SCALE. TOLERANCES ON DEC: 2 PLACE ± 3 PLACE ± ANGLES ±
ALSO SEE SPEC 90S01

CONTRACT NUMBER NAS 5-10265
ORIGINAL DATE OF DWG 26 JAN 67
DRAFTSMAN R.L. GRUND
DESIGN ACTIVITY APPROVAL
PROCURING ACTIVITY APPROVAL

Westinghouse Electric Corporation
DEFENSE AND SPACE CENTER BALTIMORE MD

TITLE T.P MASS RELEASE
ATS - BOOM SYSTEM

SIZE D CODE IDENT NO 97942 DWG NO 618R771
SCALE 1 WEIGHT SHEET

FOLDOUT FRAME 1

FOLDOUT FRAME 2

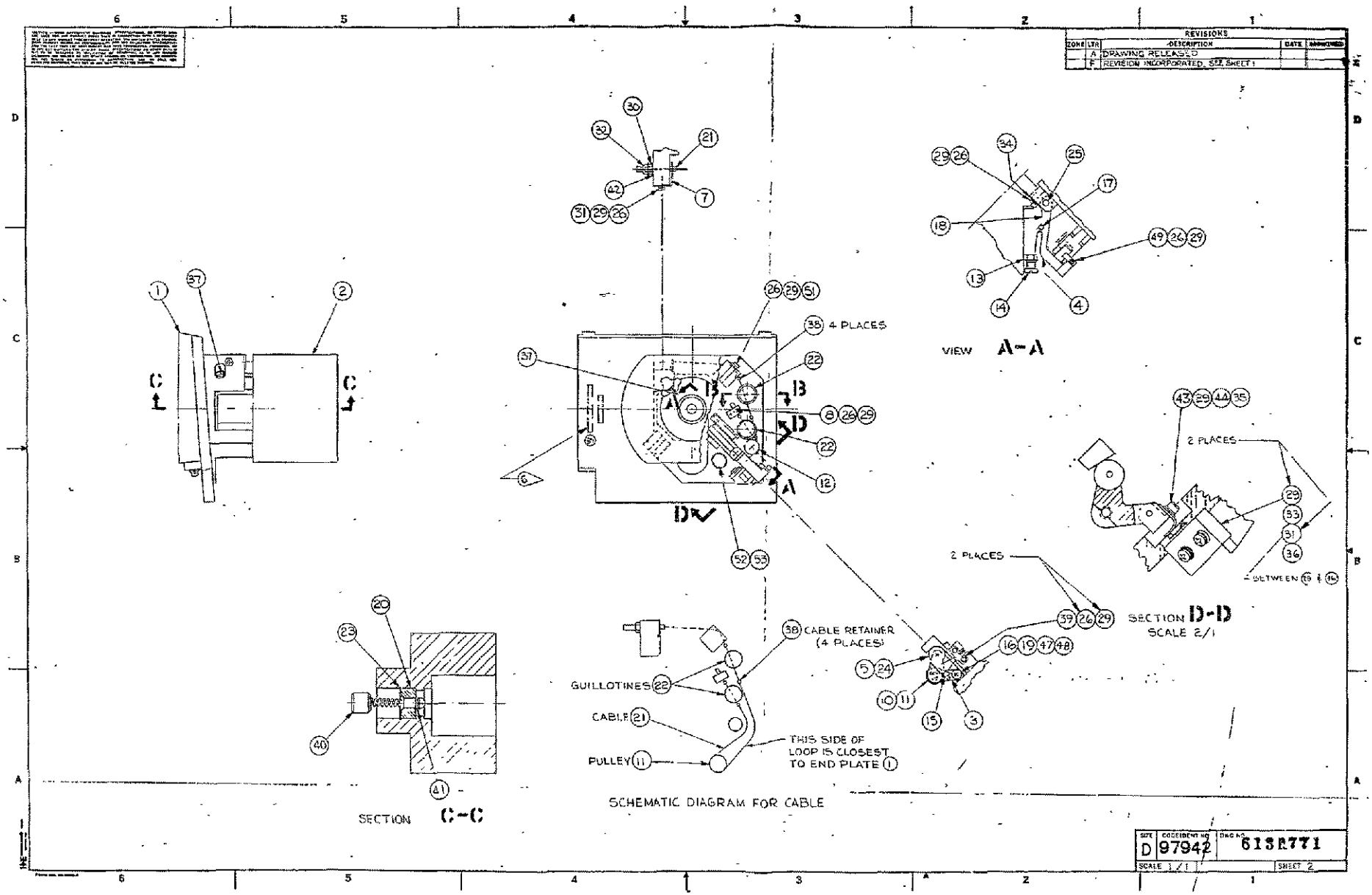

FOLDOUT FRAME 1

P-21/P-22

FOLDOUT FRAME 2

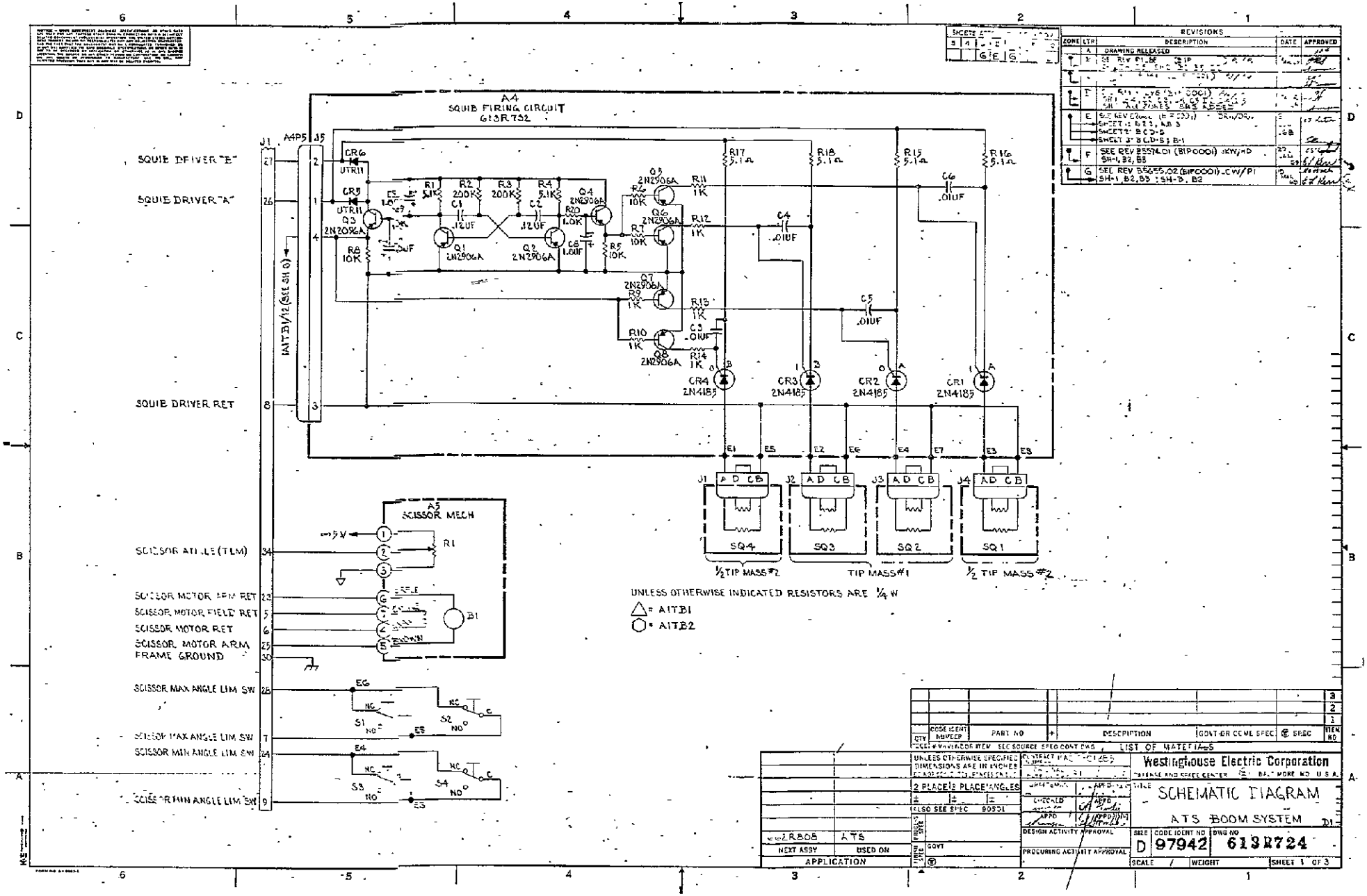

FOLDOUT FRAME 1

P-23/P-24

FOLDOUT FRAME 2

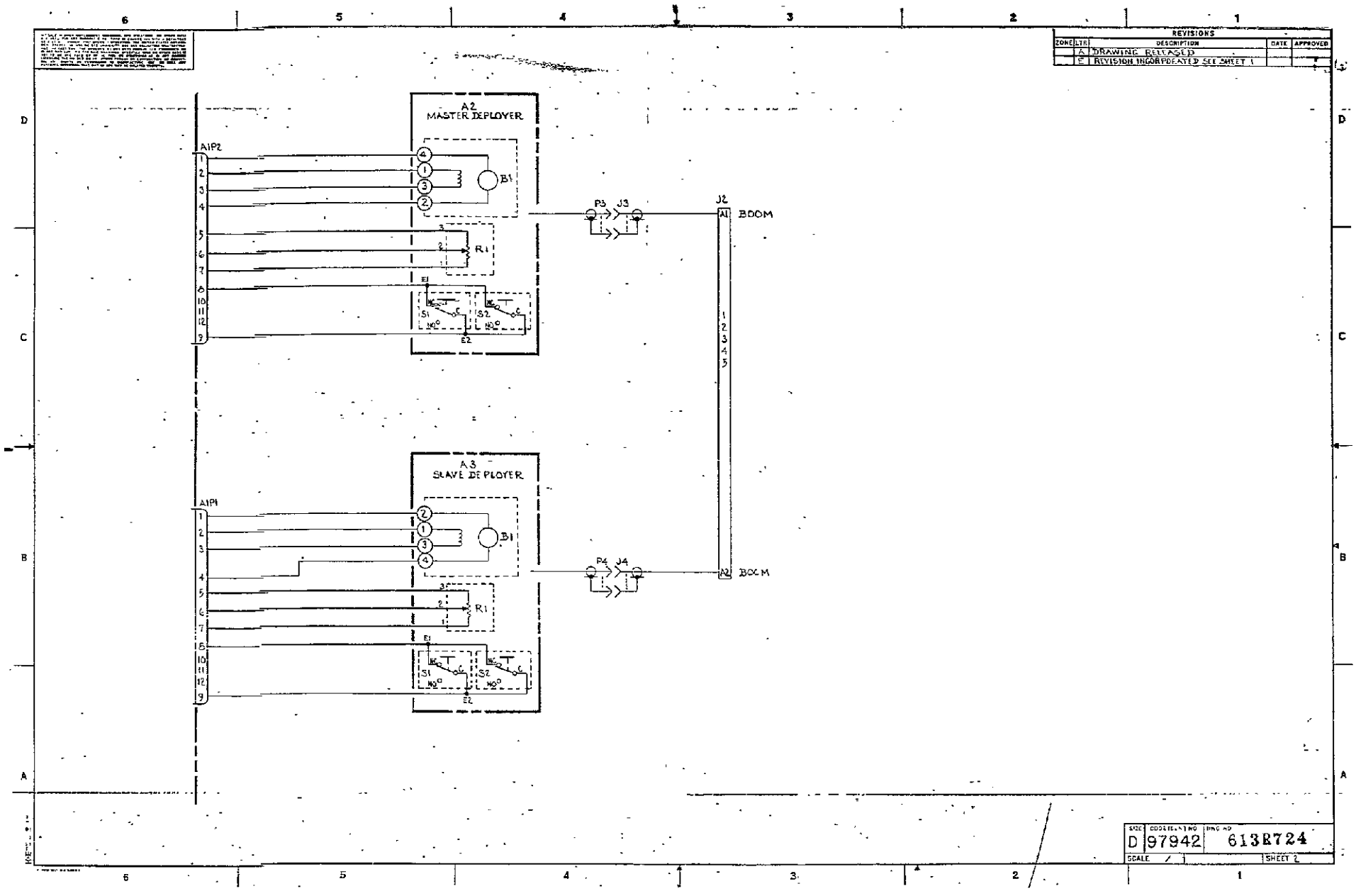

FOLDOUT FRAME 1

FOLDOUT FRAME 2

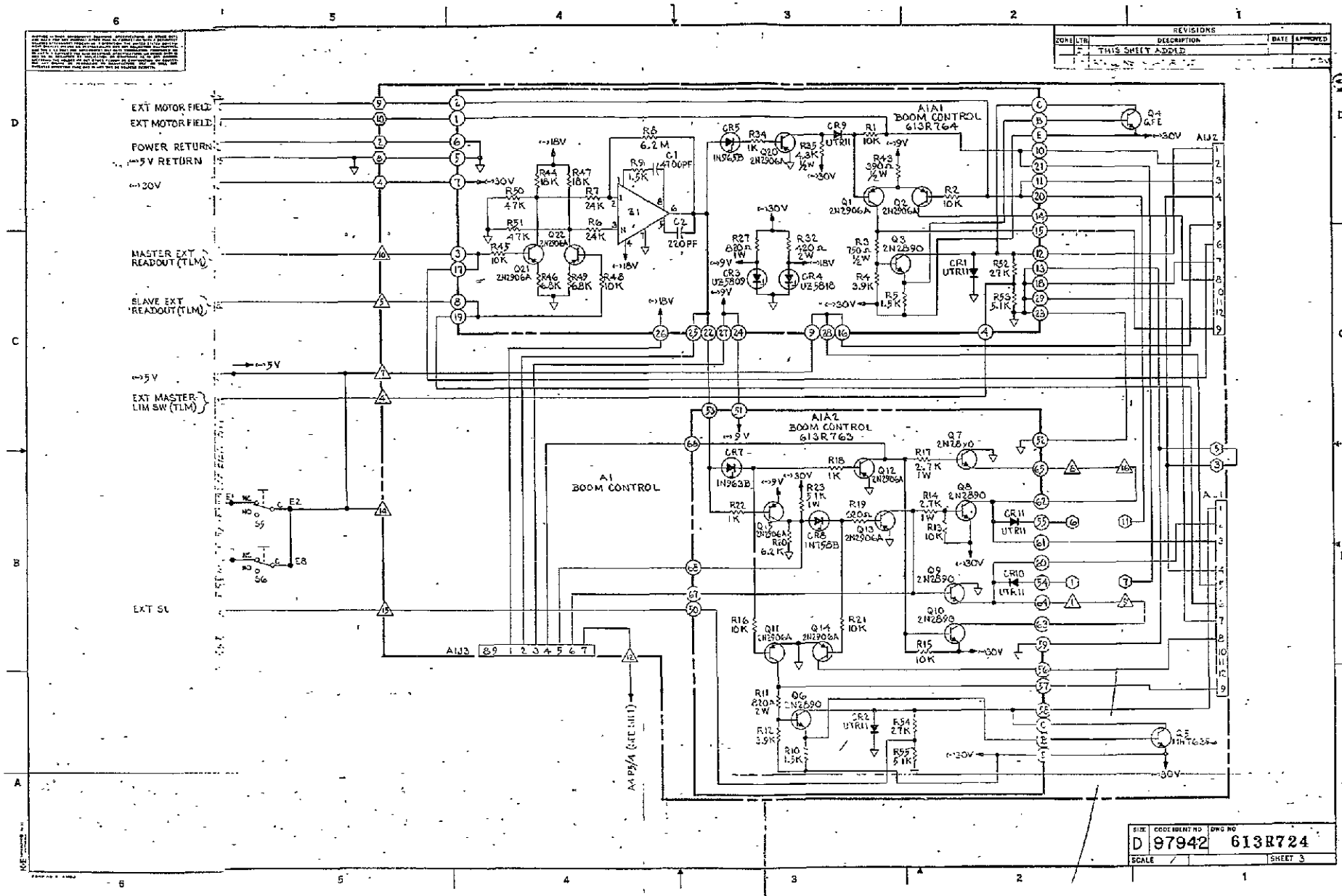

EOLDOUT FRAME 1

EOLDOUT FRAME 2